Master's thesis

NTNU
Norwegian University of Science and Technology
Faculty of Engineering
Department of Structural Engineering

Nicolas André Caronte Grønland

Steel beams with unstiffened web openings

Master's thesis in Civil and Environmental Engineering
Supervisor: Arne Aalberg
December 2021

NTNU
Norwegian University of
Science and Technology

Nicolas André Caronte Grønland

Steel beams with unstiffened web openings

Master's thesis in Civil and Environmental Engineering
Supervisor: Arne Aalberg
December 2021

Norwegian University of Science and Technology
Faculty of Engineering
Department of Structural Engineering

NTNU
Norwegian University of
Science and Technology

Department of Structural Engineering
Faculty of Engineering
NTNU- Norwegian University of Science and Technology

ACCESSIBILITY

OPEN

MASTER'S THESIS 2021

SUBJECT AREA:	DATE:	NO. OF PAGES:
Steel Structures	03.01.2022	65 + 45

TITLE:

Steel beams with unstiffened web openings

Stålbjelker med uavstivede åpninger i steget

BY:

Nicolas André Caronte Grønland

SUMMARY:

The European Committee for Standardization, CEN, have been working on an extension of *Eurocode 3: Design of steel structures – Part 1-1: General rules and rules for buildings*, to be called "EN 1993-1-13: Beams with web openings". This extension will provide design rules for steel beams with web openings, both for ultimate and serviceability limit state and is set to be published in 2026. The purpose of this master's thesis is to present the work that has been done on the topic of steel beams with web openings at Norwegian University of Science and Technology (NTNU). This includes in total five tests on steel beams with various web opening geometries. The ultimate capacities achieved in the tests have been compared against the design capacities obtained from EN 1993-1-13 and the discrepancies that were found are discussed in detail.

The work showed that the standard gives overly conservative results in some cases. In particular, it drastically underestimates the capacities of beams that have web openings where the remaining web outstands at the openings are classified as cross-sectional Class 4. To further investigate the performance of EN 1993-1-13 a parameter study was conducted. Finite element models which were calibrated against the test data gave rise to a total of 46 beams with different opening geometries. The results reinforced what was already seen about the conservatism regarding the *Vierendeel* check.

Lastly, three additional subtopics regarding beams with web openings were investigated.

RESPONSIBLE TEACHER: Prof. Arne Aalberg

SUPERVISOR(S): Prof. Arne Aalberg

CARRIED OUT AT: Department of Structural Engineering

Institutt for konstruksjonsteknikk
Fakultet for ingeniørvitenskap
NTNU- Norges teknisk- naturvitenskapelige universitet

TILGJENGELIGHET

ÅPEN

MASTEROPPGAVE 2021

FAGOMRÅDE:	DATO:	ANTALL SIDER:
Stålkonstruksjoner	03.01.2022	65 + 45

TITTEL:

Stålbjelker med uavstivede åpninger i steget

Steel beams with unstiffened web openings

UTFØRT AV:

Nicolas André Caronte Grønland

SAMMENDRAG:
Den europeiske standardiseringskomiteen, CEN, har jobbet med en utvidelse av *Eurokode 3: Design av stålkonstruksjoner – Del 1-1: Generelle regler og regler for bygninger*, som skal hete «EN 1993-1-13: Bjelker med åpninger i steget». Denne utvidelsen vil omhandle designprosedyrer for brudd- og bruksgrensetilstanden for stålbjelker med åpninger i steget og skal publiseres i 2026. Formålet med denne oppgaven er å presentere arbeidet som er gjort på dette temaet ved Norges teknisk-naturvitenskapelige universitet (NTNU). Dette inkluderer totalt fem forsøk på stålbjelker med forskjellige åpningsgeometrier. Bruddkapasitetene fra forsøkene er sammenlignet med designkapasitetene fra EN 1993-1-13, og differansene er diskutert i detalj.
Arbeidet viste at standarden gir for konservative resultater i noen tilfeller. Spesielt undervurderer den kapasiteten til de bjelkene som har åpninger der de gjenværende stegutstikkene ved åpningene er klassifisert til tverrsnittsklasse 4. For ytterligere å undersøke treffsikkerheten til EN 1993-1-13 ble det utført et parameterstudie. Finite element-modeller som ble kalibrert mot testdataene ga opphav til totalt 46 bjelker med forskjellige åpningsgeometrier. Resultatene forsterket det som allerede ble sett om konservatismen angående *Vierendeel*-sjekken i standarden.
Til slutt ble ytterligere tre undertemaer angående bjelker med åpninger i steget undersøkt.

FAGLÆRER: Professor Arne Aalberg.

VEILEDER(E): Professor Arne Aalberg.

UTFØRT VED: Institutt for konstruksjonsteknikk.

NTNU
Norges teknisk-naturvitenskapelige universitet

Fakultet for ingeniørvitenskap og teknologi

Institutt for konstruksjonsteknikk

MASTEROPPGAVE HØSTEN 2021

Nicolas André Caronte Grønland

Steel beams with unstiffened web openings

Stålbjelker med uavstivede åpninger i steget

Bakgrunn

Det kommer i løpet av et års tid en dimensjoneringsstandard for I-bjelker med store åpninger/hull i bjelkesteget, prEN 1993-1-13, «Beams with web openings». Standarden bygger på vitenskapelige undersøkelser, flere tidligere designmanualer for stålbjelker og kompositttbjelker (stål og betong), og diverse forarbeider i et EU-prosjekt.
Hull og åpninger i steget i I-bjelker er ofte nødvendige for installasjon av ledninger og rør i bjelkelag. Det er utført flere masteroppgaver ved Institutt for konstruksjonsteknikk med dette temaet de siste tre årene, med både laboratorieundersøkelser og datamaskinsimuleringer for bjelker med ulike hullstørrelser og plasseringer i bjelkesteget.

Oppgaven

Oppgaven nå er å sammenstille funnene og resultatene fra de tidligere arbeidene ved instituttet, komplettere og kvalitetssikre disse, og presentere det som en helhet. Siktemålet er å utarbeide et utkast til en vitenskapelig artikkel på området, hvor kandidaten er med som forfatter sammen med veiledere. Et egnet tidsskrift er Journal of Constructional Steel Research.

Kandidaten kan i samråd med faglærer velge å konsentrere seg om enkelte elementer i artikkelen.

Rapporten

Oppgaven skal skrives som en teknisk rapport og ha gode figurer, tabeller og foto. Rapporten skal inneholde tittelside, forord, oppgavetekst, sammendrag, innholdsfortegnelse, symbolliste (om nødvendig), utkastet til den endelige artikkelen, og nødvendige vedlegg.
Det innleveres gjennom Inspera.

Omslag kan med fordel ha en illustrasjon fra oppgaven på framsiden.

Faglærer ønsker en trykket versjon av oppgaven. Faglærer ønsker videre at det lages en pakke med filer fra arbeidet, med rapporten, forsøksresultater, bilder, bakgrunnslitteraturen, elementmodellene, etc. Dette for å lette oppstarten av studentoppgaver som evt. skal fortsette undersøkelser på området.

Masteroppgaven skal leveres innen 3. januar 2022

Arne Aalberg

Trondheim, 15. desember 2021, Arne Aalberg, Professor

Abstract

The European Committee for Standardization, CEN, have been working on an extension of *Eurocode 3: Design of steel structures – Part 1-1: General rules and rules for buildings*, to be called "EN 1993-1-13: Beams with web openings". This extension will provide design rules for steel beams with web openings, both for ultimate and serviceability limit state and is set to be published in 2026. The purpose of this master's thesis is to present the work that has been done on the topic of steel beams with web openings at Norwegian University of Science and Technology (NTNU).

This includes in total five tests on steel beams with various web opening geometries. The ultimate capacities have been compared against the design capacities obtained from EN 1993-1-13. This master's thesis then summarizes the results in a draft for a paper that is expected to be published through Journal of Constructional Steel Research. The discrepancies that are found between the design rules and the ultimate capacities are discussed in detail.

The work showed that the standard gives overly conservative results in some cases. In particular, it underestimates the capacities of beams that have web openings where the remaining web outstands at the openings are classified as cross-sectional Class 4. One of the tests achieved an ultimate capacity that was 300 % larger than the design capacity. This critical design method regards the capacity for *Vierendeel* bending where calculations with elastic capacities are forced, when in reality, plastic capacities are more likely to be developed.

To further investigate the performance of EN 1993-1-13 a parameter study was conducted. Finite element models which were calibrated against the test data gave rise to a total of 46 beams with different opening geometries. These openings were rectangular, circular or double circular and the results reinforced what was already seen about the conservatism regarding the *Vierendeel* check.

Lastly, three additional subtopics were investigated. This includes beams subjected to global axial forces, the effect of corner radius in rectangular openings and beams with loads applied at or close to an opening. The first two are not covered by EN 1993-1-13 while the last is only covered briefly. The study proposes an interaction formula for global axial forces and moment in relation to the *Vierendeel* check in the standard. In addition, a substantial increase in capacity is seen for rectangular openings when the corner radius is increased. Therefore, formulae that include this beneficiary effect is also proposed.

Preface

This master's thesis is the concluding work of a five year Civil and Environmental engineering programme at Norwegian University of Science and Technology (NTNU). It was written for the Department of Structural Engineering. The work has given greater understanding for steel as a construction material and steel beams as constructional elements. In addition, it has broadened the understanding of finite element modeling thought the use of Abaqus 2019.

I would like to extend my gratitude and thanks to my supervisor Prof. Arne Aalberg at the Department of Structural Engineering, for excellent guidance and insight. In addition, I would like to thank Christian Frugone at the Department of Structural Engineering for helping with preparing and performing tests in the laboratory.

Table of contents

List of figures

List of tables

Introduction

Background

Steel beams are widely used as constructional elements. In different occasions and for different reasons it can be practical to have single or multiple openings in the web, as shown in Fig. 1. Ventilation ducts, fire pipes or other technical equipment may be required, due to economical or architectural reasons, to pass though the web of the beam. However, this affects both the capacity and stiffness of the beam thus raising additional design considerations. A simple and much used solution is to avoid the cumbersome design process by stiffening the web around the openings with welded on plates. Still, this is not preferable and can be less cost efficient, especially if the beam in fact is strong enough without the stiffeners.

Figure 1: Example of unstiffened rectangular and circular openings in the web of a steel beam [1].

The topic has been covered by a variety of literature and different design methods have been developed. Methods that are easy to use but not too conservative are sought out. The European Committee for Standardization, CEN, have been working on preparing such methods in the form of an extension for *Eurocode 3: Design of steel structures – Part 1-1: General rules and rules for buildings* [2] and *part 1-5: Plated structural elements* [3], from her on out referred to as EN 1993-1-1 and EN 1993-1-5. The European program started based on the need to prepare an Annex for Eurocode 4, allowing for design of composite beams with web openings. In this case, rules also for steel beams with web openings were needed as a prerequisite to the design of composite beams. This led to *EN 1993-1-13: Beams with large web openings* [4], from her on out referred to as EN 1993-1-13. EN 1993-1-13 is expected to be finalized and published in 2026.

Scope

The topic of beams with web openings a have been covered extensively by several projects at Norwegian University for Science and Technology (NTNU). This in the form of master's theses and doctorates as well as other smaller projects. The scope of this master's thesis is to prepare a draft for a paper which is expected to be published through Journal of Constructional Steel Research in the near future.

The accuracy of the design rules presented in EN 1993-1-13 have been studied and evaluated up against tests performed on beams with large web openings in the laboratory at NTNU. The paper presents in detail the results obtained from these tests and discusses the discrepancies seen between the design capacity of EN 1993-1-13 and ultimate capacities reached in the tests. In addition, further examinations are done through a parameter study with FE-models. The research is extended to several new opening geometries as well as other subtopics that arise when designing steel beams with openings in the web.

Background for paper draft

In the years 2019 to 2021 there has been three master's theses on the topic of steel beams with web openings at NTNU. Marthinussen and Sandnes produced *Bjelker med rektangulære åpninger i steget* [5] in 2019. The same year Hovda and Hurum produced *Beams with circular web openings* [6]. Lastly, in 2021 Bjerch and Aksnes produced *Bjelker med åpninger i steget* [7]. Together they performed tests on five different opening geometries in the laboratory and then evaluated the results against the design methods of EN 1993-1-13. Ultimate capacities among other things were compared.

The background documents of EN 1993-1-13 reveal that the standard is built on a limited amount of laboratory testing. Luleå University of Technology performed tests on eight different rectangular opening geometries, four of these which were steel beams and four which were composite beams. In addition, RWTH AACHEN University performed five tests on composite beams with cellular openings. Even though the research was extended by parametric studies of FE-models for both cases, in total few laboratory tests have been performed. NTNU's contribution of five new tests is therefore relevant as validation of the design rules presented by the standard.

The papers main focus then becomes to present the results of these five tests and the accompanying analyzes performed by the three master's theses. It is expected that the readers have some knowledge on the topic of beams with web openings. Especially the accompanying additional failure modes that occur and terms that are used in relation to the topic. These are also extensively discussed in several of the references [4],[5], [6], [7] and [8]. Its focus lies on explaining why certain discrepancies occur between the tests and EN 1993-1-13, especially with respect to the failure mode *Vierendeel* bending.

In addition, it presents analyzes of beams with web openings that are subject to axial forces. EN 1993-1-13 limits its design rules to beams with axial forces not exceeding $N_{o,pl,Rd}/50$. $N_{o,pl,Rd}$ is here the axial resistance of the steel section at the largest opening. This means that axial forces are strictly limited by the standard. As interest on this had already been noted, especially in relation to offshore constructions, it was chosen to research it briefly. The analyzes are based on FE-models and the interaction between axial forces and moment is studied for varying opening geometries.

Another topic that is not included in the formulae of EN 1993-1-13 is the beneficial effect of an increased corner radius in rectangular openings. This is first included when the corner radius is large enough so that the opening can be considered elongated circular. Analyzes were performed on an opening with varying corner radius to quantify this increase in capacity. Formulae that include this beneficiary effect is then proposed in the paper.

The last part of the paper includes analyzes on beams that are loaded either at or close to an opening. The design methods of EN 1993-1-13 state that the local bending resistances of the Tees should be checked if the load is larger than 15 % of the shear capacity at the opening. At the same time as the length of the opening is longer than six times the depth of the Tees. The ultimate shear capacity of a beam is thought to be reduced considerably even for shorter openings due to the local effects that occur. A parameter study was therefore performed by analyzing two different load cases for beams with four different opening lengths. This included an evenly distributed load over the entire beam or a corresponding point load at the middle of the beam. A worsening of the local effects was expected for longer openings.

As a point load case could increase the shear capacities but reduce the moment capacities compared to the distributed load case, the net difference was not so straightforwardly obtained. To deal with this, the study was extended by a third load case. A point load at the middle of the beam in addition to evenly distributed loads only at the opening, on the top and bottom flange with opposite directions. This did not change the global statics compared to the point load case at the same time as it included the local bending effects of the Tees. This allowed for a more direct comparison of the ultimate capacities for each load case and is discussed in the last part of the paper.

Paper draft

IPE beam tests with unstiffened web openings evaluated against ULS design methods of EN 1993-1-13

N.A.C. Grønland[1], A. Aalberg[1a], N.C. Hagen[2]

[1]Norwegian University of Science and Technology (NTNU), N-7491, Trondheim, Norway

[2]**Stal-consult, N-4676 Kristiansand, Norway**

[a] corresponding author

Email: arne.aalberg@ntnu.no

Abstract

Key words: Steel beams, web openings, ultimate capacity, FE-modelling, *Vierendeel*

1. Introduction

2. Experiments

2.1 Beams and test setup

This section presents the general test setup of the five beams that were tested, while details for each specimen are presented in the next section. Two 12-meter-long beams, one IPE 200 and one IPE 220 were cut in four equal parts of 3 meters. To obtain a sufficiently high web slenderness, so that the tests would result in failure at the openings, the flanges were cut off and two and two pieces were welded together as illustrated in Fig. 2. This resulted in two 3-meter-long beams made from the initial IPE 200 and two 3-meter-long beams made from the initial IPE 220, in total four test beams.

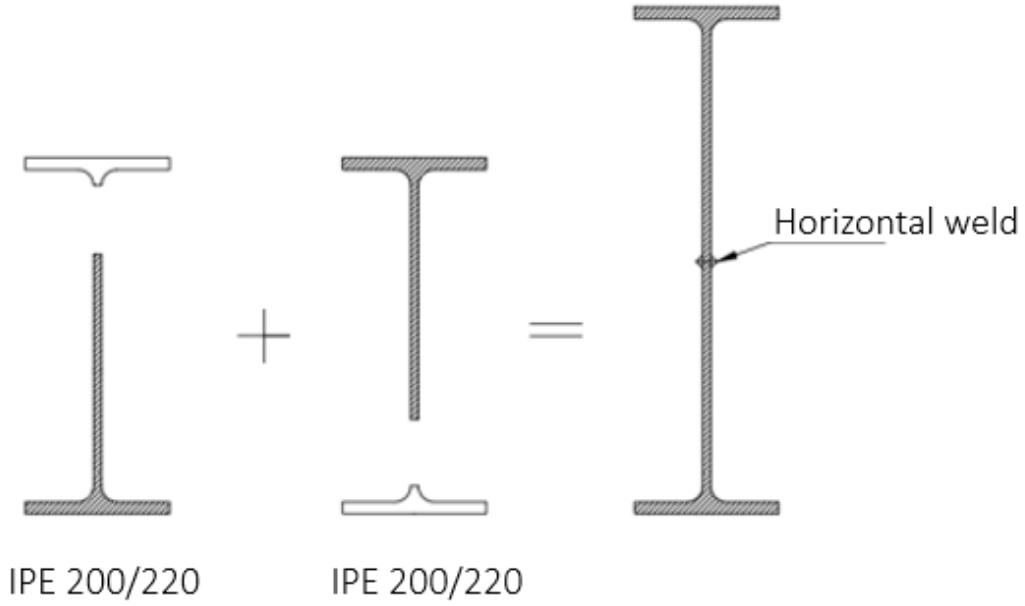

Figure 2: Illustration of how two smaller beams were cut and welded together to obtain four test beams [7].

The material strengths of the test beams were determined by tensile coupon testing of eight samples on two of the beams, in total sixteen samples. Fig. 3 illustrates the location of the samples for each beam. The main objective was to find the yield strength of the resulting test beams as it is this strength that is used for the design methods of EN 1993-1-13. Table 1 presents the corresponding yield strengths that were found for each sample. It is expected that the yield strength varies in the cross-sections due to the manufacturing process of the beams and with the chosen sample locations the diversity was thought to be covered sufficiently.

An important note to make is that the samples only were taken in the horizontal direction. As one could expect slightly different strengths in the vertical direction this choice could affect the calculations, particularly the failure modes of web-post buckling and buckling next to widely spaced openings. Nevertheless, it was accepted to only use the horizontal strengths as the differences were expected to be small.

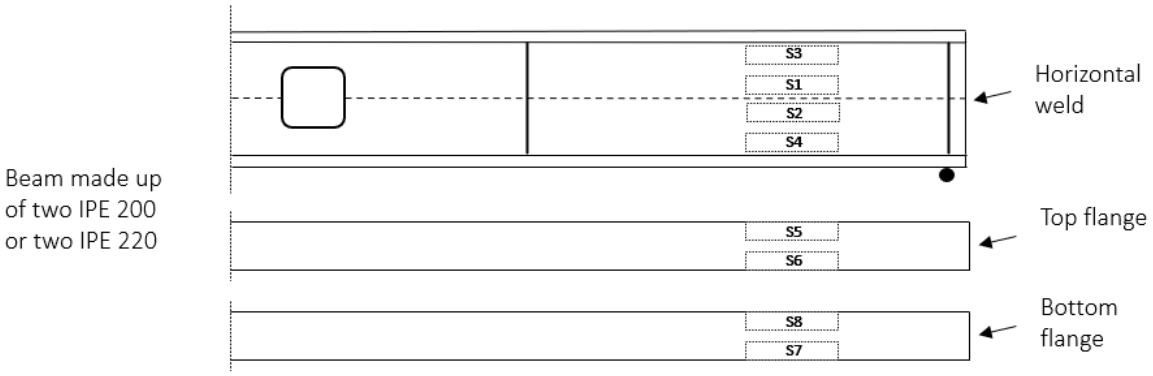

Figure 3: Location of samples for tensile coupon testing.

Table 1: Results from tensile coupon testing.

Sample location	**Beam made up of two IPE 200: f_y [MPa]**	**Beam made up of two IPE 220: f_y [MPa]**
S1- above weld	433	445
S2- below weld	443	451
S3- close to top flange	422	422
S4- close to bottom flange	410	426
S5- top flange left side	411	406
S6- top flange right side	390	395
S7- bottom flange left side	401	401
S8- bottom flange right side	403	405
Web average	**424**	**439**
S3 & S4 average	**417**	**424**
Flange average	**401**	**402**

Table 1 shows how the yield strength varies in the cross-section. The larger values were obtained from sample S1 and S2, about 40 mm from where the beams were welded together horizontally. As all the tests were secured so that failure would happen at the opening, these strengths were of lesser importance since they only were present in the cut-out part of the beams at that location.

Sample S3 and S4 were taken from the part of the web that was close to the flanges, about 20 mm from the root radius, and was the most important of the yield strengths. As the elastic neutral axis of the Tee-sections at the openings is located either close to or in the flange, the moment arm to the flange is short compared to that of the web. Thus, for elastic calculations of *Vierendeel* bending, it is this web strength that determines most of the capacity of the Tees. For plastic calculations yield stresses could be develop for the entire Tee-sections, but as the average yield strength of the flanges only were about 5% smaller than S3 and S4, the discrepancy was accepted.

As will be shown in Section 2.3, four out of five tests failed due to *Vierendeel* bending, while the last due to buckling of the web-post, all five of which are depended on the web strength more than the flange strength. Based on this it was chosen to use the average yield strength of S3 and S4 when utilizing the design methods of EN 1993-1-13 and when constructing finite element models (FE-models). This resulted in f_y=417 MPa for the beams that were made up of two IPE 200 beams, and f_y=424 MPa for the beams that were made up of two IPE 220 beams.

Fig. 4 shows the general test setup. The beams were simply supported at the ends and subjected to a concentrated load P at midspan through a half-cylinder piece to center the force. To avoid problems regarding highly concentrated loads, vertical web stiffeners were placed under the load and at the supports, on both sides of the web. The beams were restrained from transverse displacements at several points to avoid LTB, varying from specimen to specimen. For all tests the load was applied using a jack with maximum capacity of 1000 kN and run at displacement control of 1 mm/minute. Table 2 shows the exact geometries and load situations for each test. As seen, in two tests the point load at midspan was distributed to two points at the mid-region by a spreader beam.

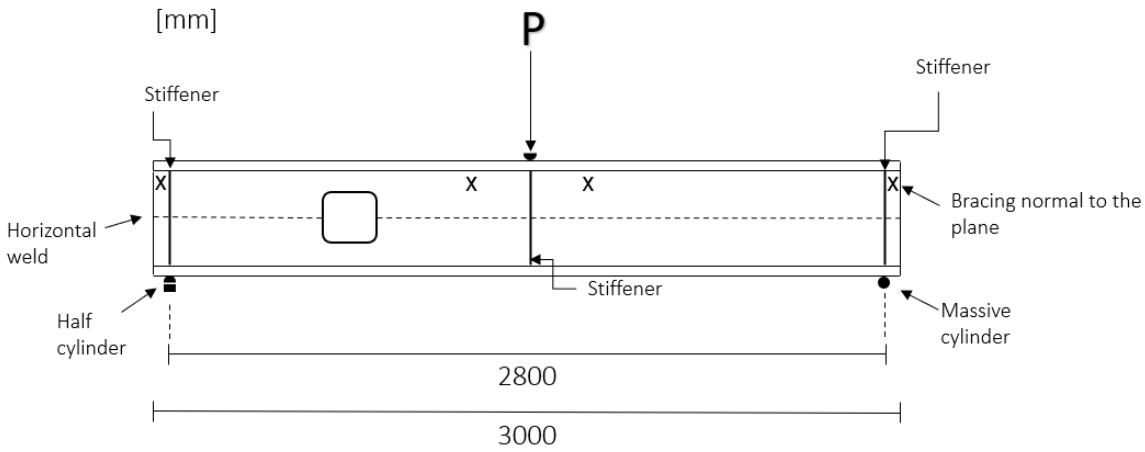

Figure 4: Illustration of general test setup.

Displacements of the beams were measured either through the jack itself or by the use of a linear voltage displacement transducer. Together this was used to obtain the load-displacement curves presented in Section 2.3. Digital Image Correlation (DIC) was used to monitor the relative displacements of a sprayed-on pattern. The displacements were then analyzed through eCorr, a computer program that plots the plastic strains, see Fig. 5.

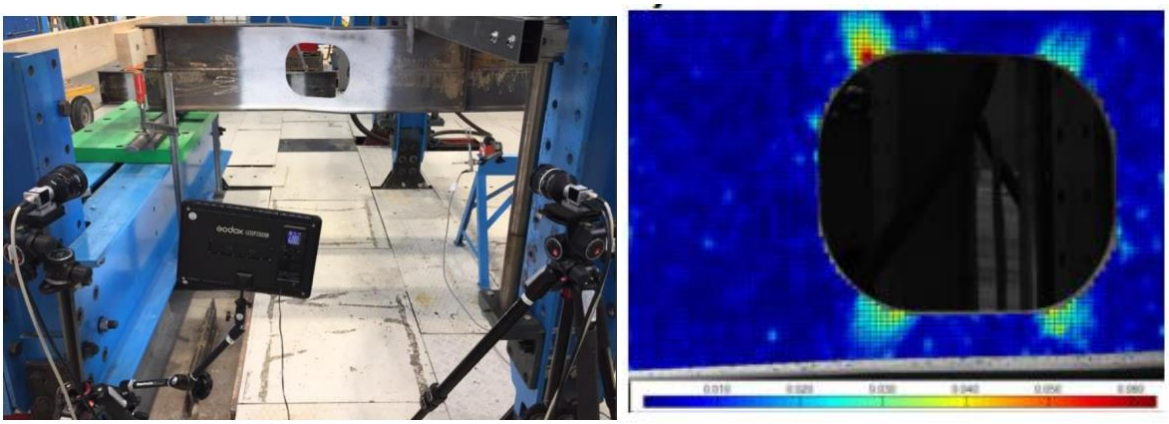

Figure 5: Digital image correlation setup (left) and example results from eCorr (right) [7].

2.2 Specimen details

The five individual test beams are denoted Specimen A, B, C, D and E, and are shown in Table 2. For each beam one web opening was made on one sides of the beam, approximately at L/4. Thus, the other side of the beam was left without openings and remained undamaged after the test. After testing Specimen A its opening was shut by welding a steel plate over it, and the beam was reused for testing Specimen B on the other side.

As seen from Table 2, Specimen A, B and C were from the original IPE 220 beams, having a final height of h=392 mm (A and B) or h=387 mm (C) for the welded test beams. Loading was a point load at midpoint. In these specimen a rectangular opening of different size was made in the web, with its center at 700 mm or 600 mm from the support point. Web opening dimensions were chosen to give a significant reduction in the beams resistance and to challenge the design methods of EN 1993-1-13. As seen, the opening heights were varied in the range 160 mm to 250 mm, and the longest opening was 380 mm, the latter specifically intended to investigate the *Vierendeel* mechanism. The cross-sectional class for the web outstands of Specimen B was Class 4, while Specimen A and C were classified to Class 3.

Specimens A and C were similar, with the only difference being the web opening corner radius increased from 16 mm in Specimen A to 100 mm in Specimen C. The motivation for this was that EN 1993-1-13 does not include the opening corner radius as a factor in its design methods for rectangular openings.

To provide test data also on beams with circular web openings, Specimen D and E were tested. The point load at midpoint was distributed to two points in the mid-region by a spreader beam. Specimen D had one opening of diameter 250 mm while Specimen E had two openings of diameter 200 mm spaced 50 mm between each other and was thus prone to web-post buckling.

Table 2: Specimen details.

Specimen	Web opening geometry [units in mm]	f_y/E used in EN-1993-1-13 calculations [MPa]
A [from IPE220]	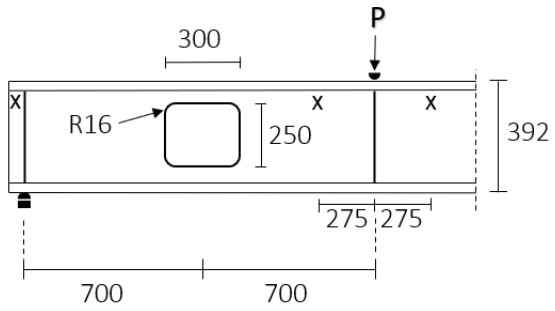	424/ 210000
B [from IPE220]	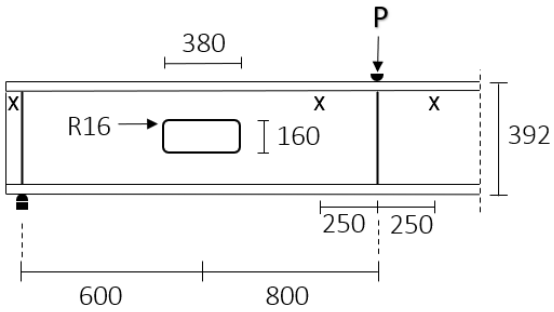	424/ 210000
C [from IPE220]	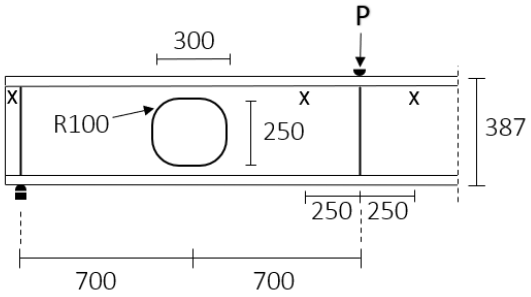	424/ 210000
D [from IPE200]	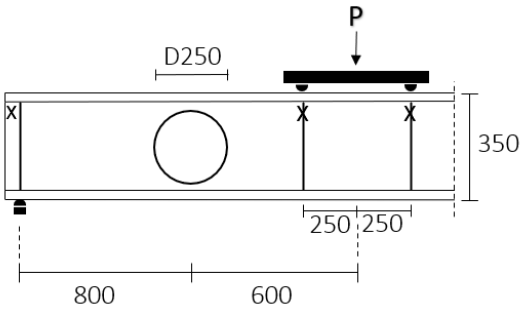	417/ 210000
E [from IPE200]	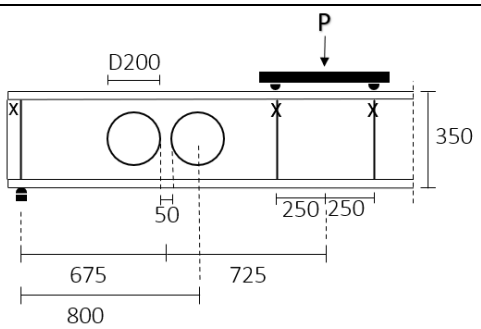	417/ 210000

Table 3 shows the cross-sectional dimensions for each specimen. The finished welded beams were joined with a weld seam at the mid-height but had surprisingly small deviations from perfect geometry. Prior to each test, after the beams were equipped with web stiffeners, the initial web imperfections were estimated with a ruler. Measurements focused on the web near the openings, (where the weld seam complicated the manual measurements), and the out-of-line deviations in the web (vertically, i.e. transverse) was in no case larger than 3 mm. These were the results of misalignment and welding. The measured deviations were later used to help calibrate each beam's FE-model.

Table 3: Cross-sectional dimensions for each specimen.

Specimen	**h [mm]**	**t_w [mm]**	**h_w/t**	**b [mm]**	**t_f [mm]**	**Amplitude of initial transverse web imperfections [mm]**
A	392 ± 1	6.0 ± 0.1	62.2	110 ± 0.7	9.4 ± 0.2	3
B	392 ± 1	6.0 ± 0.1	62.2	110 ± 0.7	9.4 ± 0.2	2
C	387 ± 0.8	6.0 ± 0.3	61.5	110 ±0.9	9.1 ± 0.2	2
D	350 ± 2	5.6 ± 0.2	59.5	100 ±1.3	8.5± 0.3	2
E	350 ± 1.5	5.6 ± 0.2	59.5	100 ± 1.3	8.5 ± 0.4	2

2.3 Test results

All the tests resulted in collapse of the beam by yielding or buckling at the opening.
The load-displacement curves for each test are presented in the following section. To account for the rig stiffness, each curve was adjusted so that the trendline of the elastic part goes through the origin. The methods used to measure the rig stiffnesses are not discussed in detail as its application only changes the corresponding displacement at maximum loading and not the ultimate capacity itself. Table 4 shows the ultimate capacities obtained for each specimen. These are compared to corresponding design capacities of EN 1993-1-13 in Section 3.

Table 4: Ultimate capacity obtained for each specimen and corresponding displacement at midpoint.

Specimen	Ultimate load [kN]	Displacement at midpoint of beam [mm]
A	228	17
B	321	13
C	300	13
D	267	13
E	265	14

2.3.1 Specimen A

Fig. 6 shows the load-displacement curve of Specimen A. The beam reached its ultimate capacity at a load of 228 kN. The bottom flange started twisting at approximately 140 kN and at 190 kN there were clearly visible deformations around the opening. The corners located closest to the middle of the beam were affected first with signs of compression of the bottom corner and tension of the top corner.

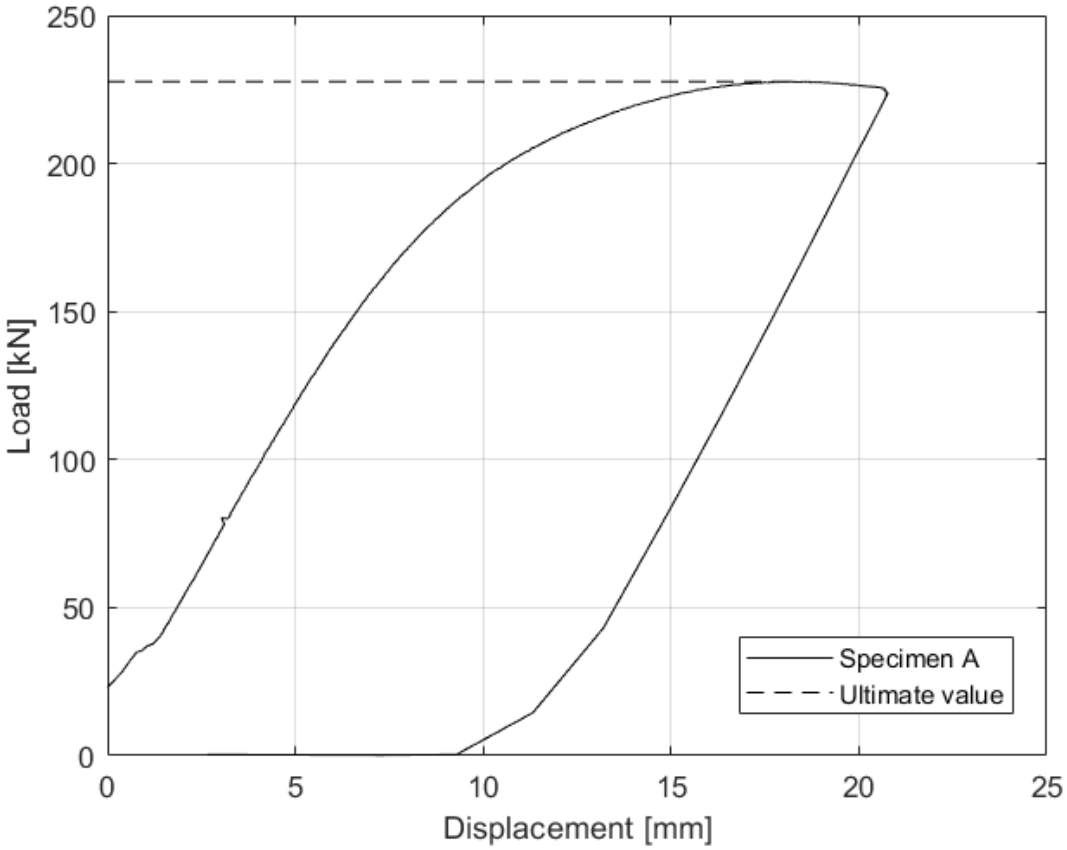

Figure 6: Load-displacement curve of Specimen A.

Interference from sun light caused problems in choosing a good reference picture for the DIC-analysis. It was chosen to use a picture from when the load was at 74 kN, which was before any major displacements or plastic behavior had taken place. Fig. 7 shows the resulting strain plot from the DIC-analysis, where blue indicates compression and red indicates tension. It can be difficult to accurately determine the cause of failure, but the resulting displacements and strains indicates failure due to *Vierendeel* bending.

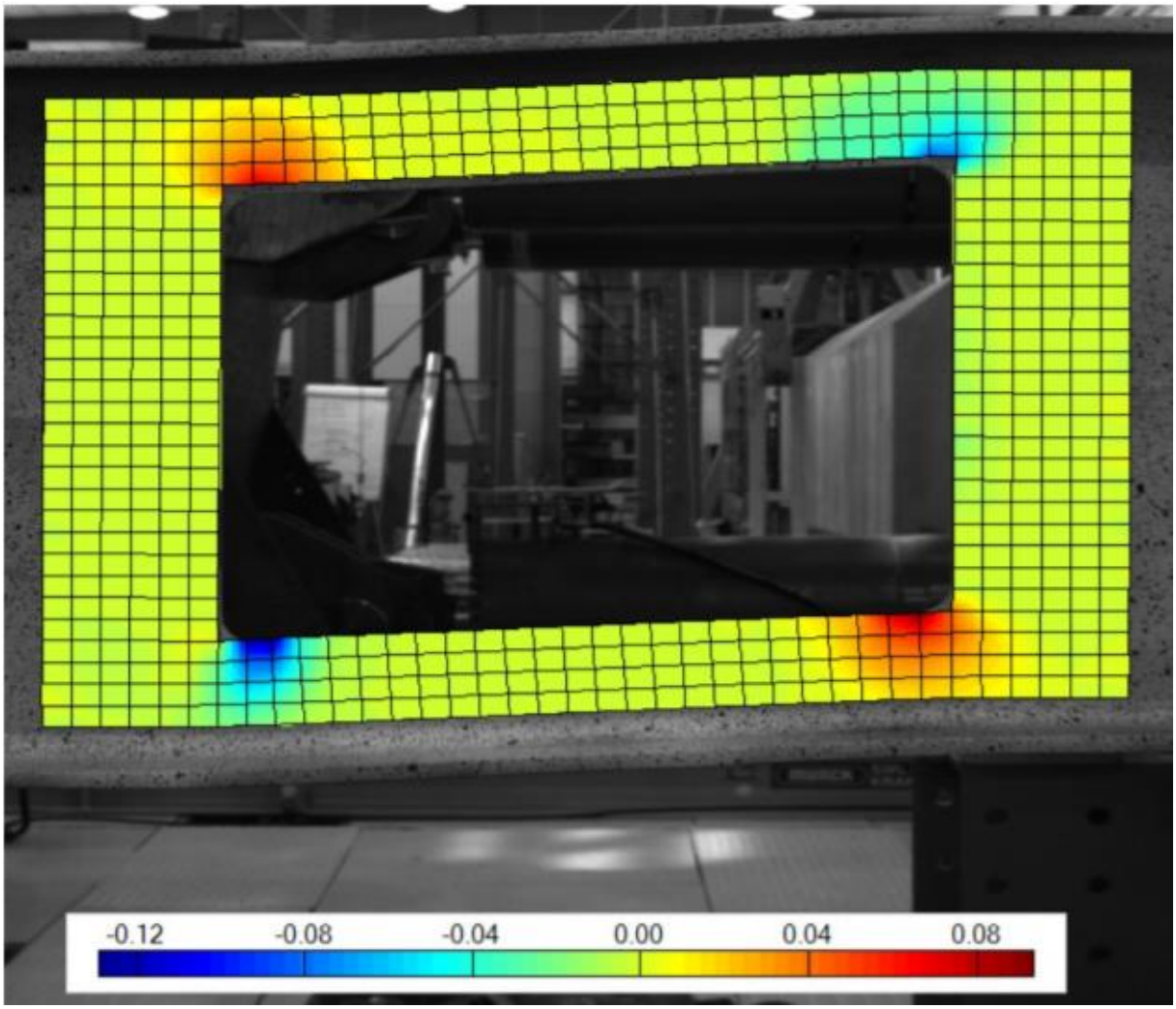

Figure 7: Plastic strain plot from DIC-analysis of Specimen A [5].

After the test, the beam was scanned with a 3D-scanner. This was done to find the transverse displacements at the corners of the opening. Fig. 8 shows the resulting deformations of Specimen A while Fig. 9 illustrates the displacements at each corner. Negative and positive values indicate inwards and outwards displacements respectively.

Figure 8: Post-test deformations of top left corner (left) and bottom right corner(right) of Specimen A [5].

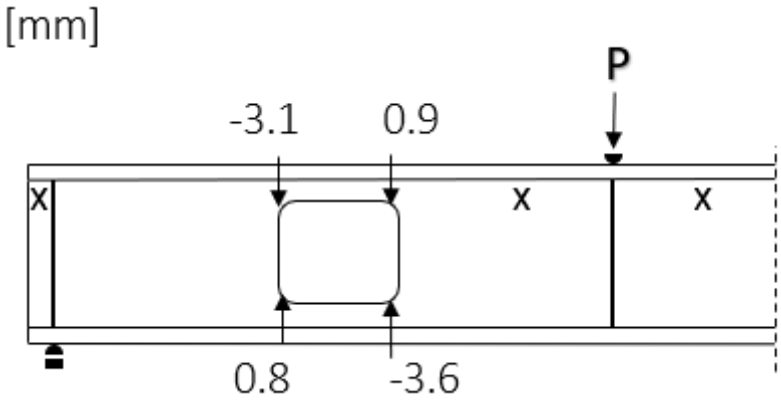

Figure 9: Post-test transverse displacement of each corner of Specimen A.

2.3.2 Specimen B

Fig. 10 shows the load-displacement curve of Specimen B. Ultimate capacity was reached at 321 kN.

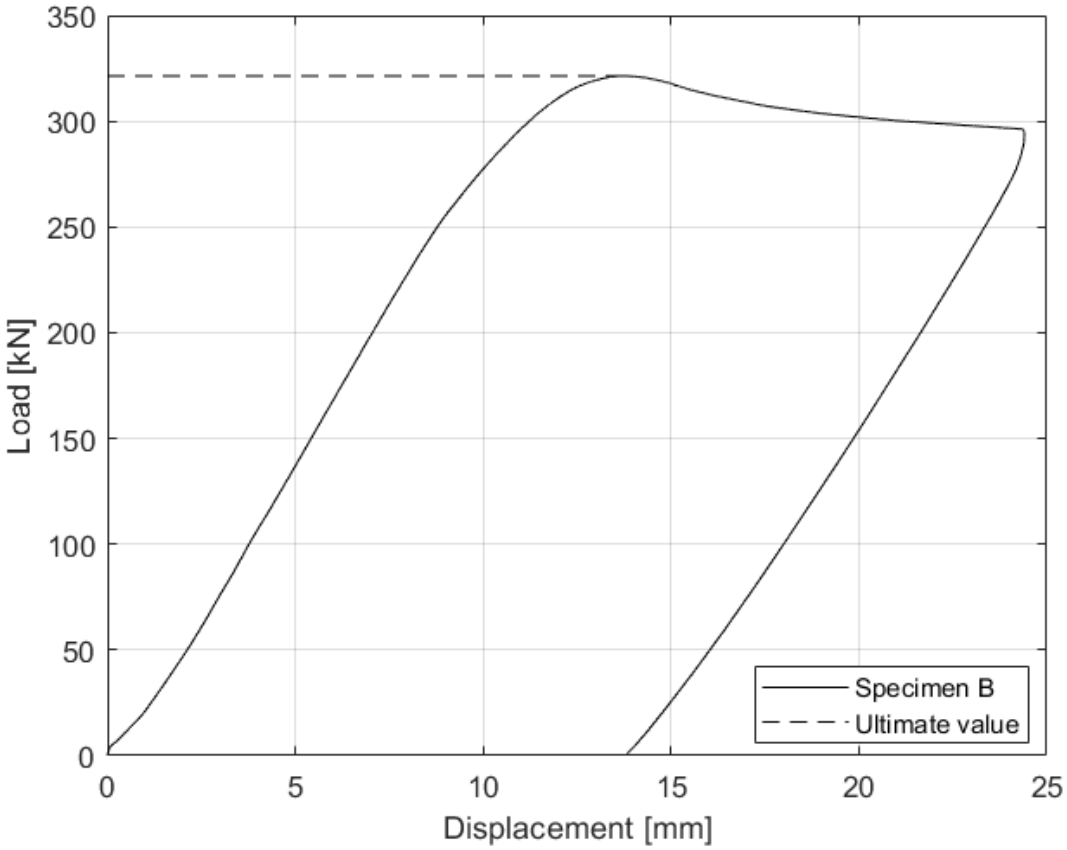

Figure 10: Load-displacement curve of Specimen B.

After the test was terminated, one could clearly see buckling of two opposite corners, again indicating failure due to *Vierendeel* bending. Fig. 11 shows transverse displacements and the accompanying strains resulting from the DIC-analysis. Red indicates larger values. The top left corner experienced the largest strains due to a combination of global bending and local T-moments, both resulting in compression at that corner. Fig. 12 shows post-test deformations at the opening obtained by 3D-scanning.

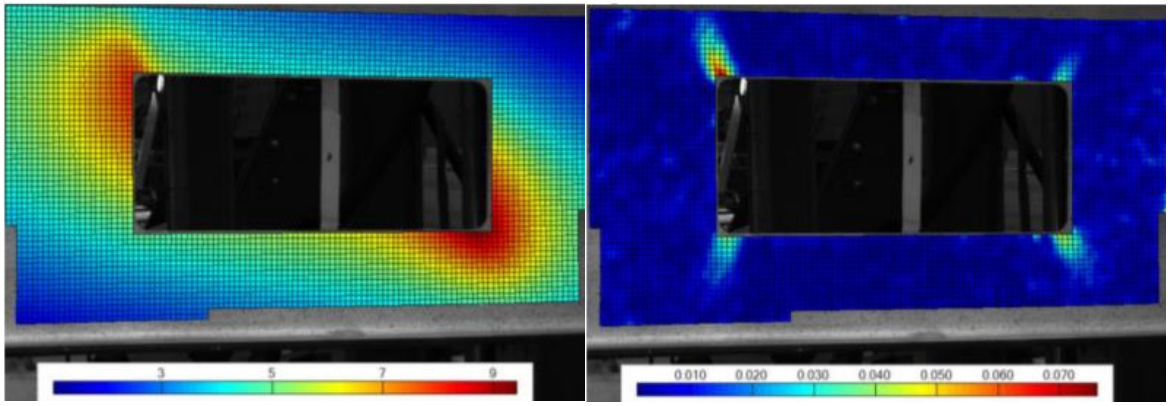

Figure 11: Post-test transverse displacements (left) and accompanying plastic strains (right) of Specimen B [7].

Figure 12: Post-test deformations of Specimen B [7].

2.3.3 Specimen C

Fig. 13 shows the load-displacement curve of Specimen B. Ultimate capacity was reached at 300 kN, 31.6 % larger than Specimen A which only differed by the corner radius. This indicates as expected that an increased corner radius also increases the ultimate capacity of the beam and is further analyzed and in Section 4.2.2.

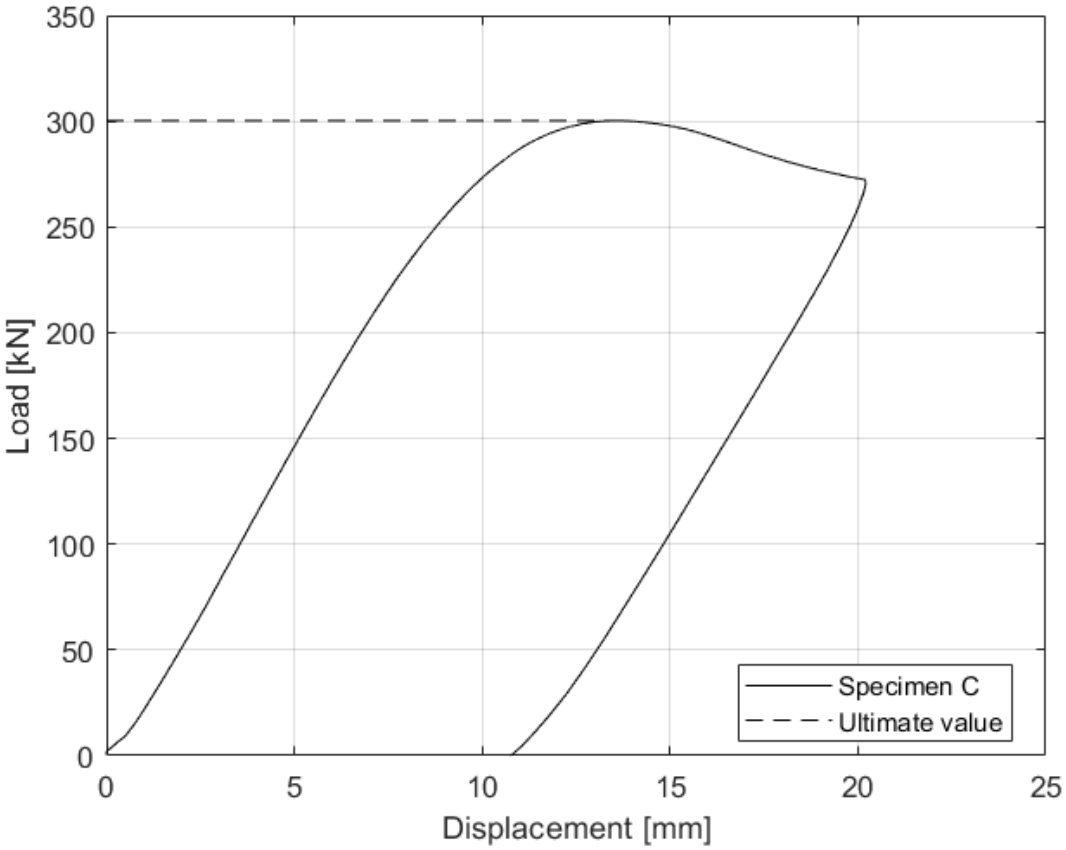

Figure 13: Load-displacement curve of Specimen C.

Fig. 14 shows transverse displacements and accompanying strains resulting from the DIC-analysis. Red indicates larger values. Insufficient layering of white paint resulted in abnormal displacements to the right of the top right corner. In reality, the beam was restrained from moving out of plane not far from that location to avoid LTB. Fig. 15 shows post-test deformations. Again, we see that the top left corner experienced the larger strains and that two opposite corners buckles, which is an indication of failure due to *Vierendeel* bending.

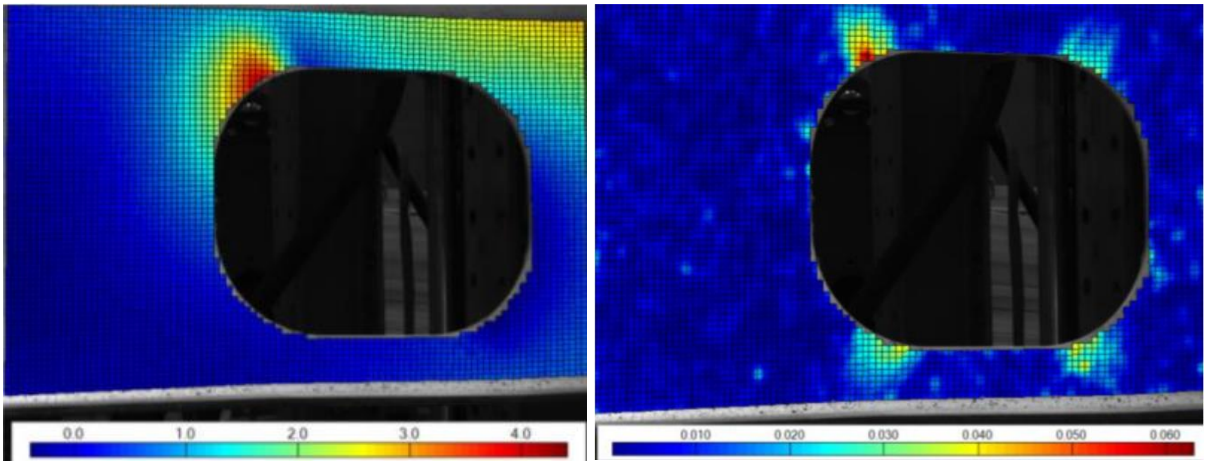

Figure 14: Post-test transverse displacements (left) and accompanying plastic strains (right) of Specimen C [7].

Figure 15: Post-test deformations of Specimen C [7].

2.3.4 Specimen D

Fig. 16 shows the load-displacement curve of Specimen D. Ultimate capacity was estimated at 267 kN. Due to failure of the hydraulics in the jack the results of this test were not logged correctly. In total, the beam was loaded and unloaded three times. This resulted in a load-displacement curve where the middle part is somewhat uncertain, seen as a dotted line. Here also, *Vierendeel* bending seemed to be the deciding failure mode, illustrated in Fig. 17 by buckling of two opposite corners.

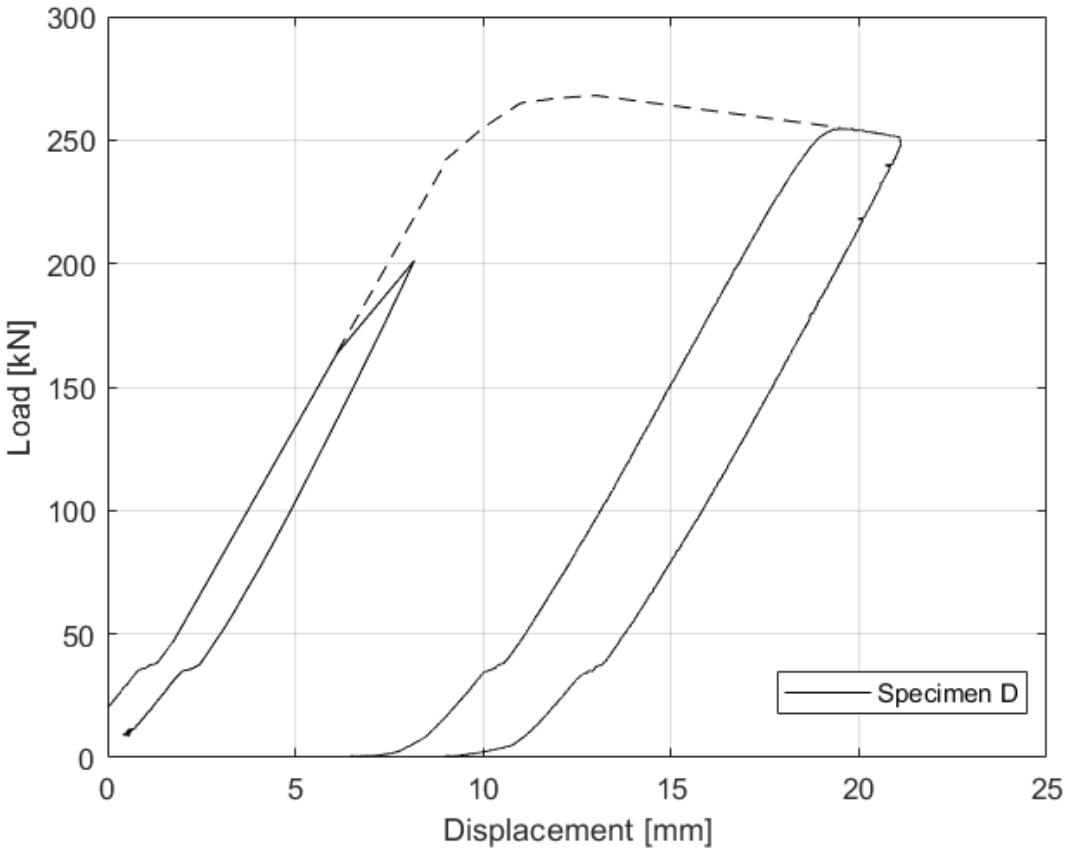

Figure 16: Load-displacement curve of Specimen D.

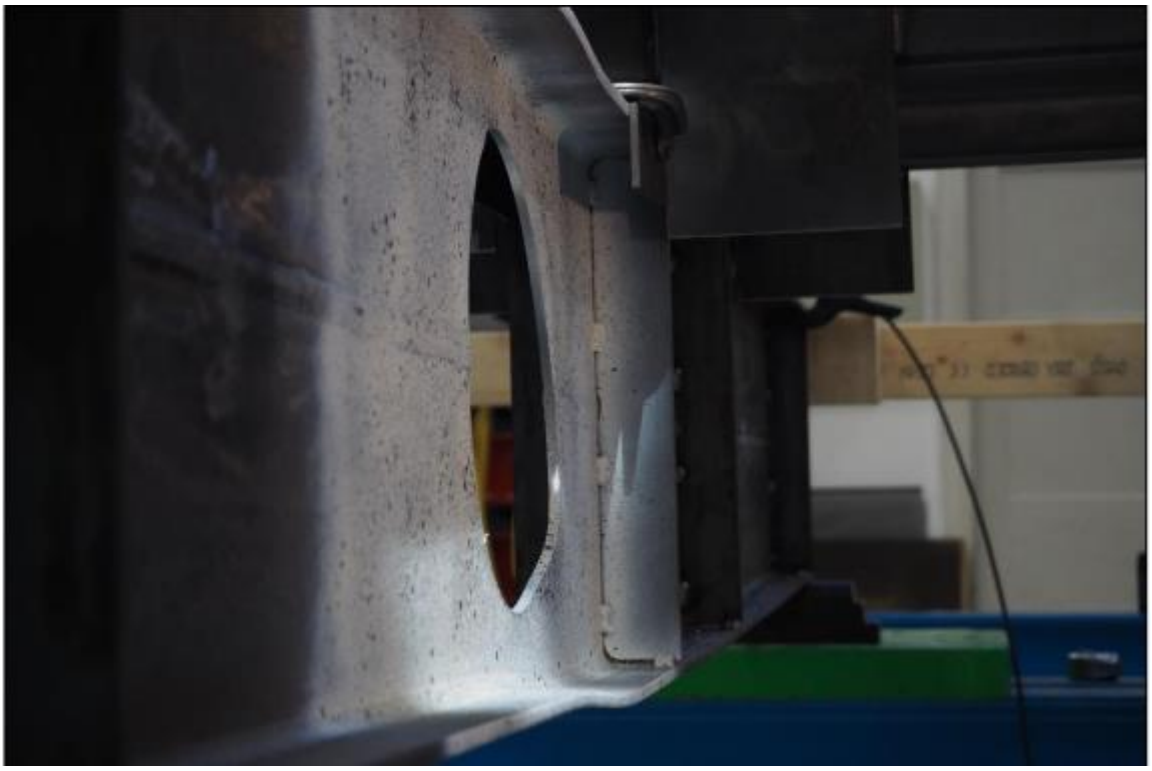

Figure 17: Post-test deformations of Specimen D [6].

2.3.5 Specimen E

Fig. 18 shows the load-displacement curve of Specimen E. Ultimate capacity was reached at 265 kN.

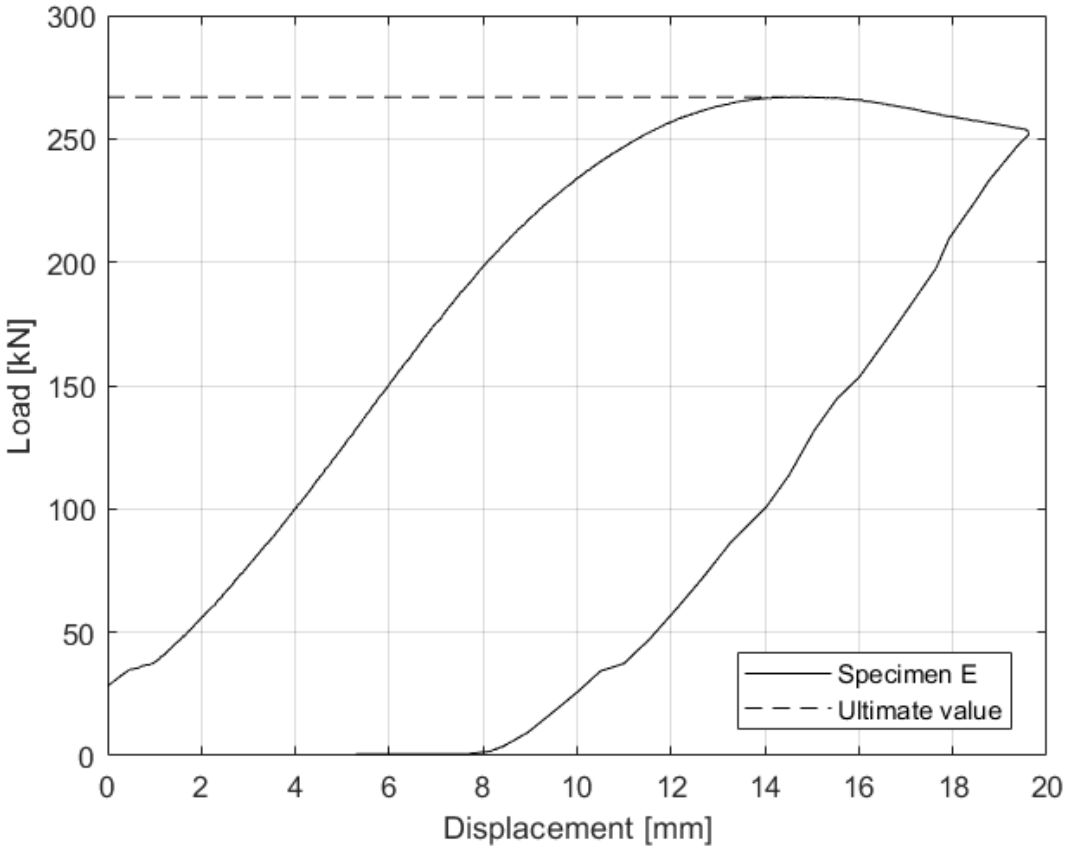

Figure 18: Load-displacement curve of Specimen E.

Failure of the beam seemed to be determined by buckling of the web-post between the openings, illustrated by the deformations in Fig. 20. After the web-post was weakened by plastic deformations, local buckling also occurred at the compressed parts of the openings. Fig. 19 shows plastic strains around the opening at ultimate load, where red indicates the larger values.

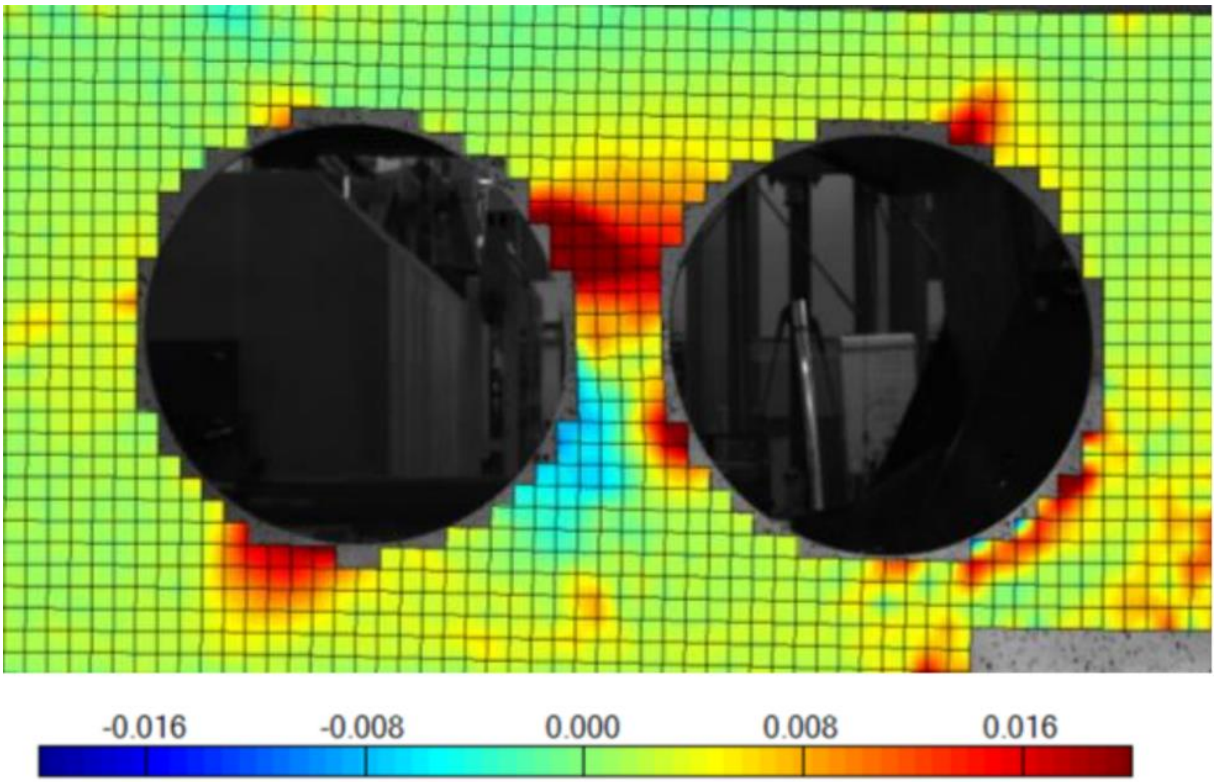

Figure 19: Plastic strain plot from DIC-analysis of Specimen E [6].

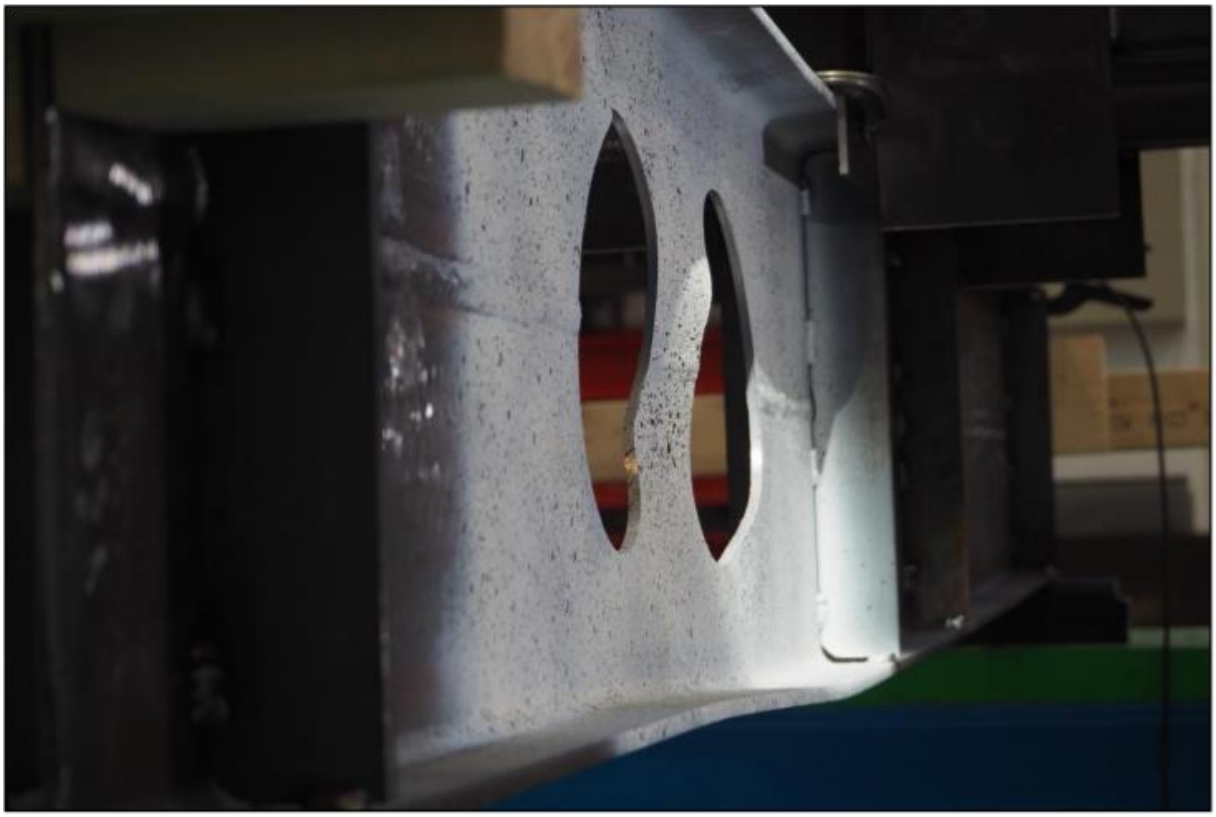

Figure 20: Post-test deformations of Specimen E [6].

3. Comparison of test results against EN 1993-1-13

To evaluate the performance of EN 1993-1-13 the design capacity of each specimen was calculated by the proposed design methods in the standard. The calculations are shown in Appendix A through E. Table 5 presents the obtained design capacities from the standard, P_{ult}, compared with the results from each test, P_{test}. The accompanying failure modes were also compared to the assessed failure mode of each test. Partial factors γ_{M0} and γ_{M1} were both set equal to 1.0 for the calculations and the material properties previously presented in Table 2 were used for each specimen.

Table 5: Design capacity of each specimen according to EN 1993-1-13.

	Calculations by EN 1993-1-13						
	$V_{Ed}/V_{o,pl,Rd}$	**$M_{o,Ed}/M_{o,Rd}$**	**$V_{Ed}/V_{Vier,\ Rd}$**	**$N_{w,Ed}/N_{w,Rd}$**	**P_{ult} [kN]**	**P_{test} [kN]**	**P_{test}/P_{ult}**
A	0.24	0.23	1.00	0.56	163	228	**1.42**
B	0.10	0.13	1.00	0.25	90.3	321	**3.55**
C	0.27	0.26	1.00	0.60	153	300	**1.96**
D	0.43	0.46	1.00	0.43	173	267	**1.54**
E	0.32	0.42	0.37	0.37 1.00(*)(**)	175	265	**1.51**

(*) As Specimen E was the only specimen with two adjacent openings the accompanying web-post failure modes are excluded from the table. EN 1993-1-13 limits Specimen E's capacity to the web post shear capacity: $V_{wp,Ed}/V_{wp,Rd}=1.00$.

(**) The web-post buckling utilization was $N_{wp,Ed}/N_{wp,Rd}=0.81$.

As seen from Table 5, the design methods of EN 1993-1-13 gave *Vierendeel* bending as the critical failure mode for the same four specimen that indicated *Vierendeel* bending in the tests. In addition to this it predicted failure of the web-post as critical for Specimen E, which was also observed in the laboratory. This indicates that EN 1993-1-13 can predict the correct failure modes well and is investigated further through the parameter study presented in Section 4.2.

The standard gave as expected conservative design capacities for all five specimens. Specimen A obtained a design capacity of 163 kN, while the test showed an ultimate capacity of 228 kN, 42% larger than what the standard allows for. The design check for *Vierendeel* bending allowed for plastic calculations and thus that the Tees were allowed to develop plastic stresses at both sides of the opening.

The most conservative results were seen for Specimen B. The design capacity was 90 kN while the test showed an ultimate capacity of 321 kN, 255 % larger than what the design methods of the standard allows for. Recall that the opening geometry of Specimen B was chosen exactly to investigate the conservatism of EN 1993-1-13 in relation to *Vierendeel* bending. As the web outstands of the Tees in compression were classified to cross-sectional Class 4, the standard restricts the capacity to elastic calculations of the bending resistance of the Tees. The depth of the outstands are to be taken as the limit of a Class 3 outstand and the resulting *Vierendeel* bending capacity then becomes the combination of elastic moment capacities of both Tees.

In reality, as the Tees are regarded as fixed at both ends, it is likely that the web outstand on one side will be in compression but that it will be in tension on the other side. Fig. 21 shows an illustration of this which is later verified in Section 4.2.1 by analyzing the stress distribution in the corresponding FE-model. Because of this, it is reasonable to assume that the classification of Class 4 only applies to one side of the Tees. Thus, if the position of zero moment across the opening is allowed to move at the ultimate limit state, then the plastic bending resistance on one side of the Tees can be developed. Furthermore, because of this change in the zero moment position the compressed length of the outstand is also reduced when assessing the classification of the Tees. Therefore, the section class may be determined from the actual length of the outstand in compression, a_c, rather than a_{eff} as the standard proposes. Equation 1 defines a_c:

Equation 1:

$$a_c = a_o \frac{M_{el.T}}{M_{el.T} + M_{pl.T}}$$

Where a_o is the opening length, $M_{el.T}$ is the elastic bending resistance of the Tees and $M_{pl.T}$ is the plastic bending resistance of the Tees.

Based on this, the capacity at opening becomes the combination of the elastic and plastic moment capacities of the Tees, rather than only the elastic. As the plastic bending resistance in this case is about three times larger than the elastic bending resistance, the total *Vierendeel* bending capacity is increased by a factor of 2. If this was allowed, one could for this geometry increase the design load to about 200 kN. Thus, the test results of 321 kN would only be about 60 % larger instead of 255 % which is the case.

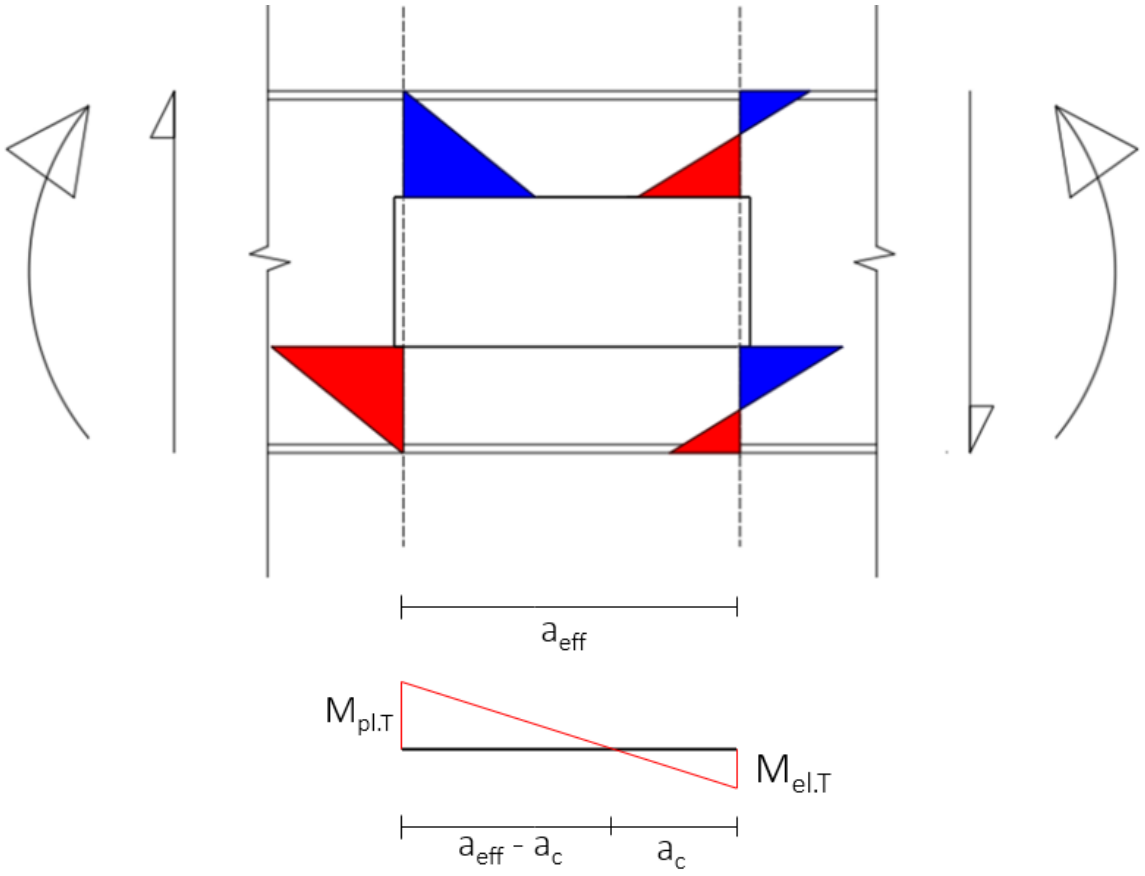

Figure 21: Illustration of stress-distribution in Tees (red is tension, blue is compression) and corresponding bending moments in bottom Tee if plastic bending resistance can be developed on one side.

For Specimen C the design capacity was 153 kN while the test showed an ultimate capacity of 300 kN, 96 % larger than what the standard predicted. For these calculations the plastic capacities of the Tees are used when assessing *Vierendeel* bending, but we still see a significant conservatism. As the opening height and length of Specimen C was equal to the one of Specimen A, it was expected that the design load achieved from the standard would be roughly equal. Table 5 shows that this was the case. At the same time the test result of Specimen C was significantly larger than that of Specimen A, about 30 %. This indicates how EN 1993-1-13 fails to account for an increased corner radius which is investigated further thought the parameter study presented in Section 4.2.

For Specimen D the design capacity was 173 kN while the test showed an ultimate capacity of 267 kN, about 54 % larger than what the standard predicted. Here again we see *Vierendeel* bending of the Tees as the limiting factor for the design. For these calculations the compressed web outstands of the Tees were classified to Class 1, and plastic capacities could be used with the full depth of the Tees.

Lastly, for Specimen E the calculated design capacity was 175 kN while the test showed an ultimate capacity of 265 kN, about 51 % larger than what the standard predicted. Failure of the web-post due to shear was the deciding failure mode according to EN 1993-1-13. This is expected for closely spaced openings as the web-post is narrow and the resulting shear area is small. In this case the width of the web-post was only 50 mm, resulting in a horizontal shear capacity of 67 kN.

4. FE-models and parameter study

4.1 Verification of FE-models

To further investigate the performance of EN 1993-1-13 numerical models of Specimen B, C, D and E were constructed in Abaqus 2019, a finite element modelling software. Sufficient accuracy of the models was achieved through calibration against each tests data. Factors such as material properties, mesh, element type and amplitude or shape of initial web imperfections were evaluated. The following section presents how each of the four specimen's models were verified. The load-displacement curve together with the observed deformations was compared to prove a sufficient accuracy of the FE-models.

4.1.1 Verification of Specimen B and C

Specimen B and C was modeled using Abaqus 2019 as a 3D deformable shell model. S4R shell elements were used for the entire model except for at the opening. Here S3R shell elements with varying size were used to handle the irregular geometry. The shell thickness varied between 9.1 mm, 6 mm and 15 mm in the flanges, web and stiffeners respectively. The corresponding plastic material properties presented in Section 2.1 was converted to true stresses/strains and used together with an elastic modulus of 210 GPa. The beam was modeled as a simply supported beam with the corresponding displacement restrains presented in Table 2. The load was applied as a downward pointing displacement in the middle of the flange width with non-linear geometry turned on. Imperfection shapes were introduced through buckling modes from linear buckling analyzes. The imperfection amplitude was chosen based on measurements in the laboratory. Different combinations of shapes and amplitudes were analyzed and chosen based on what gave the most accurate results. It was observed that choosing the correct amplitude was more important, while almost any shape would suffice. The load-displacement curves were obtained through one step and a maximal increment size of 0.5 mm.

Fig. 22 and 24, shows the load-displacement curves obtained from the FE-models together with the corresponding curves obtained in the tests of Specimen B and C respectively.

For Specimen B, the response of the numerical model was stiffer for the elastic part of the curve, but the ultimate capacities coincide well. The FE-model obtained an ultimate capacity of 321.2 kN while 321.4 kN was achieved in the test. The displacement at ultimate load was 12 mm for the numerical model and 13 mm for the test.

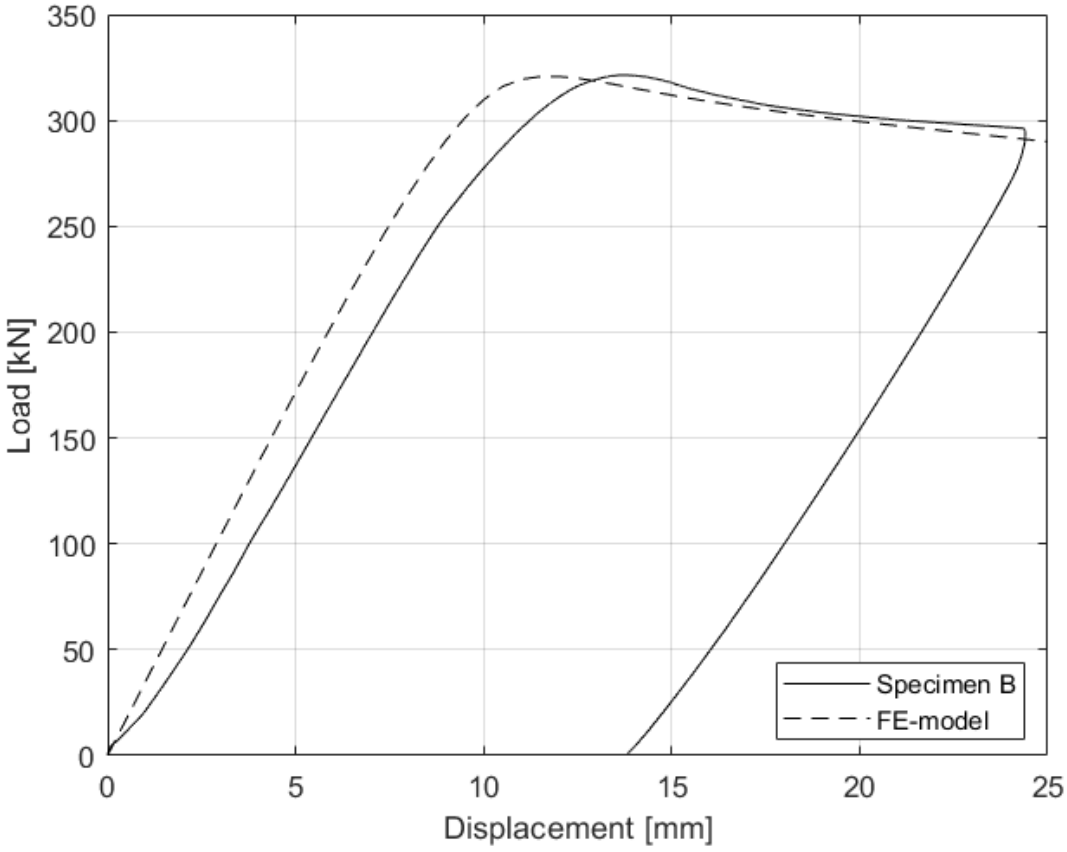

Figure 22: Load-displacement curve of Specimen B and the representative FE-model.

Fig. 23 shows a comparison of the transverse displacements of Specimen B. The left part of the figure is from the numerical model while the right part is from the laboratory test. The colors indicate a varying displacement in mm where red are the larger values. In addition, a 1:1 comparison of the deformations is shown. The results coincide well both when it comes to shape and size of displacements.

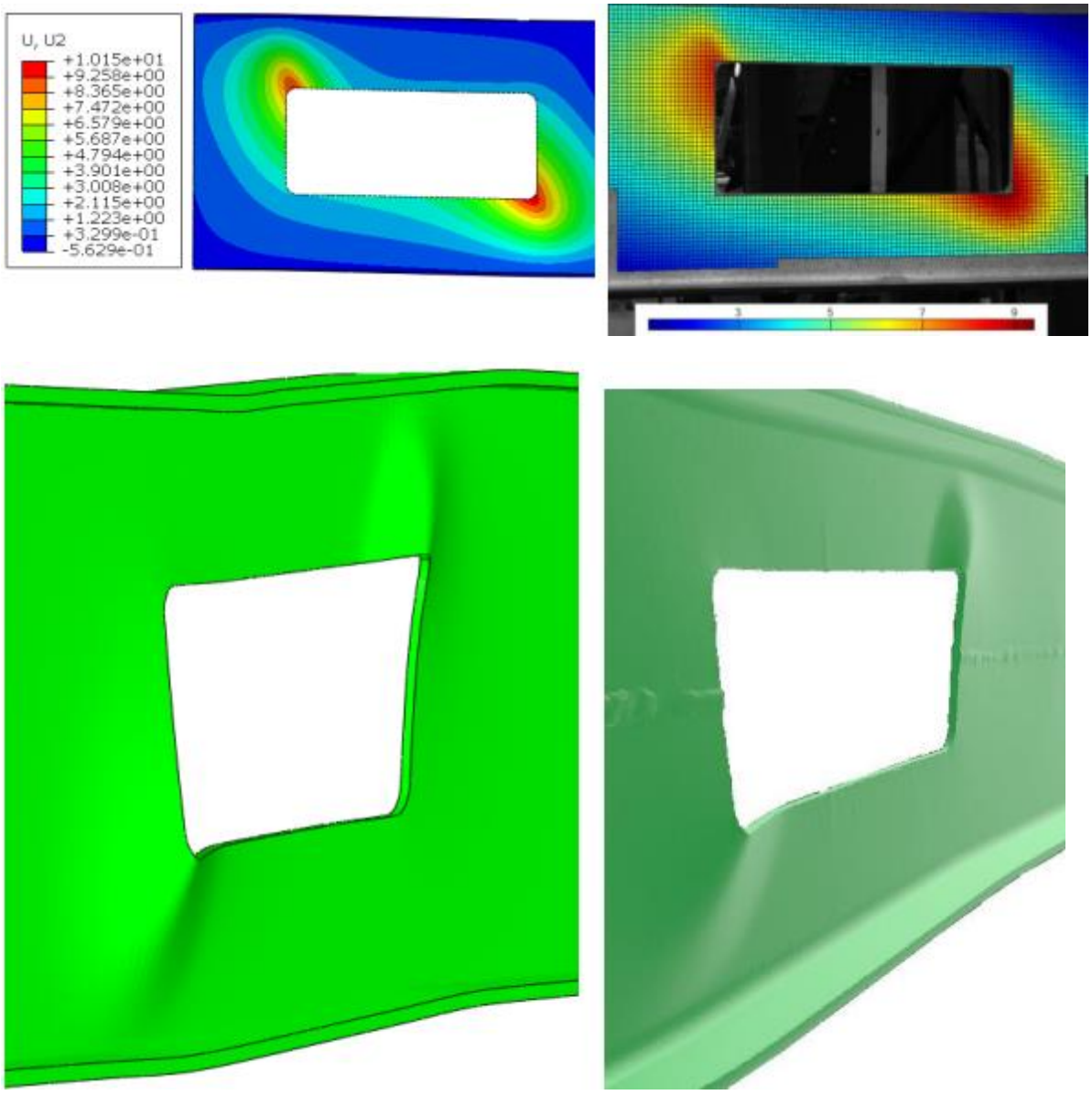

Figure 23: Comparison of transverse deformations between numerical model (left) and test (right) of Specimen B [7].

For Specimen C, both the stiffness and ultimate capacity coincide well. The ultimate capacity of the FE-model is 1.4 % smaller than that of the test and the displacement at ultimate load is 12 mm for the numerical model versus 13 mm for the test.

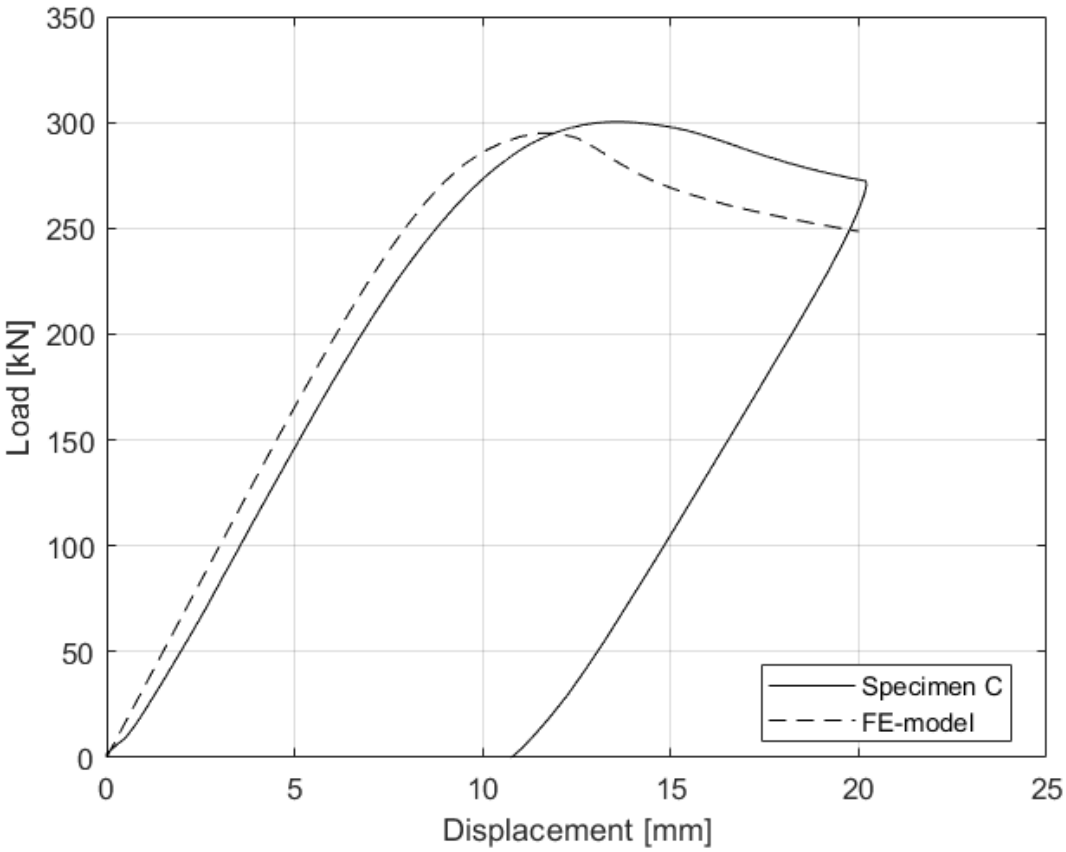

Figure 24: Load-displacement curve of Specimen C and the representative FE-model.

Fig. 25 shows a comparison of the transverse displacements of Specimen C. Again, the left part of the figure is from the numerical model and the right part is from the test. The colors indicate a varying displacement in mm where red are the larger values. In addition, a 1:1 comparison of the deformations is shown. The results coincide well both when it comes to shape and size of displacements.

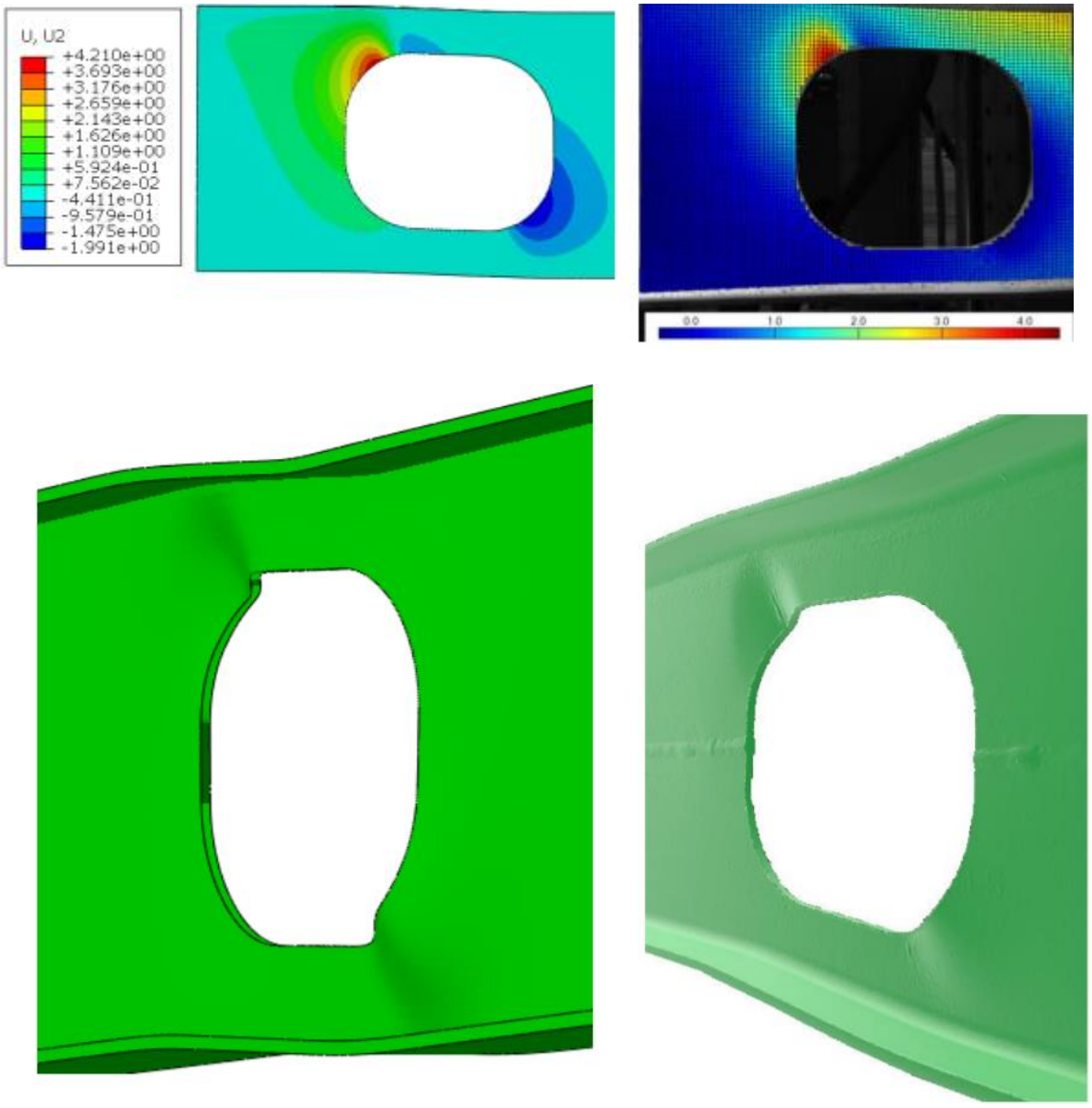

Figure 25: Comparison of transverse deformations between numerical model (left) and test (right) of Specimen C [7].

4.1.2 Verification of Specimen D and E

The process of constructing FE-models for Specimen D and E was similar to that of Specimen B and C. The models differed in element type and how the load was applied. Here, it was chosen to use C3D10 solid elements and analyzes were performed to determine the needed element sizes as well as imperfection shapes and amplitudes, similar to what was done for Specimen B and C. Since Specimen D and E were tested through four-point-bending the load application had to be modeled differently. This was done by modelling an infinitely stiff part made up of two cylinders with radius 50 mm connected with a plate, see Fig. 26. A quite refined mesh was chosen to achieve high accuracy in the contact forces.

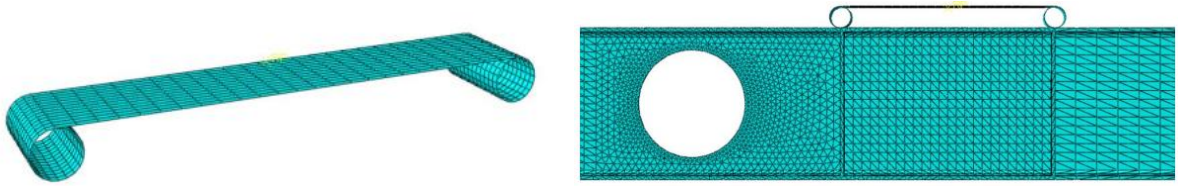

Figure 26: Illustration of how the load application was modelled for the FE-models of Specimen D and E [6].

Fig. 27 shows the load-displacement curve for Specimen D obtained from the FE-model together with the corresponding curve obtained from the test. A direct comparison between the two curves comes with a margin of error as problems with the jack occurred while testing Specimen D. The numerical model represents the stiffness of the beam well, but as the middle part of the test is less accurate, the ultimate capacities cannot be compared. Nevertheless, based on experience it is likely that the FE-model represent Specimen D sufficiently. Fig. 28 shows a 1:1 comparison of the deformations at the opening between the test (left) and the numerical model (right).

Fig. 29 and 30 shows the same comparisons for specimen E. The load-displacement curves coincide well, with discrepancies of 6 % and 1% for the stiffness and ultimate capacity respectively. The numerical model is stiffer and obtained a slightly larger ultimate load. Lastly, a 1:1 comparison of the deformations at the opening is also shown as for Specimen D.

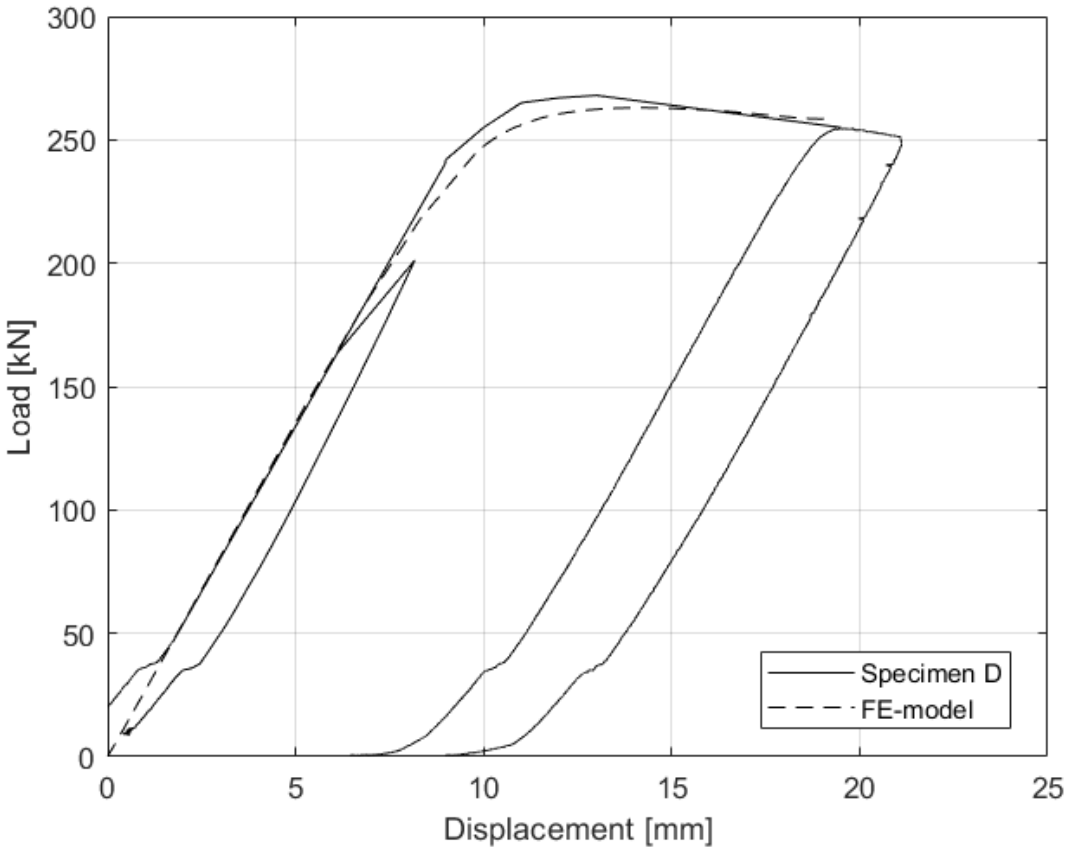

Figure 27: Load-displacement curve of Specimen D and the representative FE-model.

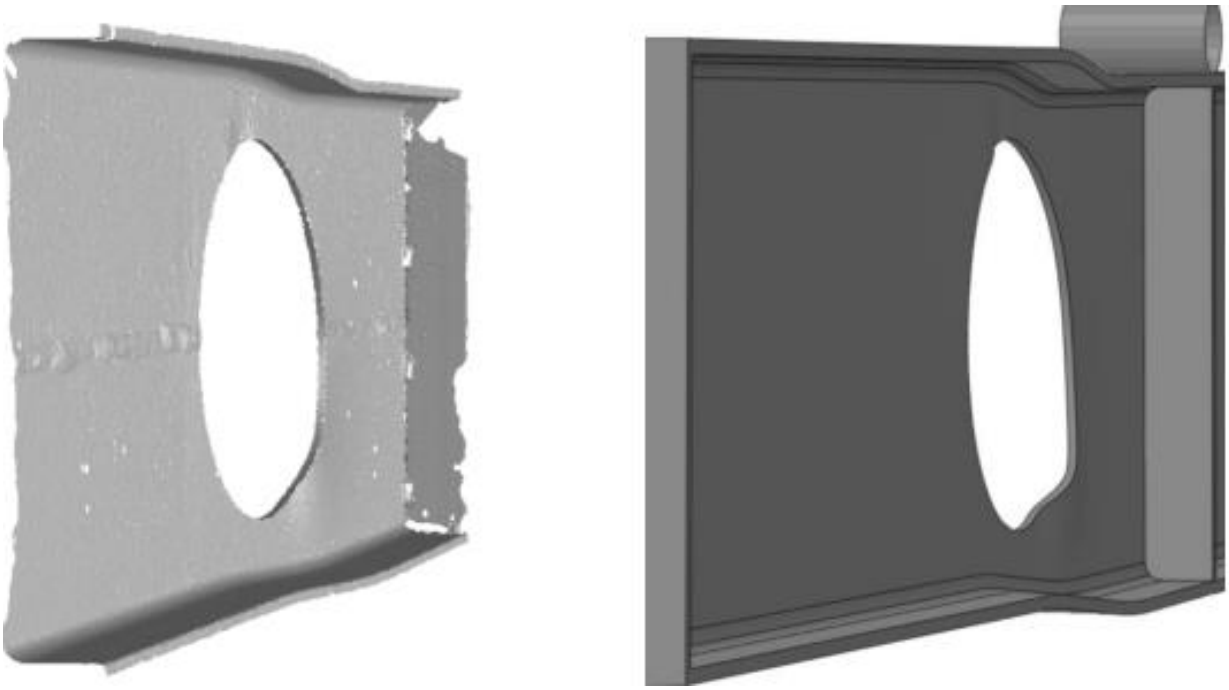

Figure 28: Comparison of transverse deformations between test (left) and numerical model (right) of Specimen D [6].

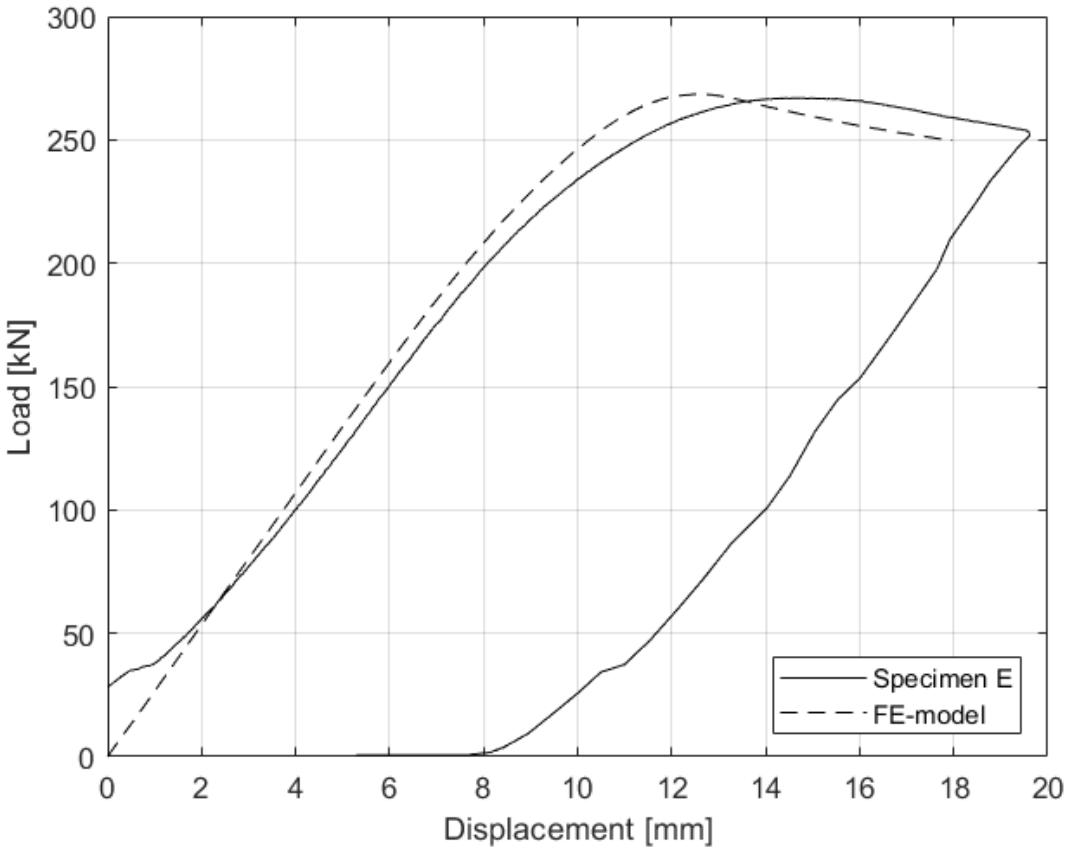

Figure 29: Load-displacement curve of Specimen E and the representative FE-model.

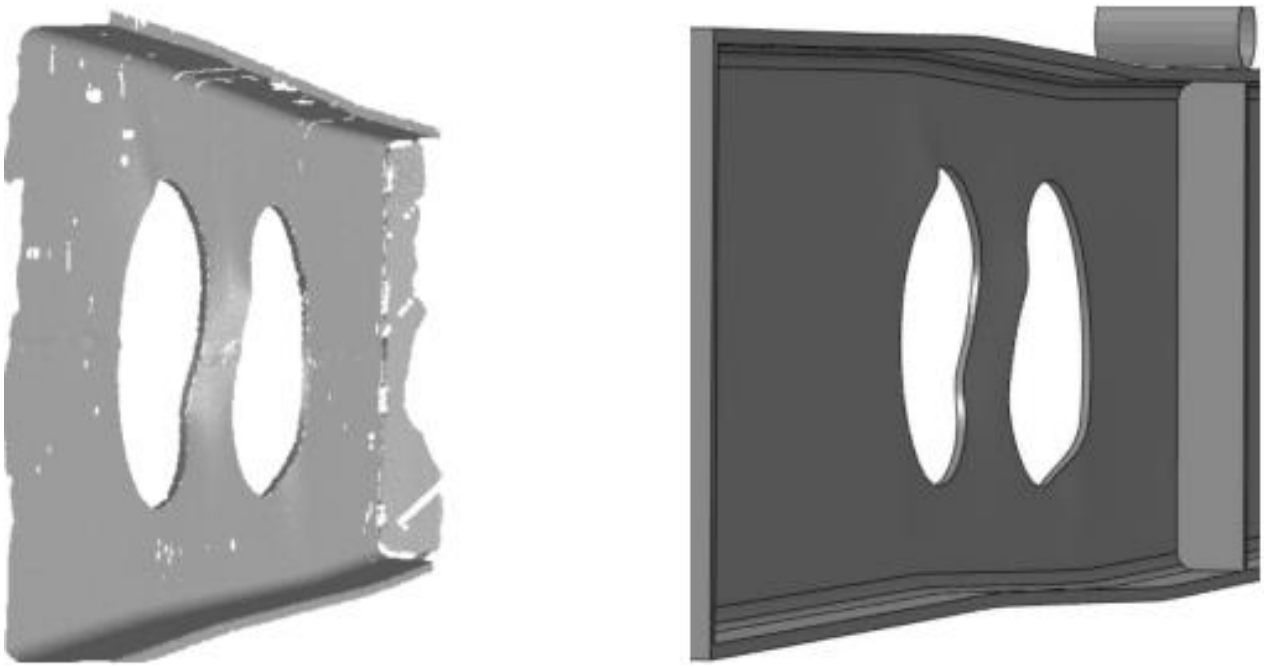

Figure 30: Comparison of transverse deformations between test (left) and numerical model (right) of Specimen E [6].

4.2 Extending the parameter range

As seen from Section 4.1 the FE-models represents the experimental data quite accurately and thus they were sufficient to be used as base models for studying several new opening geometries. The parameter study extended the base numerical models to 22 new rectangular openings, 12 combinations of single circular openings and 12 combinations of two closely spaced circular openings. Thus, a total of 46 different opening geometries were studied and compared against the ultimate design capacities from EN 1993-1-13.

Furthermore, the base numerical models were extended to study three additional subtopics. These were the effect of global axial loading, the effect of corner radius for rectangular openings, and loads applied at or close to an opening.

The effect of global axial loading was studied as EN 1993-1-13 limits it's design methods to axial forces not exceeding 2 % of the plastic capacity of the cross-section. The base model of Specimen C was extended with a varying opening height and axial forces ranging from 0-50 % of the plastic capacity.

As seen from Section 3, Specimen C achieved an ultimate load that was 30 % larger than that of Specimen A. Recall that these two specimens only differed in the corner radius. To study this discrepancy the numerical model of Specimen C was extended by varying the corner radius and the results were compared with the design capacity of the standard.

4.2.1 Rectangular openings

In Section 3 it was argued that the stress distribution at the opening of Specimen B most likely was such, that the web of two of the Tee-ends was subjected to tensile stresses and that this allowed for the development of plastic capacities. To verify this, the stress distribution of the numerical model of Specimen B was analyzed. Fig. 31 shows a plot of the stress distribution in section a-c and b-d, low moment side and high moment side of the opening respectively. The stress distribution is plotted for a varying load intensity P in increments of 20 % of the ultimate load P_{ult}=321 kN.

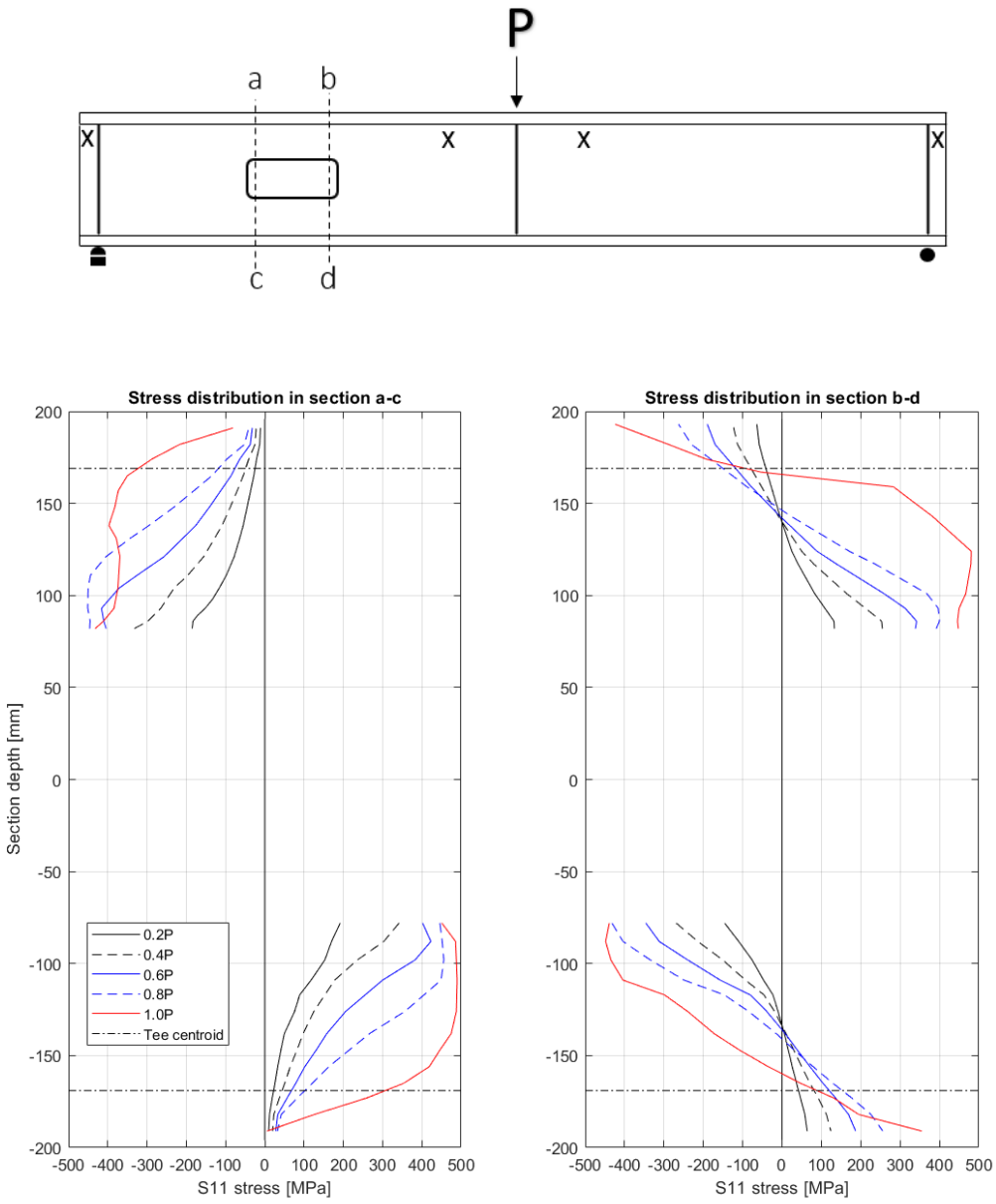

Figure 31: Plot of stress distribution at section a-c and b-d from FE-model of Specimen B, positive values indicate tension and negative values indicate compression.

It is clear from Fig. 31 that two of the Tee-ends indeed have web outstands that are subjected to tensile stresses. This is seen from the bottom left and top right corner of the figure. For all load intensities the bottom left corner of the opening experiences tensile stresses in its entire Tee-end. The local *Vierendeel* bending moment induces tensile stresses in the web and compression stresses in the flange. This combined with tensile stresses from the global bending moment results in tensile stresses for the entire Tee-end. As discussed in Section 3, EN 1993-1-13 on the other hand limits the capacity of this Tee-end as if the web was in compression, which it clearly is not.

The stresses in the Tee-end located at the top right corner of the opening (illustrated by the top right corner in Fig. 31) varies between tensile and compressive over the section of the Tee-end. This is due to the local *Vierendeel* bending in combination with compressive stresses from the global moment. Nevertheless, it is clear for all load intensities that a larger part of the web is subject to tensile stresses. Thus, the same argument holds as for the bottom left corner, and one could expect that also here plastic capacity of the section could be developed.

Combining this, it is possible to conclude on the suggested assumption of Section 3. It is indeed reasonable to assume that two of the Tee-ends could develop plastic capacities, and that the final *Vierendeel* capacity should be taken as a combination of the elastic and plastic capacities of the Tees. This is true for the opening geometry of specimen B, but a more thorough study should be done to see if this is true in general.

Table 6 shows the result of the parameter study for rectangular openings based on the FE-model of Specimen C. The calculated design capacities according to EN 1993-1-13 together with the ultimate capacities from the FE-models are listed and compared to each other. Three different web thicknesses of t_w=4 mm, t_w=6 mm and t_w=8 mm was analyzed for two opening heights h_o=160 mm and h_o=250 mm. The opening lengths a_o varied with the ratio a_o/h_o=0.6, 1.2 and 2.4, and the opening corner radius was set to r_o=16 mm.

Table 6: Results from parameter study of rectangular openings.

Opening geometry		**EN 1993-1-13 [kN]**	**FE-model [kN]**	**FE-model / EN1993-1-13**
t_w=4	h_o160a_o96	118.9	272.1	**2.29**
	h_o160a_o192	84.6	230.7	**2.73**
	h_o160a_o384	36.9	147.0	**3.98**
	h_o250a_o150	80.4	156.8	**1.95**
	h_o250a_o300	45.2	92.2	**2.04**
	h_o250a_o600	23.4	45.7	**1.95**
t_w=6	h_o160a_o96	290.2	317.3	**1.09**
	h_o160a_o192	197.5	317.1	**1.61**
	h_o160a_o384	96.5	252.9	**2.62**
	h_o250a_o150	223.8	258.3	**1.15**
	h_o250a_o300	129.1	151.1	**1.17**
	h_o250a_o600	68.3	75.9	**1.11**
t_w=8	h_o160a_o96	341.2	348.3	**1.02**
	h_o160a_o192	243.7	349.7	**1.43**
	h_o160a_o384	152.3	314.6	**2.07**
	h_o250a_o150	267.1	323.4	**1.21**
	h_o250a_o300	159.4	199.2	**1.25**
	h_o250a_o600	85.7	102.5	**1.20**

Failure modes: *Vierendeel*, Web buckling, Moment at midspan, *Vierendeel*/web buckling.

Each cell is colored based on the corresponding failure mode of the opening geometry. The failure modes for the FE-models were decided based on analyzes of the Von-Mises stresses as well as the transverse deformations at ultimate load. For some of the geometries it was hard to distinguish between *Vierendeel* or web buckling failure as the stress distribution reminded of

typical *Vierendeel* failure while the transverse displacement of typical web buckling. Thus, these got their own color (green).

It is clear from Table 6 that EN 1993-1-13 underestimates the capacity for several opening geometries. The differences are larger for beams with web thickness t_w=4 mm, which is reasonable considering that buckling of the web outstands usually is the deciding design criteria. Here the obtained ultimate capacities of the FE-models were on average 149 % larger than the allowed EN 1993-1-13 design capacities. For the beams with web thickness t_w=6 mm it was on average 46 % larger, and for the beams with a web thickness of t_w=8 mm it was 36% larger.

If the failure mode *Vierendeel*/web buckling (green cells) obtained from the FE-models is compared directly with *Vierendeel* (yellow cells) and web buckling (blue cells) of EN 1993-1-13, the standard predicted the correct failure mode in 14 of 18 cases. In the four cases where it was wrong, the numerical analyzes showed failure due to moment at mid span while the standard showed failure due to *Vierendeel* bending or buckling of the web close to the opening.

For the 12 cases where *Vierendeel* bending was the failure mode in both EN 1993-1-13 and the numerical analyzes the standard gives varying results. For 6 of the cases, a maximal difference of 25 % is observed. These are the opening geometries with h_o=250 mm and t_w=6 mm or t_w=8 mm, where plastic moment capacity of the Tees is allowed to be used.
For the remaining 6 cases the numerical results are on average 157 % larger than EN 1993-1-13. The largest discrepancy is found for geometry $t_w4h_o160a_o384$ where the capacity of the FE-model is almost 300 % larger than what EN 1993-1-13 allows for. Here the web outstands in compression are classified as Class 4 as for Specimen B, so we see the same conservatism as previously discussed. The standard only allows for elastic design of the Tees, but again, a combination of elastic and plastic capacities could give more accurate results.

Table 6 also shows that for the two cases where web buckling is the deciding failure mode according to EN 1993-1-13, the FE-models achieve an ultimate load that is about 100 % larger. This coincides with SCI Publication P355 [1], which states that the corresponding column model used to calculate the web buckling capacity next to widely spaced openings is conservative.

4.2.2 The effect of increased corner radius for rectangular openings

For rectangular openings, EN 1993-1-13 specifies a minimum corner radius of 10 mm. This is to avoid highly concentrated stresses locally. Besides this, the corner radius is not included in its design methods, and any beneficial effects of a larger radius is neglected. This means that the allowed design capacity would be the same for an opening with corner radius 10 mm or 100 mm.

Fig. 32 shows the opening geometry of Specimen C with a varying corner radius of 16, 50, 100 and 125 mm. The opening geometries of a), b) and c) should according to EN 1993-1-13 be treated equally as rectangular openings and thus the ultimate design load is equal at 153 kN. Opening d) is treated as elongated circular for which the corner radius is included in the formulae of the standard. The ultimate capacity of opening d) is thus increased to 306 kN, i.e., an increase of 100 % from geometry c) with r_o=100 mm and d) with r_o=125 mm.

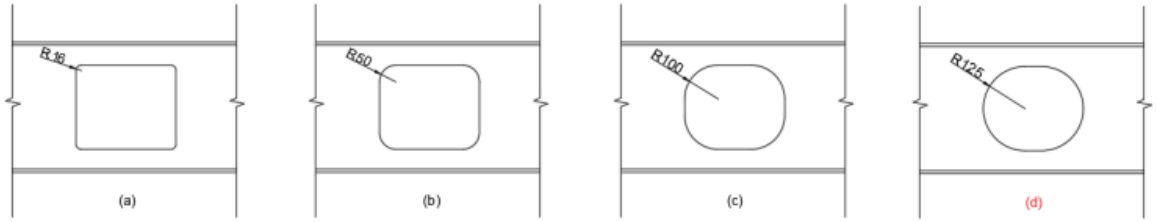

Figure 32: Opening geometry of Specimen C with corner radius varying between 16, 50, 100 and 125 mm [7].

Table 7 shows the design capacities of EN 1993-1-13 compared with the ultimate capacities obtained from numerical models of beams with the same opening geometries. It is clear that neglecting the corner radius is conservative, especially for a larger radius. For the opening with r_o=16 mm, the ultimate capacity of the numerical model is 19 % larger than the design capacity of EN 1993-1-13. For r_o=50 mm it is 38 % larger, while for r_o=100 mm it is 78 % larger. Lastly, for r_o=125 mm we see that the obtained capacities are similar.

Table 7: Ultimate capacities of opening geometries in Fig. 32 according to EN 1993-1-13 and numerical models.

Corner radius [mm]	EN 1993-1-13 [kN]	FE-models [kN]	FE-models/ EN 1993-1-13
r_o=16	153	182	**1.19**
r_o=50	153	211	**1.38**
r_o=100	153	273	**1.78**
r_o=125	306	310	**1.01**

Redwood [9] proposes that circular or elongated circular openings should be treated as equivalent rectangular openings based on the fact that yielding happens first at the corners of the opening. EN 1993-1-13 treats rectangular openings as if yielding where to happen first at the opening ends, but by analyzing the Von-Mises stresses of these openings it is clear that the larger stresses are located at the corners here as well. Based on this, it can be considered to treat rectangular openings the same way as circular or elongated openings are. This in the form of an equivalent height $h_{eq,}$ and length a_{eq}, according to the following formulas shown in Table 8.

Table 8: Proposed formulas of equivalent opening length and height for rectangular openings.

Shape of opening	Equivalent opening length, a_{eq}	Equivalent opening height, h_{eq}
Rectangular	a_o - $1.1r_o$	h_o - $0.2r_o$

The difference now, with the proposed formulas, is that the corner radius is included. The reduction of a_{eq} and h_{eq} is equivalent with what EN 1993-1-13 does for circular and elongated circular openings. Consequently, it should be considered reducing the effective length a_{eff}, used when performing checks of *Vierendeel* capacity, but in this case, it was chosen to leave it unchanged. Fig. 33 shows the equivalent opening geometries one gets when using the proposed formulas in Table 8.

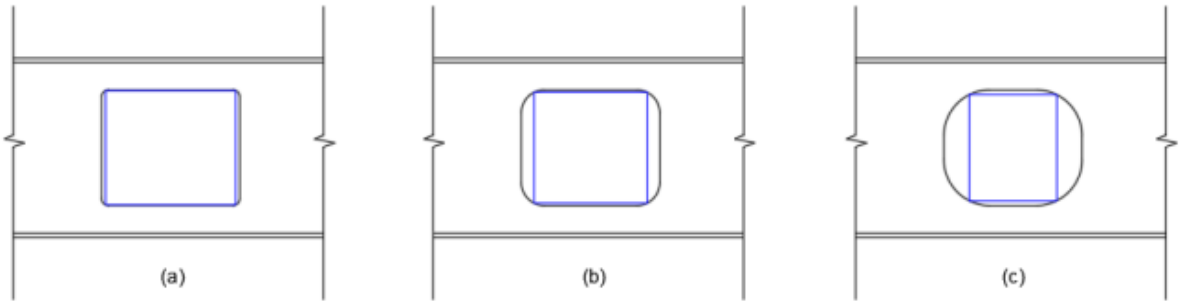

Figure 33: Illustration of rectangular openings (black) and equivalent openings (blue) when using the proposed formulas in Table 8 [7].

Table 9 is an extension of Table 7, now including the ultimate capacities of the equivalent rectangular openings. This column is named "Proposed" and the ultimate capacities from the numerical models are then compared to the proposed capacities in a separate column.

Table 9: Results from proposed formulas considering the corner radius.

Corner radius [mm]	EN 1993-1-13 [kN]	FE-models [kN]	Proposed [kN]	FE-models/ EN 1993-1-13	FE-models/ Proposed
r_o=16	153	182	170	**1.19**	**1.07**
r_o=50	153	211	205	**1.38**	**1.03**
r_o=100	153	273	270	**1.78**	**1.01**
r_o=125	306	310	306	**1.01**	**1.01**

For the opening geometries with corner radius r_o=16 mm and r_o=50 mm, the ultimate capacity of the FE-model is respectively 7 % and 3 % larger than the capacities with the proposed formulas. This means that the capacities have increased with 11 % and 34 % compared to what EN 1993-1-13 allows for. An increase of 76 % is seen for the opening geometry with r_o=100 mm.

The results of Table 9 indicate that the proposed formulas for treating a rectangular opening with an equivalent height and length is reasonable. Nevertheless, the analyzes are only performed one opening with a varying radius and further investigations should be done on a variety of geometries to conclude on whether such formulas are acceptable in general.

4.2.3 Single circular opening

Table 10 shows the results of the parameter study for single circular openings based on the FE-model of Specimen D. The calculated design capacities according to EN 1993-1-13 together with the ultimate capacities from the FE-models are listed and compared to each other. The base model was extended to four different opening heights h_o=140, 200, 250 and 273 mm each placed at three different positions as shown in Fig. 34. This was done to analyze different ratios of shear and moment.

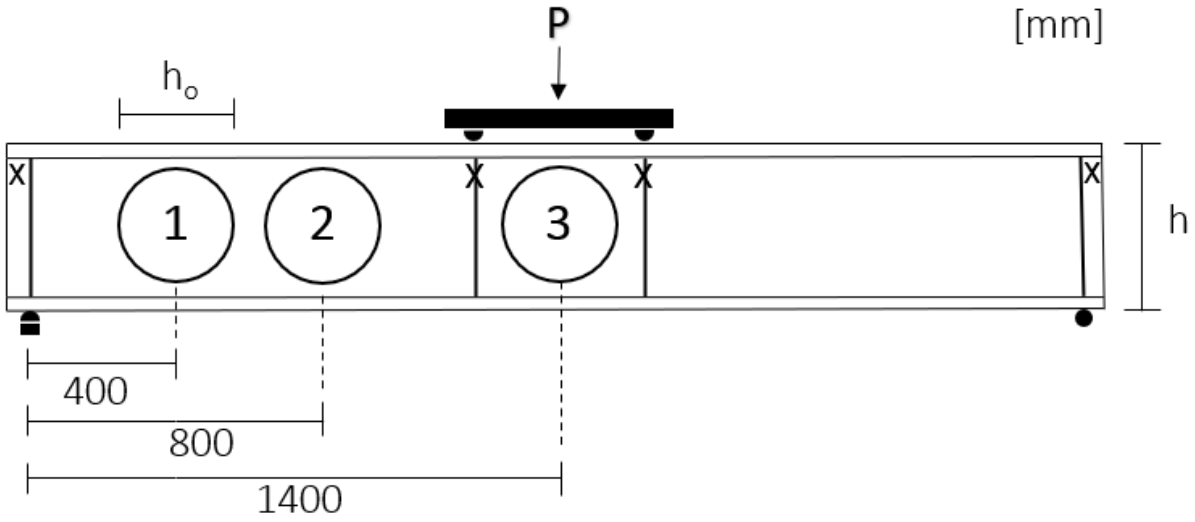

Figure 34: Illustration of opening positions for parameter study of single circular openings.

Position 1 is located close to the support resulting in a large shear force and relatively small moment. Position 2 has a large shear force and large moment, while position 3 has the largest moment but zero shear force.

As for the parameter study of rectangular openings, each cell in Table 10 is colored based on the corresponding failure mode from EN 1993-1-13 and numerical models. Together with the failure modes seen for rectangular openings, one additional is added. Failure due to moment of reduced cross-section at the opening (black). It is expected this failure mode will be critical when the opening is placed at position 3.

Table 10: Results from parameter study of single circular openings.

Opening geometry			EN 1993-1-13 [kN]	FE-model [kN]	FE / EN1993-1-13
h_o/h [%]	h_o [mm]	Pos.			
0.0	0.0	-	288.1	283.3	**0.98**
40.0	140	1	288.1	284.2	**0.99**
		2	269.4	283.2	**1.05**
		3	247.7	270.5	**1.09**
57.1	200	1	235.7	283.2	**1.20**
		2	179.4	274.4	**1.53**
		3	247.8	253.3	**1.02**
71.4	250	1	224.7	243.9	**1.09**
		2	194.4	212.8	**1.09**
		3	234.3	233.0	**0.99**
78.0	273	1	170.2	180.0	**1.06**
		2	151.2	166.4	**1.10**
		3	223.3	223.1	**1.00**

Failure modes: *Vierendeel*, Moment at opening, Moment at midspan, *Vierendeel*/web buckling.

It is clear from Table 10 that EN 1993-1-13 predicts the correct failure mode in 10 of 12 cases. In the 2 cases where it is wrong, the numerical analyzes showed failure due to moment at mid span while the standard predicted a *Vierendeel* failure mechanism. For circular openings, EN 1993-1-13 calculates the *Vierendeel* failure capacity based on equivalent rectangular openings. It is previously found that this way of calculating the capacity is conservative with up to 55 % [10].

On average the ultimate capacity of the FE-models are 10 % larger than the design capacity of EN 1993-1-13. The least conservative results are achieved for openings placed at position 3, where the average ultimate capacity is 3 % larger for the FE-models. Placing the opening at position 1 gives an average ultimate capacity that is 9 % larger, while position 2 an average that is 19 % larger.

When studying the performance of EN 1993-1-13 in relation to failure modes, it's clear that it is most conservative when *Vierendeel* bending is the critical failure mode. Here, the ultimate capacities obtained in the FE-models are on average 17 % larger. The standard predicts the ultimate capacity well when the failure mode is both moment at mid span and moment at opening.

Here again it is observed that the most conservative results are found for smaller openings. The Tees will have longer web outstands for smaller openings, and thus the local web is more prone to buckling and classified to a higher class. The restriction of elastic calculations for Class 4 is again what seems to give the most conservative results. This is true both when assessing the capacity with respect to bending moment at the opening but also for the *Vierendeel* capacity. The most prominent example is seen from h_o=200 mm at position 2, where the capacity from the FE-model is 53 % larger than that of EN 1993-1-13. Also, an interesting comparison can be done with the larger opening h_o=250 at the same position. EN 1993-1-13 gives more capacity for a larger opening, which of course is counter intuitive, and shown not to be accurate by the corresponding FE-models. All in all, it is clear that the conservatisms for circular openings are not as severe as they are for rectangular openings.

4.2.4 Two closely spaced circular openings

Table 11 shows the results from the parameter study of two closely spaced circular openings based on the FE-model of Specimen E. The calculated design capacities according to EN 1993-1-13 together with the ultimate capacities from the FE-models are listed and compared to each other. The base model was extended with the same four opening heights as for the parameter study of single circular openings, but this time with varying web-post width instead of a varying position. The web-post width s_o varied between 10, 40 and 70 % of the opening height, see Fig. 35. The smallest allowed web-post width according to EN 1993-1-13 is 10 %, while it is considered two widely spaced openings if it exceeds 100 %.

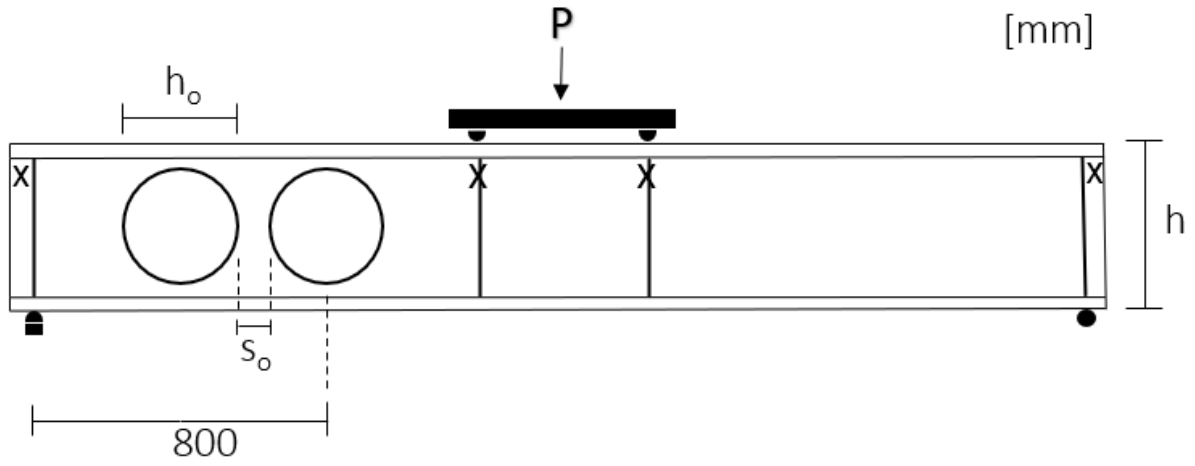

Figure 35: Illustration of a varying web-post width for the parameter study of two closely spaced circular openings.

For closely spaced openings, new failure modes regarding the web-posts between the openings are introduced. These are failure due to buckling of the web-post and failure due to horizontal shear forces in the web-post. As it is hard to distinguish between these two in the FE-models, they have the same color in Table 11 (grey).

Table 11: Results from parameter study of two closely spaced circular openings.

Opening geometry			EN 1993-1-13 [kN]	FE-model [kN]	FE-model / EN1993-1-13
h_o/h [%]	h_o [mm]	s_o/h_o [%]			
0.0	0.0	-	288.1	283.3	**0.98**
40.0	140	10	63.2	282.4	**4.47**
		40	198.3	283.6	**1.43**
		70	267.2	283.2	**1.05**
57.1	200	10	67.5	194.4	**2.88**
		40	179.3	246.2	**1.37**
		70	179.3	276.1	**1.54**
71.4	250	10	69.1	112.5	**1.63**
		40	194.8	177.7	**0.91**
		70	194.8	216.9	**1.11**
78.0	273	10	70.3	84.4	**1.20**
		40	151.2	166.1	**1.10**
		70	151.2	166.6	**1.10**

Failure modes: *Vierendeel*, Moment at opening, Moment at midspan, Web-post bucking or shear, *Vierendeel*/web-post buckling or shear.

It is clear from Table 11 that the standard predicts the correct failure mode for 7 of the 12 opening geometries.

For s_o/h_o= 70 %, the ultimate capacities from the FE-models and standard coincide well for three out of four cases. The results from the FE-models are about 10 % larger. The deviation occurs for the last case, h_o=200 mm, where failure due to moment at the opening occurred in the FE-model with an ultimate capacity that was 54 % larger. EN 1993-1-13 limits this case to *Vierendeel* bending based on elastic capacity of the Tees and as discussed this tends to be over conservative.

For s_o/h_o= 40 % the standard gave varying results. The beam with the largest openings failed due to *Vierendeel* bending at the most loaded opening, agreeing with the failure mode of 1993-1-13. The ultimate load from the FE-model was 10 % larger than what the standard

gave. For h_o=250 mm we see the only significant non-conservative result that was obtained in this study. The standard overestimates the capacity with about 9 %. According to the numerical analysis the beam fails due to buckling of the web-post, but the design capacity was limited by *Vierendeel* bending according to EN 1993-1-13. This indicates that the web-post design methods are not always conservative for circular openings.

We see the opposite for the remaining opening heights h_o=200 mm and h_o=140 mm where the standard underestimates the capacity with 27 % and 30 % respectively. For h_o=200 mm the elastic capacity of *Vierendeel* bending is critical, while for h_o=140 mm it is the web post shear capacity that is deciding. Both failure modes are different from what was seen in the FE-models.

Lastly, for the narrowest web-post s_o/h_o= 10 %, the numerical models and EN 1993-1-13 coincide well with regards to the failure modes, but not with regards to the ultimate capacities. On average the FE-models obtained an ultimate capacity that was 155 % larger than what the standard allowed. One reason for this can be that the FE-models allow for new failure modes to take over once one is reached, so as the web-post is fully plasticized the forces can be redirected to the Tees. On the other hand, EN 1993-1-13 gives ultimate design capacity as plasticization of the web-post.

This conservatism is observed to increase for smaller openings. As smaller openings have larger web outstands and thus more capacity in the Tee's, they are more capable of carrying a load increase after the web-post if fully plasticized. Which means that the difference in capacity between the FE-models and the standard increases as the openings become smaller.

4.2.5 The effect of global axial loading

EN 1993-1-13 limits ULS calculations to axial forces not exceeding 2 % of the cross-sections' net capacity at the opening. Thus, any real interaction between global moment and global axial forces is excluded from the standard. As interest on this had already been noted in relation to the design of large trusses on offshore constructions it was chosen to analyze this and propose an interaction for the design check of *Vierendeel* bending.

Firstly, the FE-model of Specimen C was extended to four different opening geometries. The opening length a_o and corner radius r_o remained constant at 300 mm and 100 mm respectively. The opening height h_o varied between 125 mm, 187.5 mm, 250 mm, and 300 mm. The four models were then subjected to global axial forces of varying intensity as well as a point load at midpoint. The intensities were decided as a percentage ranging from 0-50 % of the net axial capacity of each cross-section at the center of the opening.

Fig. 36 shows the results of the analysis with $N/N_{y,red}$ on the x-axis and M/M_{ult} on the y-axis. $N/N_{y,red}$ represents the applied axial load in relation to the net axial capacity of the reduced cross-section at the opening. M represents the moment capacity for the given axial load obtained from the FE-models, while M_{ult} is the ultimate moment capacity when the axial force is zero. M/M_{ult} then becomes a measure of the reduction of moment capacity when the beam also is loaded axially. In addition to the four analyzed opening geometries, the same is plotted for an identical beam with h_o=0, i.e, no opening. This is then compared to the design capacity of interaction between moment and axial forces according to EN 1993-1-1.

From Fig. 36 one can as expected see that beam with the largest opening, h_o=300 mm, is most affected from global axial loading. For an axial intensity of 10 % the moment capacity is reduced by 12 %. This trend continues up until an intensity of about 30 % where it from then on out slows down. This is the opposite of what we see for the other beams. For h_o=250 mm the reduction is smallest, followed by h_o=125 mm and then h_o=187.5 mm. For these three cases the reduction starts out slow, but then increases as the axial intensity gets larger. The two smaller openings head towards a very similar trend as the one EN 1993-1-1 proposes. The two larger openings head towards a trend with a slower moment capacity reduction for larger axial force intensities.

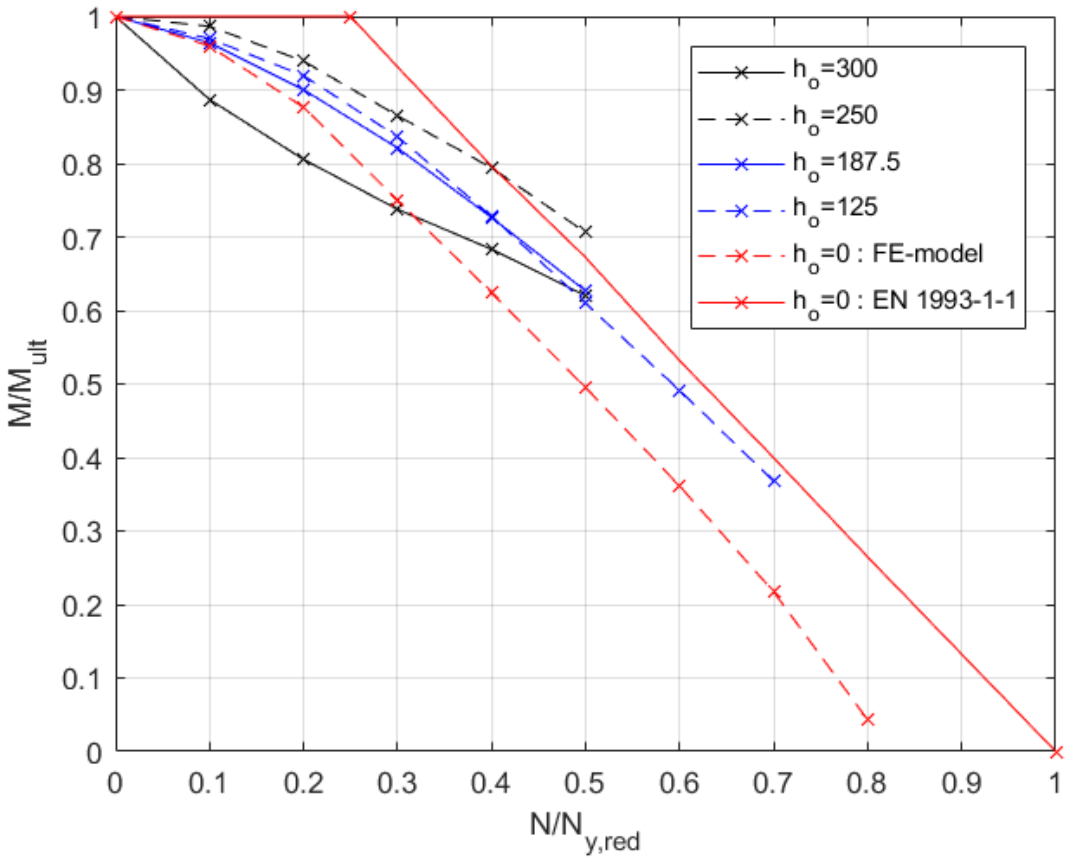

Figure 36: Results from study of moment-axial interaction.

Taking the beam with opening height h_o=250 mm the ultimate load from the FE-model is compared against a proposed interaction for *Vierendeel* bending. The results are shown in Table 12 and calculations are presented in Appendix F. In the design check for *Vierendeel* bending according to EN 1993-1-13 one is to combine the local bending of the Tees with the axial forces in the Tees resulting from the global moment. The interaction is linear if the global moment gives compressive forces in the Tee, while it is quadratic if the forces are tensile.

It is proposed to allow this interaction even for larger axial forces than 2 % and the results are shown in Table 12. The total axial force in the Tees then becomes the sum of the axial forces due to the global moment and due to the global axial forces.

Table 12: Results from proposed interaction of global axial forces.

Axial intensity $N/N_{y,red}$	FE-model [kN]	Proposed interaction [kN]	Proposed interaction/ FE-model
0	296	158	0.53
0.1	292	150	0.51
0.2	278	137	0.49
0.3	256	125	0.49
0.4	235	111	0.47
0.5	209	94	0.45

Table 12 shows that the proposed interaction in on the safe side at least for the chosen opening geometry. The ratio between the design capacity for the proposed interaction and the actual capacity obtained from the FE-models is stable. Actually, it is slightly decreasing, meaning that the proposed formulas give more conservative results as the axial intensity increases.

Indications of an unsafe interaction would have been the case if the ratio-trend was opposite. Meaning that the ratios increased as the axial intensity increased. The case of a ratio above 1.0 would have indicated that the proposed formulas give results that are on the non-conservative side. Nevertheless, the opposite is seen for the chosen geometry and indications of a valid interaction for the *Vierendeel* check are present. It should be noted that interaction also for moment at the center of the opening and moment at midspan should be checked. This was not done for this analysis as it was the *Vierendeel* bending capacity of the cross-section that was critical for the ultimate design of the beam. To conclude on whether the proposed *Vierendeel* interaction is sufficient further analyzes should be done for different opening geometries.

4.2.6 Comparison of evenly distributed load versus point load

Loading applied close to or above a web opening is covered briefly by the design methods of EN 1993-1-13. It states that the local bending resistance of the loaded Tees should be checked when $V_{Ed}>0.15\ V_{o,pl,Rd}$ and $a_{eff}>6\ h_t$ (or h_b). $V_{o,pl,Rd}$ is here the shear capacity of the cross section at the opening and a_{eff} is the effective length used to assess the stability of the web outstands in the Tees, which for rectangular openings is equal to the opening length a_o. While h_t or h_b is the depth of the top or bottom Tee respectively.

It is highly likely that large transverse concentrated forces, applied in the span of the Tee above the opening or close to it, will reduce the M-V resistance of the beam at the region of the opening considerably. Evenly distributed transverse loading along the beam's top or bottom flanges may induce local bending moment in the Tees at a magnitude sufficient to influence the beam's resistance, even for opening geometries with a_{eff} outside the criteria of EN 1993-1-13.

The latter case is therefore studied by comparing the already obtained beam response for the point load case, with a corresponding FE-model of a beam with distributed loading (q, kN/m) along the entire beam length.

The case with distributed uniform loading is easy to model, but it is not straight forward to choose an opening geometry and loading scenario that makes the point load case directly comparable to the distributed load case. It was chosen to use Specimen B as a reference, with a span length of 2,8 m, a_o=380 mm, h_o=160 mm and a centrally applied point load P. The geometry is shown in Table 2. The bending moment M_o at the center of the web opening is 0.3m*P and the shear force V_o is 0.5*P. Bending moment to shear force ratio is for such loading then M_o/V_o=0.6 kNm/kN, see Table 13 and Fig. 37.

Correspondingly, for a beam with distributed loading q the moment M_o is $0.66m^2$*q and the shear force is 0.8m*q. This gives a moment-to-shear ratio M_o/V_o=0.825 kNm/kN.

Table 13: Comparison of theoretical and analyzed moment-to-shear ratio at opening center.

Statics		Ratio M_o/V_o	FE-models		Ratio M_o/V_o
P:	M_o=0.3m*P	0.6 kNm/kN	**P_{ult}: 321 kN**	M_o=96.3 kNm	0.6 kNm/kN
	V_o=0.5P			V_o=160.5 kN	
q:	M_o=0.66m^2*q	0.825 kNm/kN	**q_{ult}: 184 kN/m**	M_o=99.5 kNm	0.675 kNm/kN
	V_o=0.8m*q			V_o=147.4 kN	

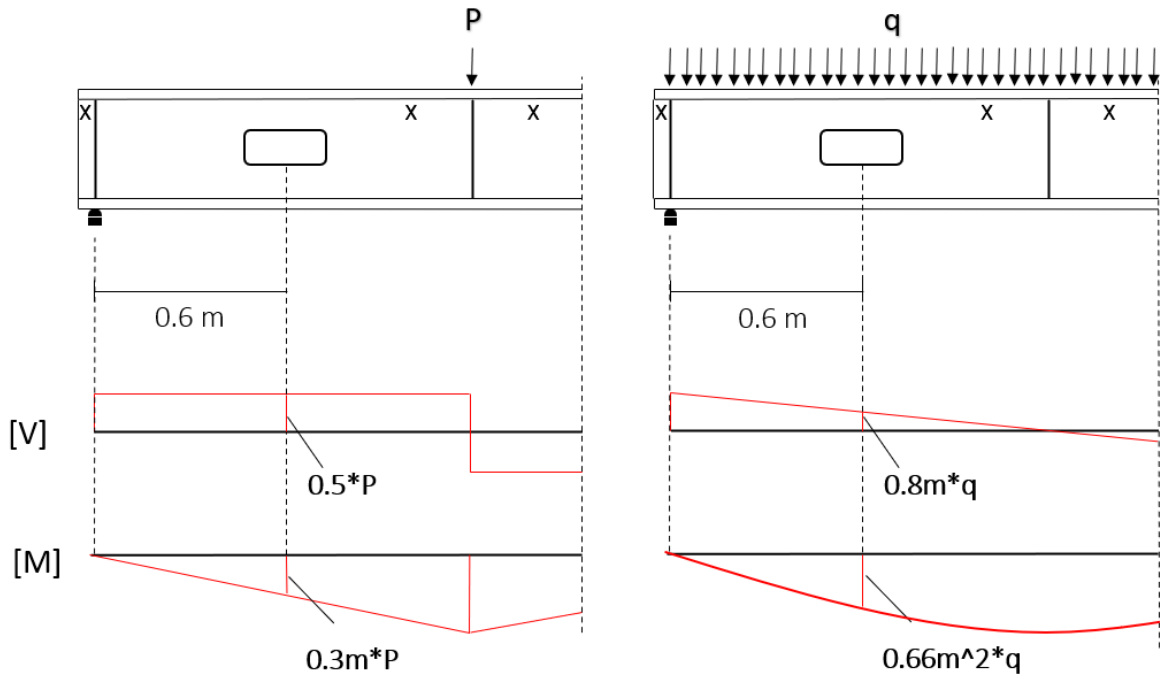

Figure 37: Illustration of statics for point load case and evenly distributed load case.

A on "equal terms" comparison of the beams ultimate load capacities (P_{ult} and q_{ult}) must then choose either moment or shear values for the basis of comparison. As the shear force V_o at the web opening center is believed to be the dominant load component for the present opening geometry case, it is chosen to compare on the shear force basis.

Ultimate loading capacity for the point load case of Specimen B gave an ultimate force P_{ult} of 321 kN as presented earlier. This gives $V_o=P_{ult}/2$=160.5 kN at the opening.

From simulation of the same beam with a distributed load q, an ultimate load capacity of q_{ult}=184 kN/m is obtained. Ultimate shear force at the center of the opening is then V_o=147 kN, which shows that the ultimate capacity is reached at shear force 9 % smaller than for the point load case. The failure pattern that defined the capacity in both simulations consisted as expected of compression of the top left and bottom right corner and tension of the bottom left and top right corner for both cases. The stress distribution and the out of plane deformations is observed to be similar for both load cases.

When interpreting this resistance drop, one must also look to the moment at the opening center M_o, which is 3 % larger for the distributed load case. The "effective" reduction in the beam's capacity due to distributed loading as an alternative for point load, may thus be smaller than 9 % if we consider the increased capacity for moment. Constructing two load/geometry scenarios with P or q loading, causing exact equal ratios of M_o and V_o, was not attempted.

When simulating also longer web openings, with constant height h_o=160 mm and varying lengths a_o=380 mm, 580 mm, 780 mm, 980 mm, one gets ultimate capacities as shown in Fig. 38. Fig. 38 shows load capacities as ultimate load versus opening lengths. One sees that the difference in capacities becomes smaller as the opening lengths become larger. For the design methods of EN 1993-1-13 to be valid, the maximum allowed opening length is set at a_o/h_o=2,5. For the chosen opening height of h_o=160 mm this corresponds to a maximal $a_{o,max}$= 400 mm, and thus the case of a_o=380 mm is representative.

It can further be commented that in the design check for the beam case with opening dimensions h_o=160 mm * a_o=380 mm, in the determining design check where the *Vierendeel* check decides, the interaction equation has two terms, $N_{Ed}/N_{T,Rd}$ and $M_{NV,Tt,Rd}/M_{el,T,Rd}$. The numerical values show that the moment utilization ($M_{NV,Tt,Rd}/M_{el,T,Rd}$) determines 88 % of the total capacity , which supports the idea that the shear force is the best foundation for an estimation of the effect of transverse loading over the opening.

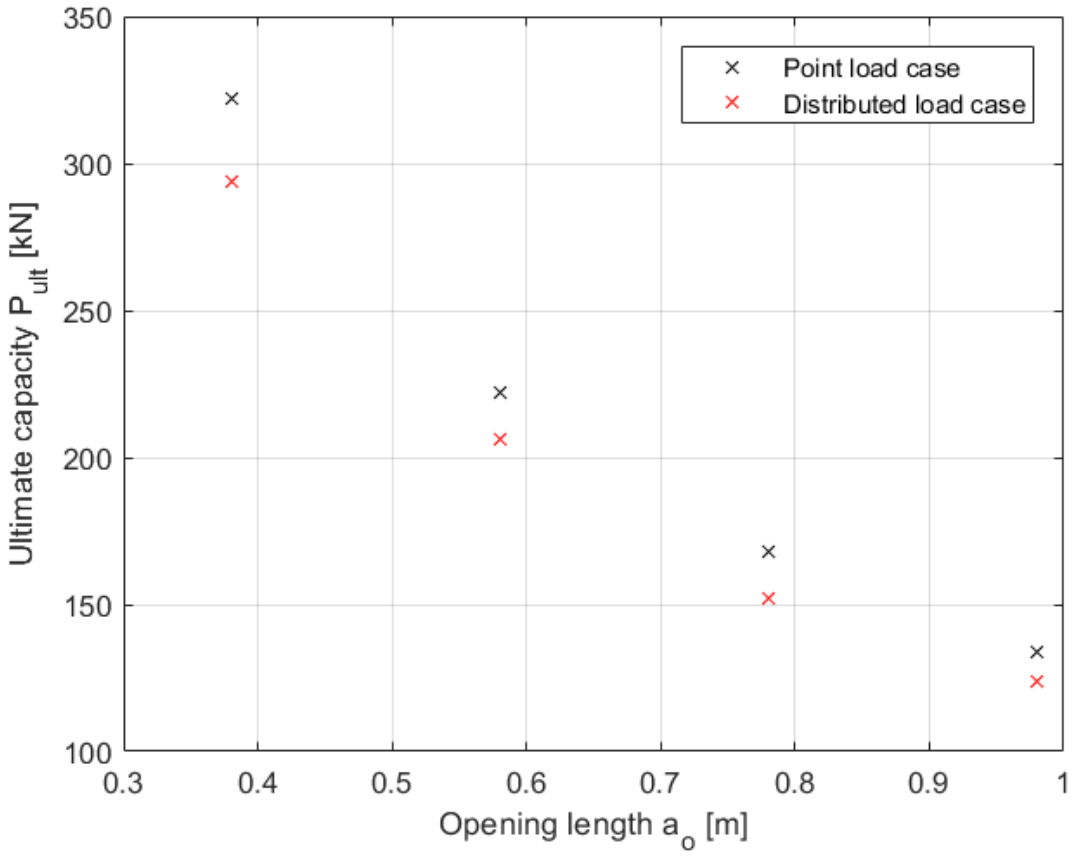

Figure 38: Ultimate capacity P_{ult} plotted versus opening length for point load case and distributed load case.

An alternative investigation on the influence of distributed loading (q) in the region of the web opening may be performed by applying two blocks of distributed loads at the opening for the point load case. Distributed vertical downwards force (q) on the upper flange and an oppositely directed distributed force (i.e., -q), on the bottom flange, see Fig. 39. This causes local bending of the Tees over and under the opening but has zero net influence on the global M and V actions on the beam, which allows a more direct comparison with the results for the point load case.

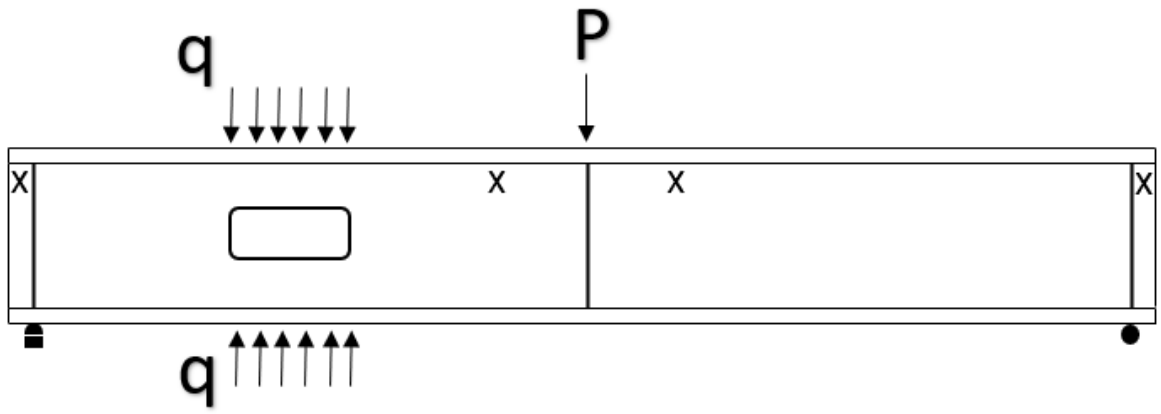

Figure 39: Illustration of alternative study with blocks of distributed load at the opening for point load case.

This approach allows the effect of distributed force to be studied for varying load intensity. Choosing the web opening case h_o=160 mm, a_o= 380 mm for this, and distributed load values q_y corresponding to what causes moment at the theoretical "fixed end" of the Tees, $M_{T,y} = 1/12 q_y a_o^2$ one gets q_y=806 kN/m using the plastic capacity of the Tees. This q_y is then used in load intervals ranging from $0q_y$ (load level 0) up until $1.0q_y$ (load level 10) in 10 percent intervals.

As seen, the resistance of the beam for point load case only, i.e., with zero distributed load q_y on the Tees, was P_{ult}=321 kN. Applied transverse distributed load on the two flanges (opposite directions) gives ultimate load capacities of the beam, P_{ult} as presented in Table 14 and plotted in Fig. 40. The reduction of the ultimate capacity is then compared to P_{ult}=321 kN to quantify the influence of distributed loading over the opening.

Table 14: Results from study of beam with blocks of distributed load as illustrated in Fig. 39.

Load level	0	1	2	3	4	5	6	7	8	9	10
Increment of q_y [kN/m]	0	81	161	242	322	403	484	564	645	725	806
P_{ult} [kN]	321	302	294	264	252	236	218	200	178	154	116
Reduction [%]	0	6.6	9.5	21.9	27.8	36.4	47.7	61	80.9	109.1	177.6

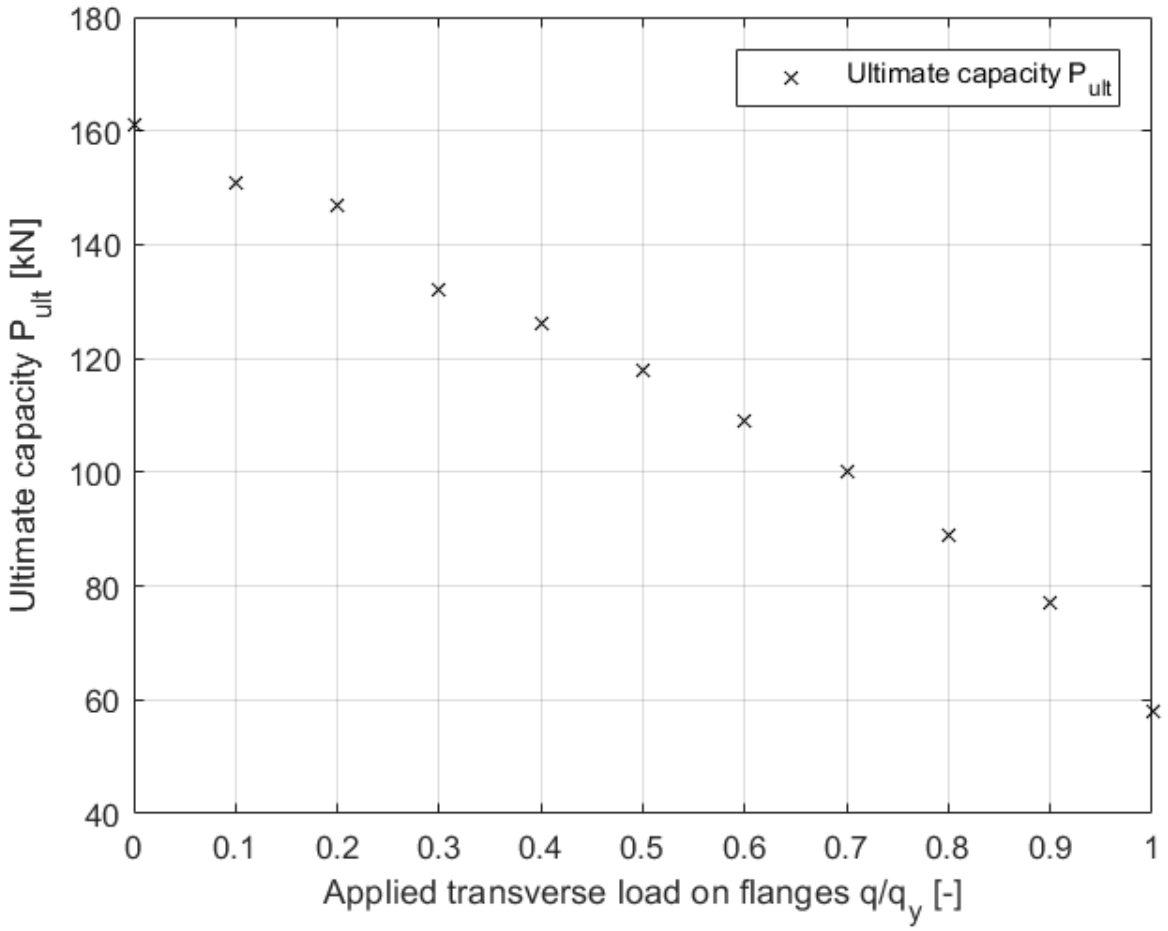

Figure 40: Ultimate capacities of beam with blocks of distributed load at the opening plotted versus the load increment of q_y.

When discussing the results of Table 14 it is important to have in mind the distributed load capacity of a representative beam without an opening. Such a beam, with span length L=2.8 m would in fact only be able to carry a distributed load q_{beam}=236 kN/m if one considers the elastic capacity. In addition, from FE-simulations of Specimen B with an evenly distributed load over the entire beam we saw an ultimate capacity of q=184 kN/m. With this in mind, it would not be reasonable to consider any load level beyond 2 or 3 when analyzing the local effects of loading above or close to an opening.

From Table 14 it is clear that when the beam is loaded at the opening with a load equivalent to that of load level 2, the reduction of ultimate capacity P_{ult}, is 9.5 %. According to EN 1993-1-13 the local capacity of the Tees does not need to be checked since the opening length is small, i.e. $a_{eff} < 6\ h_t$ (or h_b). This means that EN 1993-1-13 neglects the 9.5 % capacity reduction of the beam but does not seem unreasonable as the reduction is small.

Nevertheless, the reduction of P_{ult} is substantial when moving beyond load level 2, which could be present for traffic loads or other moving loads, and should be considered even for openings where $a_{eff} < 6\ h_t$ (or h_b).

5. Summary and conclusions

Five beams with different opening geometries were tested at Norwegian University of Science and Technology. The ultimate capacities for each test were then compared to the design capacities of EN 1993-1-13. The standard gives conservative results for all five specimen as expected, but some overly conservative results were seen in relation to rectangular openings where the web outstands are classified as cross-sectional Class 4. A proposed design method taking into consideration that two of the Tee-ends can develop plastic capacities was then discussed as an improvement to the standard.

The study was extended through a variety of FE-models which were calibrated against the tests in the laboratory. Rectangular, single circular and double circular openings were analyzed and the obtained ultimate capacities from the FE-models were compared to the design capacities of EN 1993-1-13. For rectangular openings the same conservatism regarding Class 4 web outstands was seen. For single and double circular openings some over-conservatism was seen, but the standard seemed to predict both the failure mode and ultimate capacities accurately in general.

Lastly, three subtopics regarding beams with web openings were studied. The influence of increased corner radius in rectangular openings was analyzed as EN 1993-1-13 does not include the beneficiary effects of this in its formulae. Proposed formulae for treating a rectangular opening with an equivalent length and height depending on the corner radius was verified against FE-models. The results indicated that the proposed formulae improved the accuracy of EN 1993-1-13 substantially for openings where the corner radius is large.

In addition, the design methods proposed in EN 1993-1-13 does not allow for global axial forces exceeding 2 % of the beams net axial capacity. Four different opening heights were analyzed with a varying axial intensity up to 50 % to study this. A proposed interaction with global axial force regarding the check for *Vierendeel* bending was evaluated and conservative results were seen indicating a reasonable proposed interaction.

The last subtopic regarded beams with loads applied either at the opening or close to it. This topic is covered briefly by EN 1993-1-13. FE-models with evenly distributed loads both along the entire beam length and only at the opening were analyzed. Both cases showed a reduction of the ultimate capacity of the beam. The reduction was small for the most relevant load cases and the proposed design check of EN 1993-1-13 was thus considered reasonable.

References

[1] R. M. Lawson and S. J. Hicks, «Design of composite beams with large web openings» SCI publication P355, Berkshire, 2011.

[2] CEN, «EN 1993-1-1 Eurocode 3 – Design of steel structures – Part 1–1: General rules and rules for buildings», 2005

[3] CEN, «EN 1993-1-5 Eurocode 3 – Design of steel structures – Part 1–5: Plated structural elements», 2006

[4] CEN, «EN 1993-1-13» CEN, Berlin, 2020.

[5] E. A. Marthinussen and H. H. Sandnes, «Bjelker med rektangulære åpninger i steget» NTNU, Trondheim, 2019.

[6] M. L. Hovda and V. M. Hurum, «Beams with circular web openings» NTNU, Trondheim, 2019.

[7] G.W. Bjerch and P.A. Aksnes, «Bjelker med åpninger i steget» NTNU, Trondheim, 2021.

[8] N. C. Grønland, «Bjelker med to rektangulære åpninger plassert vertikalt over hverandre,» NTNU, Trondheim, 2020.

[9] R. G. Redwood, «Design of beams with web holes» Canadian Steel Industries Construction Council, Ontario, 1973.

[10] M. Lawson, «Large web openings in steel and composite beams», Berlin: Steel Construction 10, 2017.

Appendices

Appendix A: Calculations on Specimen A according to EN 1993-1-13

Appendix B: Calculations on Specimen B according to EN 1993-1-13

Appendix C: Calculations on Specimen C according to EN 1993-1-13

Appendix D: Calculations on Specimen D according to EN 1993-1-13

Appendix E: Calculations on Specimen E according to EN 1993-1-13

Appendix F: Calculations on Specimen C with proposed interaction of moment and axial forces

Appendix A: Calculations on Specimen A according to EN 1993-1-13

Dimensions:

$L := 2800\ mm$ Span length
$h := 392\ mm$ Cross section height
$b := 110\ mm$ Flange width
$t_f := 9.4\ mm$ Flange thickness
$t_w := 6\ mm$ Web thickness
$r := 12\ mm$ Root radius

$h_o := 250\ mm$ Opening height
$a_o := 300\ mm$ Opening length
$r_o := 16\ mm$ Opening corner radius

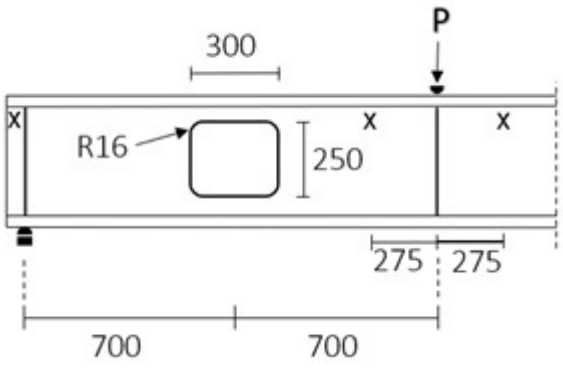

Material data:

$f_y := 424\ MPa$
$E := 210000\ MPa$
$\nu := 0.3$
$\varepsilon := \left(\frac{235\ MPa}{f_y}\right)^{0.5} = 0.744$
$\eta := 1.2$
$\gamma_{M0} := 1.0$
$\gamma_{M1} := 1.0$

Load:

$P := 163.1\ kN$ Ultimate design load according to EN 1993-1-13

$V_{Ed} := \frac{P}{2} = 81.55\ kN$ Shear load acting on cross section

$M_{o.Ed} := V_{Ed} \cdot 700\ mm = 57.085\ kN \cdot m$ Moment acting at centre of opening

$M_{mid} := V_{Ed} \cdot \frac{L}{2} = 114.17\ kN \cdot m$ Moment acting at midspan

Calculations according to EN 1993-1-1:

Shear capacity

$h_w := h - 2 \cdot t_f = 373.2\ mm$ Web height

$A := 2 \cdot b \cdot t_f + h_w \cdot t_w + 2 \cdot \frac{(2 \cdot r)^2 - \pi \cdot r^2}{2} = (4.431 \cdot 10^3)\ mm^2$ Gross area of cross section

$A_v := A - 2 \cdot b \cdot t_f + (t_w + 2 \cdot r) \cdot t_f = (2.645 \cdot 10^3)\ mm^2 \quad < \quad \eta \cdot h_w \cdot t_w = (2.687 \cdot 10^3)\ mm^2$

$A_v := \eta \cdot h_w \cdot t_w = (2.687 \cdot 10^3)\ mm^2$ Shear area

$V_{pl.Rd} := \frac{A_v \cdot f_y}{3^{0.5} \cdot \gamma_{M0}} = 657.778\ kN$ Plastic shear capacity according to (6.18)

$\frac{V_{Ed}}{V_{pl.Rd}} = 0.124 \quad < \quad 1$ OK, <0.5 do not have to reduce yield strength according 6.2.10(3)

$\frac{h_w}{t_w} = 62.2 \quad > \quad 72 \cdot \frac{\varepsilon}{\eta} = 44.669$ Need to check shear buckling according to EN 1993-1-5

Shear buckling

$a := \frac{L}{2} = (1.4 \cdot 10^3)\ mm$ Distance between vertical stiffeners

$\frac{a}{h_w} = 3.751$

$k_{\tau.sl} := 0$ No horizontal stiffeners

$k_\tau := 5.34 + 4 \cdot \left(\frac{h_w}{a}\right)^2 + k_{\tau.sl} = 5.624$

$\sigma_E := \frac{\pi^2 \cdot E \cdot t_w^2}{12 \cdot (1 - \nu^2) \cdot h_w^2} = 49.059\ MPa$

$\tau_{cr} := k_\tau \cdot \sigma_E = 275.918\ MPa$ (5.4)

$\lambda_w := 0.76 \cdot \left(\frac{f_y}{\tau_{cr}}\right)^{0.5} = 0.942$ (5.3)

$\frac{0.83}{\eta} = 0.692 \quad < \quad \lambda_w = 0.942 \quad < \quad 1.08$

$\chi_w := \frac{0.83}{\lambda_w} = 0.881$ According to table 5.1 in EN 1993-1-5

$V_{b.Rd} := \frac{\chi_w \cdot f_y \cdot h_w \cdot t_w}{3^{0.5} \cdot \gamma_{M1}} = 482.914\ kN \quad < \quad \frac{\eta \cdot f_y \cdot h_w \cdot t_w}{3^{0.5} \cdot \gamma_{M1}} = 657.778\ kN$ (5.1)

$\frac{V_{Ed}}{V_{b.Rd}} = 0.169$ < 1 OK

Moment at midspan

$c_f := \frac{b}{2} - \frac{t_w}{2} - r = 40\ mm$ Cross section classification of flenge in compression

$\frac{c_f}{t_f \cdot \varepsilon} = 5.716$ < 9 Cross sectional class 1 according to table 5.2

$c_w := h_w - 2 \cdot r = 349.2\ mm$

$c_{w1} := 72 \cdot \varepsilon \cdot t_w = 321.614\ mm$ < $c_w = 349.2\ mm$

$c_{w2} := 83 \cdot \varepsilon \cdot t_w = 370.749\ mm$ > $c_w = 349.2\ mm$ Cross sectional class 2 for web

$M_{pl.Rd} := \frac{2 \cdot \left((b \cdot t_f) \cdot \left(\frac{h}{2} - \frac{t_f}{2} \right) + \frac{h_w}{2} \cdot t_w \cdot \frac{h_w}{4} \right) \cdot f_y}{\gamma_{M0}} = 256.319\ kN \cdot m$ Plastic moment capacity at midspan

$\frac{M_{mid}}{M_{pl.Rd}} = 0.445$ < 1 OK according to (6.12)

Calculations according to EN 1993-1-13:

$a_{eff} := a_o = 300\ mm$ Defining effective opening length

$a_{eq} := a_o = 300\ mm$ Defining equivalent opening length

$h_{eq} := h_o = 250\ mm$ Defining equivalent opening height

Shear capacity at opening center, 8.2

$V_{o.Pl.Rd} := V_{pl.Rd} - \frac{h_o \cdot t_w \cdot f_y}{3^{0.5} \cdot \gamma_{M0}} = 290.583\ kN$

$\frac{V_{Ed}}{V_{o.Pl.Rd}} = 0.281$ < 1 OK according to (8.1)

< 0.5 OK, do not have to reduce yield strength according to 8.2(2)

$\frac{h_w}{t_w} = 62.2$ > $72 \cdot \frac{\varepsilon}{\eta} = 44.669$ 8.5.1(3)

$h_o = 250\ mm$ > $15 \cdot t_w \cdot \varepsilon = 67.003\ mm$ 8.5.1(4)

Both 8.5.1(3) and 8.5.1(4) are fulfilled and thus control for buckling of web next to the opening have to be done.

Buckling of web next to opening, 8.5.2

$b_w := 0.5 \cdot h_o = 125\ mm$ 8.5.2(3)

$\lambda_1 := \pi \cdot \left(\frac{E}{f_y}\right)^{0.5} = 69.916$ (8.21)

$\alpha := 0.21$ Imperfection factor for buckling curve according to EN 1993-1-1 table 6.1

$\lambda_{w.bar} := \frac{3.5 \cdot h_o}{t_w \cdot \lambda_1} = 2.086$ (8.20)

$\phi := 0.5 \cdot \left(1 + \alpha \cdot \left(\lambda_{w.bar} - 0.2\right) + \lambda_{w.bar}{}^2\right) = 2.873$

$\chi := \frac{1}{\phi + \left(\phi^2 - \lambda_{w.bar}{}^2\right)^{0.5}} = 0.206$ Buckling reduction factor according to EN 1993-1-1 (6.49)

$N_{w.Rd} := \chi \cdot b_w \cdot t_w \cdot \frac{f_y}{\gamma_{M1}} = 65.572\ kN$ (8.18)

$N_{w.Ed} := \frac{1}{2} V_{Ed} = 40.775\ kN$ According to (8.16) and (8.17)

$\frac{N_{w.Ed}}{N_{w.Rd}} = 0.622$ < 1 OK according to 8.5.2(1)

Moment capacity at opening, 8.3

$$c_{w.T} := \frac{h - 2 \cdot t_f - 2 \cdot r - h_o}{2} = 49.6 \ mm$$ Web outstands - global bending

$$\frac{c_{w.T}}{t_w \cdot \varepsilon} = 11.104 \quad < \quad 14$$ Cross sectional class 3

Since the flanges are classified as class 1, the web of the T-section that is subjected to compression can be taken as class 2 according to 7.4(2) if the effective depth of the outstand is set to the cross sectional class 2 limit according to EN 1993-1-1.

$$c_{w.T.eff} := 10 \cdot t_w \cdot \varepsilon = 44.669 \ mm$$

Calculations to find the plastic moment capacity:

$$h_{w.tT.eff} := c_{w.T.eff} + r = 56.669 \ mm$$ Height of effective web of top T

$$A_{w.tT.eff} := h_{w.tT.eff} \cdot t_w = 340.012 \ mm^2$$ Area of effective web of top T

$$A_f := b \cdot t_f = \left(1.034 \cdot 10^3\right) \ mm^2$$ Area of flange

$$A_{tT.eff} := A_f + A_{w.tT.eff} = \left(1.374 \cdot 10^3\right) \ mm^2$$ Total area of effective T neglecting area of root radius

$$z_{tT.eff} := \frac{A_f \cdot \frac{t_f}{2} + A_{w.tT.eff} \cdot \left(t_f + \frac{h_{w.tT.eff}}{2}\right)}{A_{tT.eff}} = 12.875 \ mm$$

In reality, there is a small difference between the top Tee and the bottom Tee because they have different depths. This is a small difference and is thus neglected.

$$M_{o.pl.Rd} := \frac{\left(A_{tT.eff}\right) \cdot \left(h - 2 \cdot z_{tT.eff}\right) \cdot f_y}{\gamma_{M0}} = 213.371 \ kN \cdot m$$ (8.6)

$$\frac{M_{o.Ed}}{M_{o.pl.Rd}} = 0.268 \quad < \quad 1$$ OK according to (8.5)

Buckling of T-section in compression

$$h_T := \frac{h - h_o}{2} = 71\ mm$$

$$a_{eff} = 300\ mm \quad < \quad 6 \cdot h_T \cdot \varepsilon \cdot \left(\frac{M_{o.pl.Rd}}{M_{o.Ed}} \right)^{0.5} = 613.15\ mm$$

$$< \quad 12 \cdot h_T = 852\ mm$$

Do not need to check for buckling of T-section in compression according to 8.3.2(1) and 8.3.2(2).

Vierendeel-capacity, 8.4

$$c_{w.T.V} := \frac{h - 2 \cdot t_f - 2 \cdot r - h_o}{2} = 49.6\ mm$$

$$\frac{c_{w.T.V}}{t_w \cdot \varepsilon} = 11.104 \quad < \quad 14$$ The web outstand is classfied as class 3

$$a_{eff} = 300\ mm \quad > \quad 32 \cdot t_w \cdot \varepsilon = 142.939\ mm$$

The class 3 web outstand may be taken as class 2 for Vierendeel-bending if:

$$c_{w.T.V} = 49.6\ mm \quad < \quad \frac{10 \cdot t_w \cdot \varepsilon}{\left(1 - \left(\frac{32 \cdot t_w \cdot \varepsilon}{a_{eff}} \right)^2 \right)^{0.5}} = 50.806\ mm \qquad (7.3)$$

Since (7.3) holds the Tee's can be taken as class 2 with full depth.

$$d_t := c_{w.T.V} = 49.6\ mm$$

Since the Tee's are regarded as class 2 the plastic capacity can be used.
Calculating the axial force in the Tee's as a result of global moment, and the capcaity of the Tee's in compression according to 8.4(6):

$$z_T := z_{tT.eff} = 12.875\ mm$$

$$N_{Ed} := \frac{M_{o.Ed}}{h - 2\ z_T} = 155.863\ kN$$ Axial force in Tee's as a result of global moment

$$A_{T.V} := A_{tT.eff} = \left(1.374 \cdot 10^3 \right)\ mm^2$$

$$N_{T.pl.Rd} := \frac{f_y \cdot A_{T.V}}{\gamma_{M0}} = 582.581\ kN$$ Axial capacity of Tee

$$h_{w.T.V} := d_t + r = 61.6\ mm$$

$$A_{w.T.V} := h_{w.T.V} \cdot t_w = 369.6\ mm^2$$

$$z_{pl.T} := \frac{\frac{A_{T.V}}{2}}{b} = 6.246\ mm \quad < \quad t_f = 9.4\ mm$$ Plastic neutral axis of Tee's

Have to find the cetnre of gravity of the part of the Tee's that is located "beneeth" the plastic neutral axis

$$a_{web} := t_f - z_{pl.T} + \frac{h_{w.T.V}}{2} = 33.954\ mm$$

$$a_{flange} := \frac{t_f - z_{pl.T}}{2} = 1.577\ mm$$

$$z_{Ab} := \frac{b \cdot \left(t_f - z_{pl.T}\right) \cdot a_{flange} + A_{w.T.V} \cdot a_{web}}{\frac{A_{T.V}}{2}} = 19.064\ mm$$

$$M_{pl.T.Rd} := \left(\frac{A_{T.V}}{2} \cdot \frac{z_{pl.T}}{2} + \frac{A_{T.V}}{2} \cdot z_{Ab}\right) \cdot \frac{f_y}{\gamma_{M0}} = 6.463\ kN \cdot m$$ Plastic moment capacity of the Tee's.

$$M_{NV.T.Rd} := M_{pl.T.Rd} \cdot \left(1 - \left(\frac{N_{Ed}}{N_{T.pl.Rd}}\right)^2\right) = 6\ kN \cdot m$$ (8.11)

$$V_{vier.Rd} := \frac{4 \cdot M_{NV.T.Rd}}{a_{eq}} = 80.002\ kN$$ (8.10)

$$\frac{V_{Ed}}{V_{vier.Rd}} = 1.019 \quad =1$$ OK according to (8.9).

Thus the ultimate design load P according to EN 1993-1-13 is P=142.1 kN

Appendix B: Calculations on Specimen B according to EN 1993-1-13

Dimensions:

$L := 2800\ mm$ Span length
$h := 392\ mm$ Cross section height
$b := 110\ mm$ Flange width
$t_f := 9.4\ mm$ Flange thickness
$t_w := 6\ mm$ Web thickness
$r := 12\ mm$ Root radius

$h_o := 160\ mm$ Opening height
$a_o := 380\ mm$ Opening length
$r_o := 16\ mm$ Opening corner radius

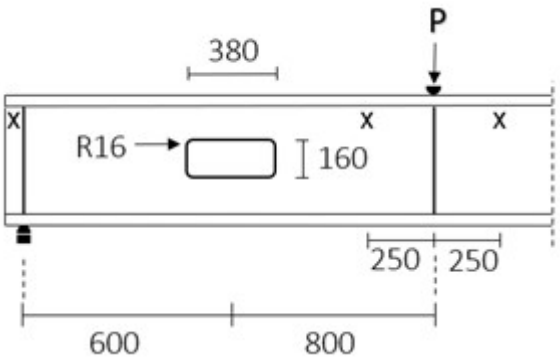

Material data:

$f_y := 424\ MPa$
$E := 210000\ MPa$
$\nu := 0.3$
$\varepsilon := \left(\frac{235\ MPa}{f_y}\right)^{0.5} = 0.744$
$\eta := 1.2$
$\gamma_{M0} := 1.0$
$\gamma_{M1} := 1.0$

Load:

$P := 90.3\ kN$ Ultimate design load according to EN 1993-1-13

$V_{Ed} := \frac{P}{2} = 45.15\ kN$ Shear load acting on cross section

$M_{o.Ed} := V_{Ed} \cdot 600\ mm = 27.09\ kN \cdot m$ Moment acting at centre of opening

$M_{mid} := V_{Ed} \cdot \frac{L}{2} = 63.21\ kN \cdot m$ Moment acting at midspan

Calculations according to EN 1993-1-1:

Shear capacity

$h_w := h - 2 \cdot t_f = 373.2\ mm$ Web height

$A := 2 \cdot b \cdot t_f + h_w \cdot t_w + 2 \cdot \frac{(2 \cdot r)^2 - \pi \cdot r^2}{2} = (4.431 \cdot 10^3)\ mm^2$ Gross area of cross section

$A_v := A - 2 \cdot b \cdot t_f + (t_w + 2 \cdot r) \cdot t_f = (2.645 \cdot 10^3)\ mm^2 \quad < \quad \eta \cdot h_w \cdot t_w = (2.687 \cdot 10^3)\ mm^2$

$A_v := \eta \cdot h_w \cdot t_w = (2.687 \cdot 10^3)\ mm^2$ Shear area

$V_{pl.Rd} := \frac{A_v \cdot f_y}{3^{0.5} \cdot \gamma_{M0}} = 657.778\ kN$ Plastic shear capacity according to (6.18)

$\frac{V_{Ed}}{V_{pl.Rd}} = 0.069 \quad < \quad 1$ OK, <0.5 do not have to reduce yield strength according 6.2.10(3)

$\frac{h_w}{t_w} = 62.2 \quad > \quad 72 \cdot \frac{\varepsilon}{\eta} = 44.669$ Need to check shear buckling according to EN 1993-1-5

Shear buckling

$a := \frac{L}{2} = (1.4 \cdot 10^3)\ mm$ Distance between vertical stiffeners

$\frac{a}{h_w} = 3.751$

$k_{\tau.sl} := 0$ No horizontal stiffeners

$k_\tau := 5.34 + 4 \cdot \left(\frac{h_w}{a}\right)^2 + k_{\tau.sl} = 5.624$

$\sigma_E := \frac{\pi^2 \cdot E \cdot t_w^2}{12 \cdot (1 - \nu^2) \cdot h_w^2} = 49.059\ MPa$

$\tau_{cr} := k_\tau \cdot \sigma_E = 275.918\ MPa$ (5.4)

$\lambda_w := 0.76 \cdot \left(\frac{f_y}{\tau_{cr}}\right)^{0.5} = 0.942$ (5.3)

$\frac{0.83}{\eta} = 0.692 \quad < \quad \lambda_w = 0.942 \quad < \quad 1.08$

$\chi_w := \frac{0.83}{\lambda_w} = 0.881$ According to table 5.1 in EN 1993-1-5

$V_{b.Rd} := \frac{\chi_w \cdot f_y \cdot h_w \cdot t_w}{3^{0.5} \cdot \gamma_{M1}} = 482.914\ kN \quad < \quad \frac{\eta \cdot f_y \cdot h_w \cdot t_w}{3^{0.5} \cdot \gamma_{M1}} = 657.778\ kN$ (5.1)

$\frac{V_{Ed}}{V_{b.Rd}} = 0.093$ < 1 OK

Moment at midspan

$c_f := \frac{b}{2} - \frac{t_w}{2} - r = 40\ mm$ Cross section classification of flenge in compression

$\frac{c_f}{t_f \cdot \varepsilon} = 5.716$ < 9 Cross sectional class 1 according to table 5.2

$c_w := h_w - 2 \cdot r = 349.2\ mm$

$c_{w1} := 72 \cdot \varepsilon \cdot t_w = 321.614\ mm$ < $c_w = 349.2\ mm$

$c_{w2} := 83 \cdot \varepsilon \cdot t_w = 370.749\ mm$ > $c_w = 349.2\ mm$ Cross sectional class 2 for web

$M_{pl.Rd} := \frac{2 \cdot \left((b \cdot t_f) \cdot \left(\frac{h}{2} - \frac{t_f}{2} \right) + \frac{h_w}{2} \cdot t_w \cdot \frac{h_w}{4} \right) \cdot f_y}{\gamma_{M0}} = 256.319\ kN \cdot m$ Plastic moment capacity at midspan

$\frac{M_{mid}}{M_{pl.Rd}} = 0.247$ < 1 OK according to (6.12)

Calculations according to EN 1993-1-13:

$a_{eff} := a_o = 380\ mm$ Defining effective opening length

$a_{eq} := a_o = 380\ mm$ Defining equivalent opening length

$h_{eq} := h_o = 160\ mm$ Defining equivalent opening height

Shear capacity at opening center, 8.2

$V_{o.Pl.Rd} := V_{pl.Rd} - \frac{h_o \cdot t_w \cdot f_y}{3^{0.5} \cdot \gamma_{M0}} = 422.773\ kN$

$\frac{V_{Ed}}{V_{o.Pl.Rd}} = 0.107$ < 1 OK according to (8.1)

< 0.5 OK, do not have to reduce yield strength according to 8.2(2)

$\frac{h_w}{t_w} = 62.2$ > $72 \cdot \frac{\varepsilon}{\eta} = 44.669$ 8.5.1(3)

$h_o = 160\ mm$ > $15 \cdot t_w \cdot \varepsilon = 67.003\ mm$ 8.5.1(4)

Both 8.5.1(3) and 8.5.1(4) are fulfilled and thus control for buckling of web next to the opening have to be done

Buckling of web next to opening, 8.5.2

$b_w := 0.5 \cdot h_o = 80\ mm$ 8.5.2(3)

$\lambda_1 := \pi \cdot \left(\frac{E}{f_y}\right)^{0.5} = 69.916$ (8.21)

$\alpha := 0.21$ Imperfection factor for buckling curve according to EN 1993-1-1 table 6.1

$\lambda_{w.bar} := \frac{3.5 \cdot h_o}{t_w \cdot \lambda_1} = 1.335$ (8.20)

$\phi := 0.5 \cdot \left(1 + \alpha \cdot \left(\lambda_{w.bar} - 0.2\right) + \lambda_{w.bar}{}^2\right) = 1.51$

$\chi := \frac{1}{\phi + \left(\phi^2 - \lambda_{w.bar}{}^2\right)^{0.5}} = 0.451$ Buckling reduction factor according to EN 1993-1-1 (6.49)

$N_{w.Rd} := \chi \cdot b_w \cdot t_w \cdot \frac{f_y}{\gamma_{M1}} = 91.827\ kN$ (8.18)

$N_{w.Ed} := \frac{1}{2} V_{Ed} = 22.575\ kN$ According to (8.16) and (8.17)

$\frac{N_{w.Ed}}{N_{w.Rd}} = 0.246$ < 1 OK according to 8.5.2(1)

Moment capacity at opening, 8.3

$$c_{w.T} := \frac{h - 2 \cdot t_f - 2 \cdot r - h_o}{2} = 94.6 \ mm$$ Web outstands - global bending

$$\frac{c_{w.T}}{t_w \cdot \varepsilon} = 21.178 \quad > \quad 14$$ Cross sectional class 4

Since the flanges are classified as class 1, the web of the T-section that is subjected to compression can be taken as class 3 according to 7.4(3) if the effective depth of the outstand is set to the cross sectional class 3 limit according to EN 1993-1-1.

$$c_{w.T.eff} := 14 \cdot t_w \cdot \varepsilon = 62.536 \ mm$$

Calculations to find the 2. moment of area:

$$h_{w.tT.eff} := c_{w.T.eff} + r = 74.536 \ mm$$ Height of effective web of top T

$$A_{w.tT.eff} := h_{w.tT.eff} \cdot t_w = 447.216 \ mm^2$$ Area of effective web of top T

$$A_f := b \cdot t_f = \left(1.034 \cdot 10^3\right) \ mm^2$$ Area of flange

$$A_{tT.eff} := A_f + A_{w.tT.eff} = \left(1.481 \cdot 10^3\right) \ mm^2$$ Total area of effective T neglecting area of root radius

$$z_{tT.eff} := \frac{A_f \cdot \frac{t_f}{2} + A_{w.tT.eff} \cdot \left(t_f + \frac{h_{w.tT.eff}}{2}\right)}{A_{tT.eff}} = 17.371 \ mm$$

$$I_{f.tT.eff} := \frac{b \cdot t_f^{\,3}}{12} + A_f \cdot \left(z_{tT.eff} - \frac{t_f}{2}\right)^2 = \left(1.736 \cdot 10^5\right) \ mm^4$$

$$I_{w.tT.eff} := \frac{t_w \cdot h_{w.tT.eff}^{\,3}}{12} + A_{w.tT.eff} \cdot \left(t_f + \frac{h_{w.tT.eff}}{2} - z_{tT.eff}\right)^2 = \left(5.909 \cdot 10^5\right) \ mm^4$$

$$I_{tT.eff} := I_{w.tT.eff} + I_{f.tT.eff} = \left(7.645 \cdot 10^5\right) \ mm^4$$ Total 2. moment of area of effective T-section in compression

The 2. moment of area for the T-section in tension is in reality larger than the one in compression, due to the use of plastic calculations. This is neglected as it is not the resulting critical design capacity.

$$z_{max} := \frac{h}{2} = 196 \ mm$$

$$I_{o.el} := 2 \cdot \left(I_{tT.eff} + A_{tT.eff} \cdot \left(z_{max} - z_{tT.eff}\right)^2\right) = \left(9.606 \cdot 10^7\right) \ mm^4$$

$$M_{o.Rd} := \frac{\frac{I_{o.el}}{z_{max}} \cdot f_y}{\gamma_{M0}} = 207.793 \ kN \cdot m$$

$\frac{M_{o.Ed}}{M_{o.Rd}} = 0.13$	<	1	OK according to (8.5)

Buckling of T-section in compression

$$h_T := \frac{h - h_o}{2} = 116 \ mm$$

$$a_{eff} = 380 \ mm \quad < \quad 6 \cdot h_T \cdot \varepsilon \cdot \left(\frac{M_{o.Rd}}{M_{o.Ed}}\right)^{0.5} = \left(1.435 \cdot 10^3\right) \ mm$$

$$< \quad 12 \cdot h_T = \left(1.392 \cdot 10^3\right) \ mm$$

Do not need to check for buckling of T-section in compression according to 8.3.2(1) and 8.3.2(2).

Vierendeel-capacity, 8.4

$$c_{w.T.V} := \frac{h - 2 \cdot t_f - 2 \cdot r - h_o}{2} = 94.6 \ mm$$

$\frac{c_{w.T.V}}{t_w \cdot \varepsilon} = 21.178$	>	14	The web outstand is classfied as class 4.

$$a_{eff} = 380 \ mm \quad > \quad 36 \cdot t_w \cdot \varepsilon = 160.807 \ mm$$

The class 4 web outstand may be taken as class 3 for Vierendeel-bending if:

$$d_t := c_{w.T.V} = 94.6 \ mm \quad < \quad \frac{14 \cdot t_w \cdot \varepsilon}{\left(1 - \left(\frac{36 \cdot t_w \cdot \varepsilon}{a_{eff}}\right)^2\right)^{0.5}} = 69.021 \ mm \quad (7.4)$$

Since (7.4) does not hold, the elastic capacity is determined by an effective depth based on the limit for a class 3 web outstands according to 7.5(6)

$$d_{t.eff} := 14 \cdot t_w \cdot \varepsilon = 62.536 \ mm$$

Since the Tee in compression is regarded as class 3 the elastic capacity have to be used.
Calculating the axial force in the Tee's as a result of global moment, and the capcaity of the Tee's in compression according to 8.4(6):

$z_{T.V.eff} := z_{tT.eff} = 17.371\ mm$

$N_{m.Ed} := \frac{M_{o.Ed}}{h - 2\ z_{T.V.eff}} = 75.828\ kN$ Axial force in Tee as a result of global moment

$A_{T.V.eff} := A_{tT.eff} = \left(1.481 \cdot 10^{3}\right)\ mm^{2}$

$N_{T.el.Rd} := \frac{f_y \cdot A_{T.V.eff}}{\gamma_{M0}} = 628.036\ kN$ Axial capacity of Tee

$h_{w.T.V.eff} := d_{t.eff} + r = 74.536\ mm$

$A_{w.T.eff.V} := h_{w.T.V.eff} \cdot t_w = 447.216\ mm^{2}$

$I_{f.T.V.eff} := \frac{b \cdot {t_f}^{3}}{12} + A_f \cdot \left(z_{T.V.eff} - \frac{t_f}{2}\right)^{2} = \left(1.736 \cdot 10^{5}\right)\ mm^{4}$

$I_{w.T.V.eff} := \frac{t_w \cdot {h_{w.T.V.eff}}^{3}}{12} + A_{w.T.eff.V} \cdot \left(t_f + \frac{h_{w.T.V.eff}}{2} - z_{T.V.eff}\right)^{2} = \left(5.909 \cdot 10^{5}\right)\ mm^{4}$

$I_{T.V.eff} := I_{f.T.V.eff} + I_{w.T.V.eff} = \left(7.645 \cdot 10^{5}\right)\ mm^{4}$ Second moment of area of Tee neglecting contribution from root radius.

$z_{max} := h_{w.T.V.eff} + t_f - z_{T.V.eff} = 66.565\ mm$

$M_{el.T.Rd} := \frac{I_{T.V.eff}}{z_{max} \cdot \gamma_{M0}} \cdot f_y = 4.87\ kN \cdot m$ Effective elastic moment capacity of Tee.

$M_{NV.Tt.Rd} := M_{el.T.Rd} \cdot \left(1 - \frac{N_{m.Ed}}{N_{T.el.Rd}}\right) = 4.282\ kN \cdot m$ (8.12)

$V_{vier.Rd} := \frac{4 \cdot \left(M_{NV.Tt.Rd}\right)}{a_{eq}} = 45.072\ kN$ (8.10)

$\frac{V_{Ed}}{V_{vier.Rd}} = 1.002$ $=1$ OK according to (8.9).

Thus the ultimate design load P according to EN 1993-1-13 is P=199.1 kN

Alternative calculations if one side of the Tees are allowed to develop plastic capacities:

$$c_{w.T.V} := \frac{h - 2 \cdot t_f - 2 \cdot r - h_o}{2} = 94.6 \ mm$$

$$A_{T.V} := c_{w.T.V} \cdot t_w + b \cdot t_f = \left(1.602 \cdot 10^3\right) \ mm^2$$

$$h_{w.T.V} := c_{w.T.V} + r = 106.6 \ mm$$

$$A_{w.T.V} := h_{w.T.V} \cdot t_w = 639.6 \ mm^2$$

$$z_{pl.T} := \frac{\frac{A_{T.V}}{2}}{b} = 7.28 \ mm \quad < \quad t_f = 9.4 \ mm$$

Plastic neutral axis of Tee's

Have to find the cetnre of gravity of the part of the Tee's that is located "beneeth" the plastic neutral axis

$$a_{web} := t_f - z_{pl.T} + \frac{h_{w.T.V}}{2} = 55.42 \ mm$$

$$a_{flange} := \frac{t_f - z_{pl.T}}{2} = 1.06 \ mm$$

$$z_{Ab} := \frac{b \cdot \left(t_f - z_{pl.T}\right) \cdot a_{flange} + A_{w.T.V} \cdot a_{web}}{\frac{A_{T.V}}{2}} = 44.573 \ mm$$

Plastic moment capacity of the Tee's.

$$M_{pl.T.Rd} := \left(\frac{A_{T.V}}{2} \cdot \frac{z_{pl.T}}{2} + \frac{A_{T.V}}{2} \cdot z_{Ab}\right) \cdot \frac{f_y}{\gamma_{M0}} = 16.37 \ kN \cdot m$$

$$N_{T.pl.Rd} := \frac{f_y \cdot A_{T.V}}{\gamma_{M0}} = 679.078 \ kN$$

$$M_{NV.Tb.Rd} := M_{pl.T.Rd} \cdot \left(1 - \left(\frac{N_{m.Ed}}{N_{T.pl.Rd}}\right)^2\right) = 16.166 \ kN \cdot m \qquad (8.11)$$

$$V_{vier.Rd} := \frac{2 \cdot \left(M_{NV.Tt.Rd} + M_{NV.Tb.Rd}\right)}{a_{eq}} = 107.62 \ kN$$

About 2 times larger capacity.

Appendix C: Calculations on Specimen C according to EN 1993-1-13

Dimensions:

$L := 2800\ mm$ Span length
$h := 387\ mm$ Cross section height
$b := 110\ mm$ Flange width
$t_f := 9.1\ mm$ Flange thickness
$t_w := 6\ mm$ Web thickness
$r := 12\ mm$ Root radius

$h_o := 250\ mm$ Opening height
$a_o := 300\ mm$ Opening length
$r_o := 100\ mm$ Opening corner radius

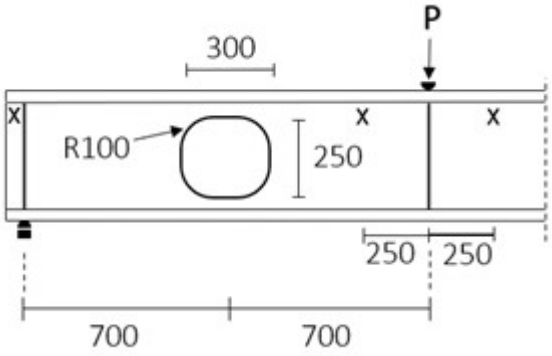

Material data:

$f_y := 424\ MPa$
$E := 210000\ MPa$
$\nu := 0.3$
$\varepsilon := \left(\frac{235\ MPa}{f_y}\right)^{0.5} = 0.744$
$\eta := 1.2$
$\gamma_{M0} := 1.0$
$\gamma_{M1} := 1.0$

Load:

$P := 153.1\ kN$ Ultimate design load according to EN 1993-1-13

$V_{Ed} := \frac{P}{2} = 76.55\ kN$ Shear load acting on cross section

$M_{o.Ed} := V_{Ed} \cdot 700\ mm = 53.585\ kN \cdot m$ Moment acting at centre of opening

$M_{mid} := V_{Ed} \cdot \frac{L}{2} = 107.17\ kN \cdot m$ Moment acting at midspan

Calculations according to EN 1993-1-1:

Shear capacity

$h_w := h - 2 \cdot t_f = 368.8\ mm$ Web height

$A := 2 \cdot b \cdot t_f + h_w \cdot t_w + 2 \cdot \frac{(2 \cdot r)^2 - \pi \cdot r^2}{2} = (4.338 \cdot 10^3)\ mm^2$ Gross area of cross section

$A_v := A - 2 \cdot b \cdot t_f + (t_w + 2 \cdot r) \cdot t_f = (2.609 \cdot 10^3)\ mm^2 \quad < \quad \eta \cdot h_w \cdot t_w = (2.655 \cdot 10^3)\ mm^2$

$A_v := \eta \cdot h_w \cdot t_w = (2.655 \cdot 10^3)\ mm^2$ Shear area

$V_{pl.Rd} := \frac{A_v \cdot f_y}{3^{0.5} \cdot \gamma_{M0}} = 650.023\ kN$ Plastic shear capacity according to (6.18)

$\frac{V_{Ed}}{V_{pl.Rd}} = 0.118 \quad < \quad 1$ OK, <0.5 do not have to reduce yield strength according 6.2.10(3)

$\frac{h_w}{t_w} = 61.467 \quad > \quad 72 \cdot \frac{\varepsilon}{\eta} = 44.669$ Need to check shear buckling according to EN 1993-1-5

Shear buckling

$a := \frac{L}{2} = (1.4 \cdot 10^3)\ mm$ Distance between vertical stiffeners

$\frac{a}{h_w} = 3.796$

$k_{\tau.sl} := 0$ No horizontal stiffeners

$k_\tau := 5.34 + 4 \cdot \left(\frac{h_w}{a}\right)^2 + k_{\tau.sl} = 5.618$

$\sigma_E := \frac{\pi^2 \cdot E \cdot t_w^2}{12 \cdot (1 - \nu^2) \cdot h_w^2} = 50.236\ MPa$

$\tau_{cr} := k_\tau \cdot \sigma_E = 282.206\ MPa$ (5.4)

$\lambda_w := 0.76 \cdot \left(\frac{f_y}{\tau_{cr}}\right)^{0.5} = 0.932$ (5.3)

$\frac{0.83}{\eta} = 0.692 \quad < \quad \lambda_w = 0.932 \quad < \quad 1.08$

$\chi_w := \frac{0.83}{\lambda_w} = 0.891$ According to table 5.1 in EN 1993-1-5

$V_{b.Rd} := \frac{\chi_w \cdot f_y \cdot h_w \cdot t_w}{3^{0.5} \cdot \gamma_{M1}} = 482.628\ kN \quad < \quad \frac{\eta \cdot f_y \cdot h_w \cdot t_w}{3^{0.5} \cdot \gamma_{M1}} = 650.023\ kN$ (5.1)

$$\frac{V_{Ed}}{V_{b.Rd}} = 0.159 \quad < \quad 1$$ OK

Moment at midspan

$c_f := \frac{b}{2} - \frac{t_w}{2} - r = 40\ mm$ Cross section classification of flenge in compression

$$\frac{c_f}{t_f \cdot \varepsilon} = 5.904 \quad < \quad 9$$ Cross sectional class 1 according to table 5.2

$c_w := h_w - 2 \cdot r = 344.8\ mm$

$c_{w1} := 72 \cdot \varepsilon \cdot t_w = 321.614\ mm \quad < \quad c_w = 344.8\ mm$

$c_{w2} := 83 \cdot \varepsilon \cdot t_w = 370.749\ mm \quad > \quad c_w = 344.8\ mm$ Cross sectional class 2 for web

$$M_{pl.Rd} := \frac{2 \cdot \left((b \cdot t_f) \cdot \left(\frac{h}{2} - \frac{t_f}{2} \right) + \frac{h_w}{2} \cdot t_w \cdot \frac{h_w}{4} \right) \cdot f_y}{\gamma_{M0}} = 246.894\ kN \cdot m$$ Plastic moment capacity at midspan

$$\frac{M_{mid}}{M_{pl.Rd}} = 0.434 \quad < \quad 1$$ OK according to (6.12)

Calculations according to EN 1993-1-13:

$a_{eff} := a_o = 300\ mm$ Defining effective opening length

$a_{eq} := a_o = 300\ mm$ Defining equivalent opening length

$h_{eq} := h_o = 250\ mm$ Defining equivalent opening height

Shear capacity at opening center, 8.2

$$V_{o.Pl.Rd} := V_{pl.Rd} - \frac{h_o \cdot t_w \cdot f_y}{3^{0.5} \cdot \gamma_{M0}} = 282.828\ kN$$

$$\frac{V_{Ed}}{V_{o.Pl.Rd}} = 0.271 \quad < \quad 1$$ OK according to (8.1)

$< \quad 0.5$ OK, do not have to reduce yield strength according to 8.2(2)

$\frac{h_w}{t_w} = 61.467$ > $72 \cdot \frac{\varepsilon}{\eta} = 44.669$ 8.5.1(3)

$h_o = 250\ mm$ > $15 \cdot t_w \cdot \varepsilon = 67.003\ mm$ 8.5.1(4)

Both 8.5.1(3) and 8.5.1(4) are fulfilled and thus control for buckling of web next to the opening have to be done

Buckling of web next to opening, 8.5.2

$b_w := 0.5 \cdot h_o = 125\ mm$ 8.5.2(3)

$\lambda_1 := \pi \cdot \left(\frac{E}{f_y}\right)^{0.5} = 69.916$ (8.21)

$\alpha := 0.21$ Imperfection factor for buckling curve according to EN 1993-1-1 table 6.1

$\lambda_{w.bar} := \frac{3.5 \cdot h_o}{t_w \cdot \lambda_1} = 2.086$ (8.20)

$\phi := 0.5 \cdot \left(1 + \alpha \cdot \left(\lambda_{w.bar} - 0.2\right) + \lambda_{w.bar}{}^2\right) = 2.873$

$\chi := \frac{1}{\phi + \left(\phi^2 - \lambda_{w.bar}{}^2\right)^{0.5}} = 0.206$ Buckling reduction factor according to EN 1993-1-1 (6.49)

$N_{w.Rd} := \chi \cdot b_w \cdot t_w \cdot \frac{f_y}{\gamma_{M1}} = 65.572\ kN$ (8.18)

$N_{w.Ed} := \frac{1}{2} V_{Ed} = 38.275\ kN$ According to (8.16) and (8.17)

$\frac{N_{w.Ed}}{N_{w.Rd}} = 0.584$ < 1 OK according to 8.5.2(1)

Moment capacity at opening, 8.3

$$c_{w.T} := \frac{h - 2 \cdot t_f - 2 \cdot r - h_o}{2} = 47.4 \ mm$$ Web outstands - global bending

$$\frac{c_{w.T}}{t_w \cdot \varepsilon} = 10.611 \quad < \quad 14$$ Cross sectional class 3

Since the flanges are classified as class 1, the web of the T-section that is subjected to compression can be taken as class 2 according to 7.4(2) if the effective depth of the outstand is set to the cross sectional class 2 limit according to EN 1993-1-1.

$$c_{w.T.eff} := 10 \cdot t_w \cdot \varepsilon = 44.669 \ mm$$

Calculations to find the plastic moment capacity:

$$h_{w.tT.eff} := c_{w.T.eff} + r = 56.669 \ mm$$ Height of effective web of top T

$$A_{w.tT.eff} := h_{w.tT.eff} \cdot t_w = 340.012 \ mm^2$$ Area of effective web of top T

$$A_f := b \cdot t_f = \left(1.001 \cdot 10^3\right) \ mm^2$$ Area of flange

$$A_{tT.eff} := A_f + A_{w.tT.eff} = \left(1.341 \cdot 10^3\right) \ mm^2$$ Total area of effective T neglecting area of root radius

$$z_{tT.eff} := \frac{A_f \cdot \frac{t_f}{2} + A_{w.tT.eff} \cdot \left(t_f + \frac{h_{w.tT.eff}}{2}\right)}{A_{tT.eff}} = 12.888 \ mm$$

In reality, there is a small difference between the top Tee and the bottom Tee because they have different depths. This is a small difference and is thus neglected.

$$M_{o.Rd} := \frac{\left(A_{tT.eff}\right) \cdot \left(h - 2 \cdot z_{tT.eff}\right) \cdot f_y}{\gamma_{M0}} = 205.388 \ kN \cdot m$$

$$\frac{M_{o.Ed}}{M_{o.Rd}} = 0.261 \quad < \quad 1$$ OK according to (8.5)

Buckling of T-section in compression

$$h_T := \frac{h - h_o}{2} = 68.5\ mm$$

$$a_{eff} = 300\ mm \quad < \quad 6 \cdot h_T \cdot \varepsilon \cdot \left(\frac{M_{o.Rd}}{M_{o.Ed}}\right)^{0.5} = 599.044\ mm$$

$$< \quad 12 \cdot h_T = 822\ mm$$

Do not need to check for buckling of T-section in compression according to 8.3.2(1) and 8.3.2(2).

Vierendeel-capacity, 8.4

$$c_{w.T.V} := \frac{h - 2 \cdot t_f - 2 \cdot r - h_o}{2} = 47.4\ mm$$

$$\frac{c_{w.T.V}}{t_w \cdot \varepsilon} = 10.611 \quad < \quad 14$$ The web outstand is classfied as class 3

$$a_{eff} = 300\ mm \quad > \quad 32 \cdot t_w \cdot \varepsilon = 142.939\ mm$$

The class 3 web outstand may be taken as class 2 for Vierendeel-bending if:

$$c_{w.T.V} = 47.4\ mm \quad < \quad \frac{10 \cdot t_w \cdot \varepsilon}{\left(1 - \left(\frac{32 \cdot t_w \cdot \varepsilon}{a_{eff}}\right)^2\right)^{0.5}} = 50.806\ mm \qquad (7.3)$$

Since (7.3) holds the Tee can be taken as class 2.

$$d_t := c_{w.T.V} = 47.4\ mm$$

Since the Tee's are regarded as class 2 the plastic capacity can be used.
Calculating the axial force in the Tee's as a result of global moment, and the capcaity of the Tee's in compression according to 8.4(6):

$h_{w.T.V} := d_t + r = 59.4\ mm$ Height of web of Tee's

$A_{w.T.V} := h_{w.T.V} \cdot t_w = 356.4\ mm^2$ Area of web of Tee's

$A_f := b \cdot t_f = \left(1.001 \cdot 10^3\right)\ mm^2$ Area of flange

$A_{T.V} := A_f + A_{w.T.V} = \left(1.357 \cdot 10^3\right)\ mm^2$ Total area of Tee's neglecting area of root radius

$$z_{T.V} := \frac{A_f \cdot \frac{t_f}{2} + A_{w.T.V} \cdot \left(t_f + \frac{h_{w.T.V}}{2}\right)}{A_{T.V}} = 13.543\ mm$$

$$N_{Ed} := \frac{M_{o.Ed}}{h - 2\ z_{T.V}} = 148.883\ kN$$ Axial force in Tee's as a result of global moment

$$N_{T.pl.Rd} := \frac{f_y \cdot A_{T.V}}{\gamma_{M0}} = 575.538\ kN$$ Axial capacity of Tee

$$z_{pl.T} := \frac{\frac{A_{T.V}}{2}}{b} = 6.17\ mm \quad < \quad t_f = 9.1\ mm$$ Plastic neutral axis of Tee's

Finding the cetnre of gravity of the part of the Tee's that is located "beneeth" the plastic neutral axis.

$$a_{web} := t_f - z_{pl.T} + \frac{h_{w.T.V}}{2} = 32.63\ mm$$

$$a_{flenge} := \frac{t_f - z_{pl.T}}{2} = 1.465\ mm$$

$$z_{Ab} := \frac{b \cdot \left(t_f - z_{pl.T}\right) \cdot a_{flenge} + A_{w.T.V} \cdot a_{web}}{\frac{A_{T.V}}{2}} = 17.83\ mm$$

$$M_{pl.T.Rd} := \left(\frac{A_{T.V}}{2} \cdot \frac{z_{pl.T}}{2} + \frac{A_{T.V}}{2} \cdot z_{Ab}\right) \cdot \frac{f_y}{\gamma_{M0}} = 6.019\ kN \cdot m$$ Plastic moment capacity of the Tee's.

$$M_{NV.T.Rd} := M_{pl.T.Rd} \cdot \left(1 - \left(\frac{N_{Ed}}{N_{T.pl.Rd}}\right)^2\right) = 5.616\ kN \cdot m$$ (8.11)

$$V_{vier.Rd} := \frac{4 \cdot M_{NV.T.Rd}}{a_{eq}} = 74.881\ kN$$ (8.10)

$$\frac{V_{Ed}}{V_{vier.Rd}} = 1.022 \quad =1$$ OK according to (8.9).

Thus the ultimate design load P according to EN 1993-1-13 is P=153.1 kN

Appendix D: Calculations on Specimen D according to EN 1993-1-13

Dimensions:

$L := 2800\ mm$ Span length
$h := 350\ mm$ Cross section height
$b := 100\ mm$ Flange width
$t_f := 8.5\ mm$ Flange thickness
$t_w := 5.6\ mm$ Web thickness
$r := 12\ mm$ Root radius

$h_o := 250\ mm$ Opening height

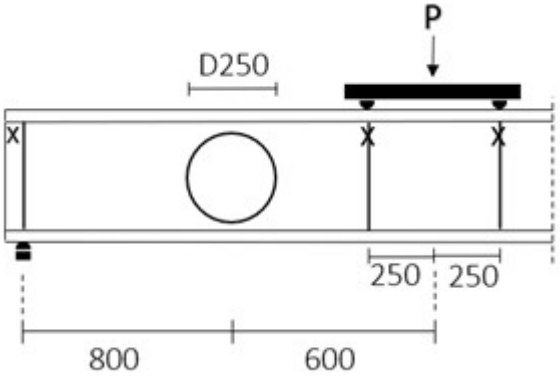

Material data:

$f_y := 417\ MPa$
$E := 210000\ MPa$
$\nu := 0.3$
$\varepsilon := \left(\frac{235\ MPa}{f_y}\right)^{0.5} = 0.751$
$\eta := 1.2$
$\gamma_{M0} := 1.0$
$\gamma_{M1} := 1.0$

Load:

$P := 173.1\ kN$ Ultimate design load according to EN 1993-1-13

$V_{Ed} := \frac{P}{2} = 86.55\ kN$ Shear load acting on cross section

$M_{o.Ed} := V_{Ed} \cdot 800\ mm = 69.24\ kN \cdot m$ Moment acting at centre of opening

$M_{mid} := V_{Ed} \cdot 1150\ mm = 99.533\ kN \cdot m$ Moment acting at midspan

Calculations according to EN 1993-1-1:

Shear capacity

$h_w := h - 2 \cdot t_f = 333\ mm$ Web height

$A := 2 \cdot b \cdot t_f + h_w \cdot t_w + 2 \cdot \frac{(2 \cdot r)^2 - \pi \cdot r^2}{2} = (3.688 \cdot 10^3)\ mm^2$ Gross area of cross section

$A_v := A - 2 \cdot b \cdot t_f + (t_w + 2 \cdot r) \cdot t_f = (2.24 \cdot 10^3)\ mm^2 \quad < \quad \eta \cdot h_w \cdot t_w = (2.238 \cdot 10^3)\ mm^2$

$A_v := \eta \cdot h_w \cdot t_w = (2.238 \cdot 10^3)\ mm^2$ Shear area

$V_{pl.Rd} := \frac{A_v \cdot f_y}{3^{0.5} \cdot \gamma_{M0}} = 538.752\ kN$ Plastic shear capacity according to (6.18)

$\frac{V_{Ed}}{V_{pl.Rd}} = 0.161 \quad < \quad 1$ OK, <0.5 do not have to reduce yield strength according 6.2.10(3)

$\frac{h_w}{t_w} = 59.464 \quad > \quad 72 \cdot \frac{\varepsilon}{\eta} = 45.042$ Need to check shear buckling according to EN 1993-1-5

Shear buckling

$a := \frac{L}{2} = (1.4 \cdot 10^3)\ mm$ Distance between vertical stiffeners

$\frac{a}{h_w} = 4.204$

$k_{\tau.sl} := 0$ No horizontal stiffeners

$k_\tau := 5.34 + 4 \cdot \left(\frac{h_w}{a}\right)^2 + k_{\tau.sl} = 5.566$

$\sigma_E := \frac{\pi^2 \cdot E \cdot t_w^2}{12 \cdot (1 - \nu^2) \cdot h_w^2} = 53.676\ MPa$

$\tau_{cr} := k_\tau \cdot \sigma_E = 298.78\ MPa$ (5.4)

$\lambda_w := 0.76 \cdot \left(\frac{f_y}{\tau_{cr}}\right)^{0.5} = 0.898$ (5.3)

$\frac{0.83}{\eta} = 0.692 \quad < \quad \lambda_w = 0.898 \quad < \quad 1.08$

$\chi_w := \frac{0.83}{\lambda_w} = 0.924$ According to table 5.1 in EN 1993-1-5

$V_{b.Rd} := \frac{\chi_w \cdot f_y \cdot h_w \cdot t_w}{3^{0.5} \cdot \gamma_{M1}} = 415.03\ kN \quad < \quad \frac{\eta \cdot f_y \cdot h_w \cdot t_w}{3^{0.5} \cdot \gamma_{M1}} = 538.752\ kN$ (5.1)

$$\frac{V_{Ed}}{V_{b.Rd}} = 0.209 \quad < \quad 1$$ OK

Moment at midspan

$c_f := \frac{b}{2} - \frac{t_w}{2} - r = 35.2\ mm$ Cross section classification of flenge in compression

$\frac{c_f}{t_f \cdot \varepsilon} = 5.516 \quad < \quad 9$ Cross sectional class 1 according to table 5.2

$c_w := h_w - 2 \cdot r = 309\ mm$

$c_{w1} := 72 \cdot \varepsilon \cdot t_w = 302.682\ mm \quad < \quad c_w = 309\ mm$

$c_{w2} := 83 \cdot \varepsilon \cdot t_w = 348.925\ mm \quad > \quad c_w = 309\ mm$ Cross sectional class 2 for web

$$M_{pl.Rd} := \frac{2 \cdot \left((b \cdot t_f) \cdot \left(\frac{h}{2} - \frac{t_f}{2} \right) + \frac{h_w}{2} \cdot t_w \cdot \frac{h_w}{4} \right) \cdot f_y}{\gamma_{M0}} = 185.782\ kN \cdot m$$ Plastic moment capacity at midspan

$\frac{M_{mid}}{M_{pl.Rd}} = 0.536 \quad < \quad 1$ OK according to (6.12)

Calculations according to EN 1993-1-13:

$a_{eff} := 0.7\ h_o = 175\ mm$ Defining effective opening length

$a_{eq} := 0.45 \cdot h_o = 112.5\ mm$ Defining equivalent opening length

$h_{eq} := 0.9 \cdot h_o = 225\ mm$ Defining equivalent opening height

Shear capacity at opening center, 8.2

$$V_{o.Pl.Rd} := V_{pl.Rd} - \frac{h_o \cdot t_w \cdot f_y}{3^{0.5} \cdot \gamma_{M0}} = 201.695\ kN$$

$\frac{V_{Ed}}{V_{o.Pl.Rd}} = 0.429 \quad < \quad 1$ OK according to (8.1)

$< \quad 0.5$ OK, do not have to reduce yield strength according to 8.2(2)

$\frac{h_w}{t_w} = 59.464$ > $72 \cdot \frac{\varepsilon}{\eta} = 45.042$ 8.5.1(3)

$h_o = 250\ mm$ > $25 \cdot t_w \cdot \varepsilon = 105.098\ mm$ 8.5.1(4)

Both 8.5.1(3) and 8.5.1(4) are fulfilled and thus control for buckling of web next to the opening have to be done

Buckling of web next to opening, 8.5.2

$b_w := 0.5 \cdot h_o = 125\ mm$ 8.5.2(3)

$\lambda_1 := \pi \cdot \left(\frac{E}{f_y}\right)^{0.5} = 70.5$ (8.21)

$\alpha := 0.21$ Imperfection factor for buckling curve according to EN 1993-1-1 table 6.1

$\lambda_{w.bar} := \frac{2.4 \cdot h_o}{t_w \cdot \lambda_1} = 1.52$ (8.20)

$\phi := 0.5 \cdot \left(1 + \alpha \cdot \left(\lambda_{w.bar} - 0.2\right) + {\lambda_{w.bar}}^2\right) = 1.793$

$\chi := \frac{1}{\phi + \left(\phi^2 - {\lambda_{w.bar}}^2\right)^{0.5}} = 0.364$ Buckling reduction factor according to EN 1993-1-1 (6.49)

$N_{w.Rd} := \chi \cdot b_w \cdot t_w \cdot \frac{f_y}{\gamma_{M1}} = 106.317\ kN$ (8.18)

$N_{w.Ed} := \frac{1}{2} V_{Ed} = 43.275\ kN$ According to (8.16) and (8.17)

$\frac{N_{w.Ed}}{N_{w.Rd}} = 0.407$ < 1 OK according to 8.5.2(1)

Moment capacity at opening, 8.3

$$c_{w.T} := \frac{h - 2 \cdot t_f - 2 \cdot r - h_o}{2} = 29.5 \ mm$$ Web outstands - global bending

$$\frac{c_{w.T}}{t_w \cdot \varepsilon} = 7.017 \quad < \quad 9$$ Cross sectional class 1

Calculations to find the plastic moment capacity:

$h_{w.tT} := c_{w.T} + r = 41.5 \ mm$ Height of web of top T

$A_{w.tT} := h_{w.tT} \cdot t_w = 232.4 \ mm^2$ Area of web of top T

$A_f := b \cdot t_f = 850 \ mm^2$ Area of flange

$A_{tT} := A_f + A_{w.tT} = \left(1.082 \cdot 10^3\right) \ mm^2$ Total area of T neglecting area of root radius

$$z_{tT} := \frac{A_f \cdot \frac{t_f}{2} + A_{w.tT} \cdot \left(t_f + \frac{h_{w.tT}}{2}\right)}{A_{tT}} = 9.618 \ mm$$ Elastic neutral axis depth from outer edge of flange

$$M_{o.Rd} := \frac{A_{tT} \cdot \left(h - 2 \cdot z_{tT}\right) \cdot f_y}{\gamma_{M0}} = 149.294 \ kN \cdot m$$

$\frac{M_{o.Ed}}{M_{o.Rd}} = 0.464 \quad < \quad 1$ OK according to (8.5)

Buckling of T-section in compression

$$h_T := \frac{h - h_o}{2} = 50 \ mm$$

$$a_{eff} = 175 \ mm \quad < \quad 6 \cdot h_T \cdot \varepsilon \cdot \left(\frac{M_{o.Rd}}{M_{o.Ed}}\right)^{0.5} = 330.697 \ mm$$

$$< \quad 12 \cdot h_T = 600 \ mm$$

Do not need to check for buckling of T-section in compression according to 8.3.2(1) and 8.3.2(2).

Vierendeel-capacity, 8.4

$$c_{w.T.V} := \frac{h - 2 \cdot t_f - 2 \cdot r - h_o}{2} = 29.5 \ mm$$

$$\frac{c_{w.T.V}}{t_w \cdot \varepsilon} = 7.017 \quad < \quad 9$$ The web outstand is classfied as class 1

$$d_t := c_{w.T.V} = 29.5 \ mm$$

Since the Tee's are regarded as class 1 the plastic capacity can be used.
Calculating the axial force in the Tee's as a result of global moment, and the capcaity of the Tee's in compression according to 8.4(6):

$z_T := z_{tT} = 9.618 \ mm$ Elastic neutral axis of Tee's meassured from outside of flange

$$N_{Ed} := \frac{M_{o.Ed}}{h - 2 \ z_T} = 209.333 \ kN$$ Axial force in Tee's as a result of global moment

$$A_T := A_{tT} = \left(1.082 \cdot 10^3\right) \ mm^2$$

$$N_{T.pl.Rd} := \frac{f_y \cdot A_T}{\gamma_{M0}} = 451.361 \ kN$$ Axial capacity of Tee

$$h_{w.T.V} := d_t + r = 41.5 \ mm$$

$$A_{w.T.V} := h_{w.T.V} \cdot t_w = 232.4 \ mm^2$$

$$A_{T.V} := A_f + A_{w.T.V} = \left(1.082 \cdot 10^3\right) \ mm^2$$

$$z_{pl.T} := \frac{\frac{A_{T.V}}{2}}{b} = 5.412 \ mm \quad < \quad t_f = 8.5 \ mm$$ Plastic neutral axis of Tee's negelcting root radius

Have to find the cetnre of gravity of the part of the Tee's that is located "beneeth" the plastic neutral axis

$$a_{web} := t_f - z_{pl.T} + \frac{h_{w.T.V}}{2} = 23.838 \ mm$$

$$a_{flenge} := \frac{t_f - z_{pl.T}}{2} = 1.544 \ mm$$

$$z_{Ab} := \frac{b \cdot \left(t_f - z_{pl.T}\right) \cdot a_{flenge} + A_{w.T.V} \cdot a_{web}}{\frac{A_{T.V}}{2}} = 11.117\ mm$$

$$M_{pl.T.Rd} := \left(\frac{A_{T.V}}{2} \cdot \frac{z_{pl.T}}{2} + \frac{A_{T.V}}{2} \cdot z_{Ab}\right) \cdot \frac{f_y}{\gamma_{M0}} = 3.12\ kN \cdot m$$

Plastic moment capacity of the Tee's.

$$M_{NV.T.Rd} := M_{pl.T.Rd} \cdot \left(1 - \left(\frac{N_{Ed}}{N_{T.pl.Rd}}\right)^2\right) = 2.449\ kN \cdot m \quad (8.11)$$

$$V_{vier.Rd} := \frac{4 \cdot M_{NV.T.Rd}}{a_{eq}} = 87.063\ kN \quad (8.10)$$

$$\frac{V_{Ed}}{V_{vier.Rd}} = 0.994 \quad = 1$$

OK according to (8.9).

Thus the ultimate design load P according to EN 1993-1-13 is P=173.1kN

Appendix E: Calculations on Specimen E according to EN 1993-1-13

Dimensions:

$L := 2800\ mm$	Span length
$h := 350\ mm$	Cross section height
$b := 100\ mm$	Flange width
$t_f := 8.5\ mm$	Flange thickness
$t_w := 5.6\ mm$	Web thickness
$r := 12\ mm$	Root radius
$h_o := 200\ mm$	Opening height
$s_o := 50\ mm$	Distance between openings

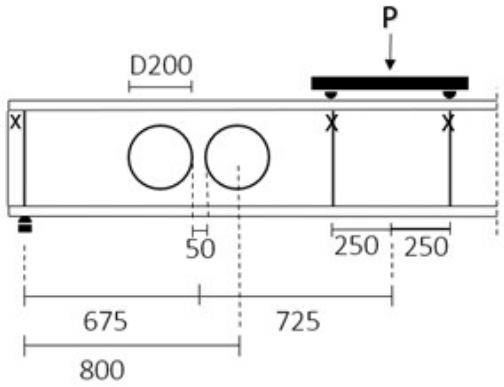

Material data:

$f_y := 417\ MPa$

$E := 210000\ MPa$

$\nu := 0.3$

$$\varepsilon := \left(\frac{235\ MPa}{f_y}\right)^{0.5} = 0.751$$

$\eta := 1.2$

$\gamma_{M0} := 1.0$

$\gamma_{M1} := 1.0$

Load:

$P := 174.5\ kN$ — Ultimate design load according to EN 1993-1-13

$V_{Ed} := \frac{P}{2} = 87.25\ kN$ — Shear load acting on cross section

$M_{o.Ed} := V_{Ed} \cdot 800\ mm = 69.8\ kN \cdot m$ — Largest moment acting at centre of opening

$M_{so.Ed} := V_{Ed} \cdot 675\ mm = 58.894\ kN \cdot m$ — Moment acting inbetween openings

$M_{mid} := V_{Ed} \cdot 1150\ mm = 100.338\ kN \cdot m$ — Moment acting at midspan

Calculations according to EN 1993-1-1:

Shear capacity

$h_w := h - 2 \cdot t_f = 333\ mm$ Web height

$A := 2 \cdot b \cdot t_f + h_w \cdot t_w + 2 \cdot \frac{(2 \cdot r)^2 - \pi \cdot r^2}{2} = (3.688 \cdot 10^3)\ mm^2$ Gross area of cross section

$A_v := A - 2 \cdot b \cdot t_f + (t_w + 2 \cdot r) \cdot t_f = (2.24 \cdot 10^3)\ mm^2 \quad < \quad \eta \cdot h_w \cdot t_w = (2.238 \cdot 10^3)\ mm^2$

$A_v := \eta \cdot h_w \cdot t_w = (2.238 \cdot 10^3)\ mm^2$ Shear area

$V_{pl.Rd} := \frac{A_v \cdot f_y}{3^{0.5} \cdot \gamma_{M0}} = 538.752\ kN$ Plastic shear capacity according to (6.18)

$\frac{V_{Ed}}{V_{pl.Rd}} = 0.162 \quad < \quad 1$ OK, <0.5 do not have to reduce yield strength according 6.2.10(3)

$\frac{h_w}{t_w} = 59.464 \quad > \quad 72 \cdot \frac{\varepsilon}{\eta} = 45.042$ Need to check shear buckling according to EN 1993-1-5

Shear buckling

$a := \frac{L}{2} = (1.4 \cdot 10^3)\ mm$ Distance between vertical stiffeners

$\frac{a}{h_w} = 4.204$

$k_{\tau.sl} := 0$ No horizontal stiffeners

$k_\tau := 5.34 + 4 \cdot \left(\frac{h_w}{a}\right)^2 + k_{\tau.sl} = 5.566$

$\sigma_E := \frac{\pi^2 \cdot E \cdot t_w^2}{12 \cdot (1 - \nu^2) \cdot h_w^2} = 53.676\ MPa$

$\tau_{cr} := k_\tau \cdot \sigma_E = 298.78\ MPa$ (5.4)

$\lambda_w := 0.76 \cdot \left(\frac{f_y}{\tau_{cr}}\right)^{0.5} = 0.898$ (5.3)

$\frac{0.83}{\eta} = 0.692 \quad < \quad \lambda_w = 0.898 \quad < \quad 1.08$

$\chi_w := \frac{0.83}{\lambda_w} = 0.924$ According to table 5.1 in EN 1993-1-5

$V_{b.Rd} := \frac{\chi_w \cdot f_y \cdot h_w \cdot t_w}{3^{0.5} \cdot \gamma_{M1}} = 415.03\ kN \quad < \quad \frac{\eta \cdot f_y \cdot h_w \cdot t_w}{3^{0.5} \cdot \gamma_{M1}} = 538.752\ kN$ (5.1)

$\frac{V_{Ed}}{V_{b.Rd}} = 0.21$ < 1 OK

Moment at midspan

$c_f := \frac{b}{2} - \frac{t_w}{2} - r = 35.2\ mm$ Cross section classification of flenge in compression

$\frac{c_f}{t_f \cdot \varepsilon} = 5.516$ < 9 Cross sectional class 1 according to table 5.2

$c_w := h_w - 2 \cdot r = 309\ mm$

$c_{w1} := 72 \cdot \varepsilon \cdot t_w = 302.682\ mm$ < $c_w = 309\ mm$

$c_{w2} := 83 \cdot \varepsilon \cdot t_w = 348.925\ mm$ > $c_w = 309\ mm$ Cross sectional class 2 for web

$M_{pl.Rd} := \frac{2 \cdot \left((b \cdot t_f) \cdot \left(\frac{h}{2} - \frac{t_f}{2} \right) + \frac{h_w}{2} \cdot t_w \cdot \frac{h_w}{4} \right) \cdot f_y}{\gamma_{M0}} = 185.782\ kN \cdot m$ Plastic moment capacity at midspan

$\frac{M_{mid}}{M_{pl.Rd}} = 0.54$ < 1 OK according to (6.12)

Calculations according to EN 1993-1-13:

$a_{eff} := 0.7\ h_o = 140\ mm$ Defining effective opening length

$a_{eq} := 0.45 \cdot h_o = 90\ mm$ Defining equivalent opening length

$h_{eq} := 0.9 \cdot h_o = 180\ mm$ Defining equivalent opening height

Shear capacity at opening center, 8.2

$V_{o.Pl.Rd} := V_{pl.Rd} - \frac{h_o \cdot t_w \cdot f_y}{3^{0.5} \cdot \gamma_{M0}} = 269.106\ kN$

$\frac{V_{Ed}}{V_{o.Pl.Rd}} = 0.324$ < 1 OK according to (8.1)

< 0.5 OK, do not have to reduce yield strength according to 8.2(2)

$\frac{h_w}{t_w} = 59.464$ > $72 \cdot \frac{\varepsilon}{\eta} = 45.042$ 8.5.1(3)

$h_o = 200\ mm$ > $25 \cdot t_w \cdot \varepsilon = 105.098\ mm$ 8.5.1(4)

Both 8.5.1(3) and 8.5.1(4) are fulfilled and thus control for buckling of web next to the opening have to be done

Buckling of web next to opening, 8.5.2

$b_w := 0.5 \cdot h_o = 100\ mm$ 8.5.2(3)

$\lambda_1 := \pi \cdot \left(\frac{E}{f_y}\right)^{0.5} = 70.5$ (8.21)

$\alpha := 0.21$ Imperfection factor for buckling curve according to EN 1993-1-1 table 6.1

$\lambda_{w.bar} := \frac{2.4 \cdot h_o}{t_w \cdot \lambda_1} = 1.216$ (8.20)

$\phi := 0.5 \cdot \left(1 + \alpha \cdot \left(\lambda_{w.bar} - 0.2\right) + {\lambda_{w.bar}}^2\right) = 1.346$

$\chi := \frac{1}{\phi + \left(\phi^2 - {\lambda_{w.bar}}^2\right)^{0.5}} = 0.52$ Buckling reduction factor according to EN 1993-1-1 (6.49)

$N_{w.Rd} := \chi \cdot b_w \cdot t_w \cdot \frac{f_y}{\gamma_{M1}} = 121.456\ kN$ (8.18)

$N_{w.Ed} := \frac{1}{2} V_{Ed} = 43.625\ kN$ According to (8.16) and (8.17)

$\frac{N_{w.Ed}}{N_{w.Rd}} = 0.359$ < 1 OK according to 8.5.2(1)

Moment capacity at opening, 8.3

$c_{w.T} := \frac{h - 2 \cdot t_f - 2 \cdot r - h_o}{2} = 54.5\ mm$ Web outstands - global bending

$\frac{c_{w.T}}{t_w \cdot \varepsilon} = 12.964 \quad < \quad 14$ Cross sectional class 3

Since the flanges are classified as class 1, the web of the T-section that is subjected to compression can be taken as class 2 according to 7.4(2) if the effective depth of the outstand is set to the cross sectional class 2 limit according to EN 1993-1-1.

$c_{w.T.eff} := 10 \cdot t_w \cdot \varepsilon = 42.039\ mm$

Calculations to find the plastic moment capacity:

$h_{w.tT.eff} := c_{w.T} + r = 66.5\ mm$ Height of effective web of top T

$A_{w.tT.eff} := h_{w.tT.eff} \cdot t_w = 372.4\ mm^2$ Area of effective web of top T

$A_f := b \cdot t_f = 850\ mm^2$ Area of flange

$A_{tT.eff} := A_f + A_{w.tT.eff} = \left(1.222 \cdot 10^3\right)\ mm^2$ Total area of effective T neglecting area of root radius

$z_{tT} := \frac{A_f \cdot \frac{t_f}{2} + A_{w.tT.eff} \cdot \left(t_f + \frac{h_{w.tT.eff}}{2}\right)}{A_{tT.eff}} = 15.674\ mm$ Elastic neutral axis depth from outer edge of flange

$M_{o.Rd} := \frac{A_{tT.eff} \cdot \left(h - 2 \cdot z_{tT}\right) \cdot f_y}{\gamma_{M0}} = 162.43\ kN \cdot m$

$\frac{M_{o.Ed}}{M_{o.Rd}} = 0.43 \quad < \quad 1$ OK according to (8.5)

Buckling of T-section in compression

$h_T := \frac{h - h_o}{2} = 75\ mm$

$a_{eff} = 140\ mm \quad < \quad 6 \cdot h_T \cdot \varepsilon \cdot \left(\frac{M_{o.Rd}}{M_{o.Ed}}\right)^{0.5} = 515.328\ mm$

$< \quad 12 \cdot h_T = 900\ mm$

Do not need to check for buckling of T-section in compression according to 8.3.2(1) and 8.3.2(2).

Vierendeel-capacity, 8.3

$$c_{w.T.V} := \frac{h - 2 \cdot t_f - 2 \cdot r - h_o}{2} = 54.5 \ mm$$

$$\frac{c_{w.T.V}}{t_w \cdot \varepsilon} = 12.964 \quad < \quad 14$$ The web outstand is classfied as class 3

$$a_{eff} = 140 \ mm \quad > \quad 32 \cdot t_w \cdot \varepsilon = 134.525 \ mm$$

The class 3 web outstand may be taken as class 2 for Vierendeel-bending if:

$$c_{w.T.V} = 54.5 \ mm \quad < \quad \frac{10 \cdot t_w \cdot \varepsilon}{\left(1 - \left(\frac{32 \cdot t_w \cdot \varepsilon}{a_{eff}}\right)^2\right)^{0.5}} = 151.813 \ mm \qquad (7.3)$$

Since (7.3) holds the Tee can be taken as class 2.

$$d_t := c_{w.T.V} = 54.5 \ mm$$

Since the Tee's are regarded as class 2 the plastic capacity can be used.
Calculating the axial force in the Tee's as a result of global moment, and the capcaity of the Tee's in compression according to 8.4(6):

$h_{w.T.V} := d_t + r = 66.5 \ mm$ Height of web of Tee's

$A_{w.T.V} := h_{w.T.V} \cdot t_w = 372.4 \ mm^2$ Area of web of Tee's

$A_f := b \cdot t_f = 850 \ mm^2$ Area of flange

$A_{T.V} := A_f + A_{w.T.V} = \left(1.222 \cdot 10^3\right) \ mm^2$ Total area of Tee's neglecting area of root radius

$$z_{T.V} := \frac{A_f \cdot \frac{t_f}{2} + A_{w.T.V} \cdot \left(t_f + \frac{h_{w.T.V}}{2}\right)}{A_{T.V}} = 15.674 \ mm$$ Elastic neutral axis of Tee from outside of flange

$$N_{Ed} := \frac{M_{o.Ed}}{h - 2 \ z_{T.V}} = 219.048 \ kN$$ Axial force in Tee's as a result of global moment

$$N_{T.pl.Rd} := \frac{f_y \cdot A_{T.V}}{\gamma_{M0}} = 509.741\ kN$$ Axial capacity of Tee

$$z_{pl.T} := \frac{\frac{A_{T.V}}{2}}{b} = 6.112\ mm \quad < \quad t_f = 8.5\ mm$$ Plastic neutral axis of Tee's

Finding the cetnre of gravity of the part of the Tee's that is located "beneeth" the plastic neutral axis.

$$a_{web} := t_f - z_{pl.T} + \frac{h_{w.T.V}}{2} = 35.638\ mm$$

$$a_{flenge} := \frac{t_f - z_{pl.T}}{2} = 1.194\ mm$$

$$z_{Ab} := \frac{b \cdot \left(t_f - z_{pl.T}\right) \cdot a_{flenge} + A_{w.T.V} \cdot a_{web}}{\frac{A_{T.V}}{2}} = 22.18\ mm$$

$$M_{pl.T.Rd} := \left(\frac{A_{T.V}}{2} \cdot \frac{z_{pl.T}}{2} + \frac{A_{T.V}}{2} \cdot z_{Ab}\right) \cdot \frac{f_y}{\gamma_{M0}} = 6.432\ kN \cdot m$$ Plastic moment capacity of the Tee's.

$$M_{NV.T.Rd} := M_{pl.T.Rd} \cdot \left(1 - \left(\frac{N_{Ed}}{N_{T.pl.Rd}}\right)^2\right) = 5.244\ kN \cdot m$$ (8.11)

$$V_{vier.Rd} := \frac{4 \cdot M_{NV.T.Rd}}{a_{eq}} = 233.079\ kN$$ (8.10)

$$\frac{V_{Ed}}{V_{vier.Rd}} = 0.374$$ =1 OK according to (8.9).

Web-post buckling, 8.6.3

$$\lambda_{wp.bar} := \frac{1.75 \cdot \left(s_o{}^2 + h_o{}^2\right)^{0.5}}{t_w} \cdot \frac{1}{\lambda_1} = 0.914 \quad < \quad \frac{2.4 \cdot h_o}{t_w} \cdot \frac{1}{\lambda_1} = 1.216 \qquad (8.30)$$

$\alpha := 0.21$ Imperfection factor for buckling curve according to EN 1993-1-1 table 6.1

$$\phi := 0.5 \cdot \left(1 + \alpha \cdot \left(\lambda_{wp.bar} - 0.2\right) + \lambda_{wp.bar}{}^2\right) = 0.992$$

$$\chi_{wp} := \frac{1}{\phi + \left(\phi^2 - \lambda_{wp.bar}{}^2\right)^{0.5}} = 0.725$$ Buckling reduction factor according to EN 1993-1-1 (6.49)

$$N_{wp.Rd} := s_o \cdot t_w \cdot \chi_{wp} \cdot \frac{f_y}{\gamma_{M1}} = 84.627\ \mathit{kN}$$ (8.29) Web-post buckling capacity

$$\Delta M := V_{Ed} \cdot \left(800\ \mathit{mm} - 550\ \mathit{mm}\right) = 21.813\ \mathit{kN} \cdot \mathit{m}$$

$$\Delta N_{Ed.T} := \frac{\Delta M}{h - 2 \cdot z_{T.V}} = 68.453\ \mathit{kN}$$

$N_{wp.Ed} := \Delta N_{Ed.T} = 68.453\ \mathit{kN}$ Web-post buckling load according to figure 8.3

$\frac{N_{wp.Ed}}{N_{wp.Rd}} = 0.809$ <1 OK (8.26)

Web-post shear, 8.6.4

$$V_{wp.Rd} := s_o \cdot t_w \cdot \frac{f_y}{3^{0.5} \cdot \gamma_{M0}} = 67.411\ \mathit{kN}$$ (8.34)

$V_{wp.Ed} := \Delta N_{Ed.T} = 68.453\ \mathit{kN}$ Web-post shear load according to figure 8.3

$\frac{V_{wp.Ed}}{V_{wp.Rd}} = 1.015$ =1 OK (8.33)

Thus the ultimate design load P according to EN 1993-1-13 is P=174.5 kN

Appendix F: Calculations on Specimen C with proposed interaction of moment and axial forces

Dimensions:

$L := 2800\ mm$ Span length
$h := 387\ mm$ Cross section height
$b := 110\ mm$ Flange width
$t_f := 9.1\ mm$ Flange thickness
$t_w := 6\ mm$ Web thickness
$r := 12\ mm$ Root radius

$h_o := 250\ mm$ Opening height
$a_o := 300\ mm$ Opening length
$r_o := 100\ mm$ Opening corner radius

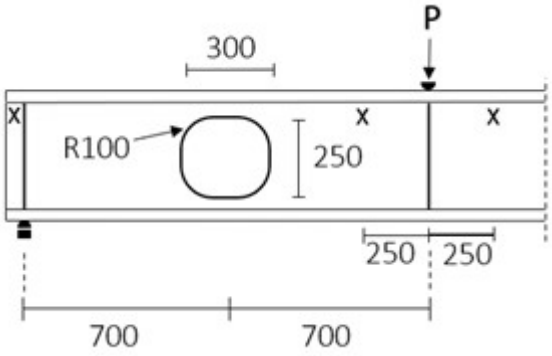

Material data:

$f_y := 445\ MPa$ Same yield strenght that was used in the FE analyses.

$E := 210000\ MPa$
$\nu := 0.3$
$\varepsilon := \left(\frac{235\ MPa}{f_y}\right)^{0.5} = 0.727$
$\eta := 1.2$
$\gamma_{M0} := 1.0$
$\gamma_{M1} := 1.0$

Vierendeel-capacity, 8.4

$a_{eff} := a_o = 300\ mm$ Defining effective opening length

$$c_{w.T.V} := \frac{h - 2 \cdot t_f - 2 \cdot r - h_o}{2} = 47.4\ mm$$

$$\frac{c_{w.T.V}}{t_w \cdot \varepsilon} = 10.871 \quad < \quad 14$$ The web outstand is classfied as class 3

$$a_{eff} = 300\ mm \quad > \quad 32 \cdot t_w \cdot \varepsilon = 139.526\ mm$$

The class 3 web outstand may be taken as class 2 for Vierendeel-bending if:

$$c_{w.T.V} = 47.4\ mm \quad < \quad \frac{10 \cdot t_w \cdot \varepsilon}{\left(1 - \left(\frac{32 \cdot t_w \cdot \varepsilon}{a_{eff}}\right)^2\right)^{0.5}} = 49.253\ mm \qquad (7.3)$$

Since (7.3) holds the Tee can be taken as class 2.

$d_t := c_{w.T.V} = 47.4\ mm$

Since the Tee's are regarded as class 2 the plastic capacity can be used.
Calculating the axial force in the Tee's as a result of global moment, and the capcaity of the Tee's in compression according to 8.4(6):

$h_{w.T.V} := d_t + r = 59.4\ mm$ Height of web of Tee's

$A_{w.T.V} := h_{w.T.V} \cdot t_w = 356.4\ mm^2$ Area of web of Tee's

$A_f := b \cdot t_f = \left(1.001 \cdot 10^3\right)\ mm^2$ Area of flange

$A_{T.V} := A_f + A_{w.T.V} = \left(1.357 \cdot 10^3\right)\ mm^2$ Total area of Tee's neglecting area of root radius

$$z_{T.V} := \frac{A_f \cdot \frac{t_f}{2} + A_{w.T.V} \cdot \left(t_f + \frac{h_{w.T.V}}{2}\right)}{A_{T.V}} = 13.543\ mm$$

$N_{T.pl.Rd} := \frac{f_y \cdot A_{T.V}}{\gamma_{M0}} = 604.043\ kN$ Axial capacity of Tee

$$z_{pl.T} := \frac{\frac{A_{T.V}}{2}}{b} = 6.17\ mm \quad < \quad t_f = 9.1\ mm$$ Plastic neutral axis of Tee's

Finding the cetnre of gravity of the part of the Tee's that is located "beneeth" the plastic neutral axis.

$$a_{web} := t_f - z_{pl.T} + \frac{h_{w.T.V}}{2} = 32.63\ mm$$

$$a_{flenge} := \frac{t_f - z_{pl.T}}{2} = 1.465\ mm$$

$$z_{Ab} := \frac{b \cdot \left(t_f - z_{pl.T}\right) \cdot a_{flenge} + A_{w.T.V} \cdot a_{web}}{\frac{A_{T.V}}{2}} = 17.83\ mm$$

$$M_{pl.T.Rd} := \left(\frac{A_{T.V}}{2} \cdot \frac{z_{pl.T}}{2} + \frac{A_{T.V}}{2} \cdot z_{Ab}\right) \cdot \frac{f_y}{\gamma_{M0}} = 6.317\ kN \cdot m$$

Plastic moment capacity of the Tee's.

0% global axial force:

$$P_{0.0} := 158\ kN$$

Ultimate design load taking into account global axial forces

$$V_{Ed} := \frac{P_{0.0}}{2} = 79\ kN$$

Shear load acting on cross section

$$M_{o.Ed} := V_{Ed} \cdot 700\ mm = 55.3\ kN \cdot m$$

Moment acting at center of opening

$$N_{m.Ed} := \frac{M_{o.Ed}}{h - 2\ z_{T.V}} = 153.648\ kN$$

Axial force in Tee's as a result of global moment and global axial forces

$$M_{NV.T.Rd} := M_{pl.T.Rd} \cdot \left(1 - \left(\frac{N_{m.Ed}}{N_{T.pl.Rd}}\right)^2\right) = 5.908\ kN \cdot m$$

Plastic moment capacity in Tees reduced for axial forces from global moment and global axial loading

$$V_{vier.Rd} := \frac{4 \cdot M_{NV.T.Rd}}{a_o} = 78.776\ kN$$

$$\frac{V_{Ed}}{V_{vier.Rd}} = 1.003$$

=1

Check for Vierendeel-capacity

10% global axial force:

$h_w := h - t_f = 377.9\ mm$

$A_{tot} := h_w \cdot t_w + 2 \cdot b \cdot t_f = \left(4.269 \cdot 10^3\right)\ mm^2$

$A_{net} := A_{tot} - h_o \cdot t_w = \left(2.769 \cdot 10^3\right)\ mm^2$ Area of net cross section

$N_{Pl.Rd} := A_{net} \cdot f_y = \left(1.232 \cdot 10^3\right)\ kN$ Axial capacity of net cross section

$N_{0.1} := 0.1 \cdot N_{Pl.Rd} = 123.238\ kN$ Global axial load

$P_{0.1} := 149.8\ kN$ Ultimate design load taking into account global axial forces

$V_{Ed} := \frac{P_{0.1}}{2} = 74.9\ kN$ Shear load acting on cross section

$M_{o.Ed} := V_{Ed} \cdot 700\ mm = 52.43\ kN \cdot m$ Moment acting at center of opening

$N_{m.Ed} := \frac{M_{o.Ed}}{h - 2\ z_{T.V}} + \frac{N_{0.1}}{2} = 207.293\ kN$ Axial force in Tee's as a result of global moment and global axial forces

$M_{NV.T.Rd} := M_{pl.T.Rd} \cdot \left(1 - \left(\frac{N_{m.Ed}}{N_{T.pl.Rd}}\right)^2\right) = 5.573\ kN \cdot m$ Plastic moment capacity in Tees reduced for axial forces from global moment and global axial loading

$V_{vier.Rd} := \frac{4 \cdot M_{NV.T.Rd}}{a_o} = 74.306\ kN$

$\frac{V_{Ed}}{V_{vier.Rd}} = 1.008$ $=1$ Check for Vierendeel-capacity

20% global axial force:

$N_{0.2} := 0.2 \cdot N_{Pl.Rd} = 246.477\ kN$ Global axial load

$P_{0.2} := 137.3\ kN$ Ultimate design load taking into account global axial forces

$V_{Ed} := \frac{P_{0.2}}{2} = 68.65\ kN$ Shear load acting on cross section

$M_{o.Ed} := V_{Ed} \cdot 700\ mm = 48.055\ kN \cdot m$ Moment acting at center of opening

$N_{m.Ed} := \frac{M_{o.Ed}}{h - 2\ z_{T.V}} + \frac{N_{0.2}}{2} = 256.756\ kN$ Axial force in Tee's as a result of global moment and global axial forces

$M_{NV.T.Rd} := M_{pl.T.Rd} \cdot \left(1 - \left(\frac{N_{m.Ed}}{N_{T.pl.Rd}}\right)^2\right) = 5.176\ kN \cdot m$ Plastic moment capacity in Tees reduced for axial forces from global moment and global axial loading

$V_{vier.Rd} := \frac{4 \cdot M_{NV.T.Rd}}{a_o} = 69.008\ kN$

$\frac{V_{Ed}}{V_{vier.Rd}} = 0.995$ =1 Check for Vierendeel-capacity

30% global axial force:

$N_{0.3} := 0.3 \cdot N_{Pl.Rd} = 369.715\ kN$ Global axial load

$P_{0.3} := 125.2\ kN$ Ultimate design load taking into account global axial forces

$V_{Ed} := \frac{P_{0.3}}{2} = 62.6\ kN$ Shear load acting on cross section

$M_{o.Ed} := V_{Ed} \cdot 700\ mm = 43.82\ kN \cdot m$ Moment acting at center of opening

$N_{m.Ed} := \frac{M_{o.Ed}}{h - 2\ z_{T.V}} + \frac{N_{0.3}}{2} = 306.609\ kN$ Axial force in Tee's as a result of global moment and global axial forces

$M_{NV.T.Rd} := M_{pl.T.Rd} \cdot \left(1 - \left(\frac{N_{m.Ed}}{N_{T.pl.Rd}}\right)^2\right) = 4.689\ kN \cdot m$ Plastic moment capacity in Tees reduced for axial forces from global moment and global axial loading

$V_{vier.Rd} := \frac{4 \cdot M_{NV.T.Rd}}{a_o} = 62.525\ kN$

$\frac{V_{Ed}}{V_{vier.Rd}} = 1.001$ =1 Check for Vierendeel-capacity

40% global axial force:

$N_{0.4} := 0.4 \cdot N_{Pl.Rd} = 492.953\ kN$ Global axial load

$P_{0.4} := 110.5\ kN$ Ultimate design load taking into account global axial forces

$V_{Ed} := \frac{P_{0.4}}{2} = 55.25\ kN$ Shear load acting on cross section

$M_{o.Ed} := V_{Ed} \cdot 700\ mm = 38.675\ kN \cdot m$ Moment acting at center of opening

$N_{m.Ed} := \frac{M_{o.Ed}}{h - 2\ z_{T.V}} + \frac{N_{0.4}}{2} = 353.933\ kN$ Axial force in Tee's as a result of global moment and global axial forces

$M_{NV.T.Rd} := M_{pl.T.Rd} \cdot \left(1 - \left(\frac{N_{m.Ed}}{N_{T.pl.Rd}}\right)^2\right) = 4.148\ kN \cdot m$ Plastic moment capacity in Tees reduced for axial forces from global moment and global axial loading

$V_{vier.Rd} := \frac{4 \cdot M_{NV.T.Rd}}{a_o} = 55.309\ kN$

$\frac{V_{Ed}}{V_{vier.Rd}} = 0.999$ =1 Check for Vierendeel-capacity

50% global axial force:

$N_{0.5} := 0.5 \cdot N_{Pl.Rd} = 616.192\ kN$ Global axial load

$P_{0.5} := 94.4\ kN$ Ultimate design load taking into account global axial forces

$V_{Ed} := \frac{P_{0.5}}{2} = 47.2\ kN$ Shear load acting on cross section

$M_{o.Ed} := V_{Ed} \cdot 700\ mm = 33.04\ kN \cdot m$ Moment acting at center of opening

$N_{m.Ed} := \frac{M_{o.Ed}}{h - 2\ z_{T.V}} + \frac{N_{0.5}}{2} = 399.895\ kN$ Axial force in Tee's as a result of global moment and global axial forces

$M_{NV.T.Rd} := M_{pl.T.Rd} \cdot \left(1 - \left(\frac{N_{m.Ed}}{N_{T.pl.Rd}}\right)^2\right) = 3.548\ kN \cdot m$ Plastic moment capacity in Tees reduced for axial forces from global moment and global axial loading

$V_{vier.Rd} := \frac{4 \cdot M_{NV.T.Rd}}{a_o} = 47.311\ kN$

$\frac{V_{Ed}}{V_{vier.Rd}} = 0.998$ =1 Check for Vierendeel-capacity

Nicolas André Caronte Grønland

Steel beams with unstiffened web openings

NTNU
Norwegian University of
Science and Technology